Unraveling Carbohydrate-Mediated Host-Pathogen Interactions: Surface Chemistry and Label-Free Biosensing

Jing Shang

A dissertation

submitted in partial fulfillment of the

requirements for the degree of

Doctor of Philosophy

University of Washington

2012

Reading Committee:

Daniel M. Ratner, Chair

James D. Bryers

David S. Newburg

Program Authorized to Offer Degree:

Department of Bioengineering

University of Washington

Abstract

Unraveling Carbohydrate-Mediated Host-Pathogen Interactions: Surface Chemistry and Label-Free Biosensing

Jing Shang

Chair of the Supervisory Committee:

Dr. Daniel M. Ratner

Department of Bioengineering

Infectious diseases present a significant challenge to public health, and there is an urgent need to develop new strategies to address bacterial and viral pathogenesis. As the initial interaction between pathogen and the host cell is often mediated by a carbohydrate recognition event, a straightforward and effective strategy to prevent infection is to block host-pathogen protein-carbohydrate binding. By mimicking carbohydrate ligands present on the host mucosa, human milk glycans have been proven to function as soluble inhibitors capable of preventing a variety of pathogens from binding to the host. These glycans hold great promise to be employed as anti-infective prophylactics to combat infectious disease in both pediatric and adult populations. However, among the hundreds of carbohydrate structures found in human milk, it is challenging to establish the inhibitory relationship between discrete glycan entities and specific pathogens. To address this problem and accelerate the development of anti-infective glycans, we apply high-throughput and label-free biosensing platforms for characterizing the anti-viral activities of human milk glycans against norovirus and HIV. Surface plasmon resonance (SPR) and silicon

photonic microring resonators are two types of label-free biosensors capable of quantifying binding events in real-time. However, the lack of efficient biofunctionalization strategies limits the application of these devices in characterizing carbohydrate-mediated interactions. In this study, reliable and versatile conjugation methods were developed to functionalize biosensors with carbohydrates. These methods utilize a homobifunctional linker, divinylsulfone (DVS), to conjugate natural sugars or carbohydrates modified with nucleophilic linkers ($-NH_2$, -SH) onto the sensor surface. Compared to previous immobilization strategies, our DVS-based method greatly simplifies the process for carbohydrate immobilization and demonstrates high stability for biosensing. Next, the carbohydrate-functionalized biosensors were applied to study human milk glycan-norovirus interactions. We identified glycans that bind to two strains of norovirus and confirmed the activity of specific glycans against norovirus-host receptor interactions. Finally, the inhibitory mechanism of human milk glycosaminoglycans (GAGs) against HIV infection was investigated by SPR. The biosensing platforms and the binding studies in this dissertation advance our understanding of the anti-infective mechanism of human milk glycans and promote the application of glycan-based agents to prevent norovirus and HIV infection.

Table of Contents

List of Figures

List of Tables

Acknowledgements

I am grateful to all the people who provided help and support during my PhD study. I would like to thank my advisor, Dr. Daniel Ratner, for his long-term guidance on my research projects, his great suggestions on my career development and my writing and speaking skills, and his help on many other aspects related with work and living in the United States. I would like to thank my supervisory committee, Dr. James Bryers, Dr. Kim Woodrow, Dr. Hong Ma and Dr. David Newburg for their support and advice on my research and dissertation. I am also grateful to all the present and past members in Ratner lab. They are like my family, and always willing to give me a hand when I need help. In addition, I want to thank all the collaborators involved in my PhD project, Dr. David Newburg, Dr. Vladimir Piskarev, Dr. Xi Jiang, Dr. Joe Zaia, Dr. Mao Yang, Dr. Rodrigo B. Andrade and Justin M. Kaplan. Because of their generous supply of reagents, my experiments were completed as expected. I want to express my gratitude to all my friends. Connie Cheng and Julie Shi gave me many useful suggestions on research and writing. Dan Wang, Sijie Sun and Lin Yan shared their living experiences in U.S. and offered me a lot of support to my study. Finally, I would like to thank my husband, Dr. Wei Lu. Because of Wei's persistence and optimism, I was able to pass through the hardest time in my life. I appreciate all he did for me in the past years. I also want to thank my parents in China. Their selfless care always encouraged me to pursue my dream without fear.

Chapter 1: Introduction

1.1 Motivation

Bacterial and viral infections are major causes of death, disability and socioeconomic disruption for hundreds of millions of people worldwide.[1] For example, human immunodeficiency virus (HIV) has newly affected 2.5 million people in 2011, with a total global prevalence of 34.2 million infections.[2] Acquired immunodeficiency syndrome (AIDS) caused by HIV infection resulted in 1.7 million deaths worldwide in 2011.[2] Domestic and international funding for HIV/AIDS services (including prevention, diagnosis and treatment) have expanded from $1.6 billion in 2001 to $15 billion in 2010.[2, 3] In addition to the rapid transmission of pathogens and huge consequences to global health and economy, the lack of long-effective and universally accessible treatment for HIV/AIDS is a formidable problem.[4] Another example is norovirus, a leading cause of acute gastroenteritis. It affects 21 million people of all ages every year in the United States.[5] Although the outcome of norovirus infection is normally mild, severe illness has been observed in the elderly, infants and immunocompromised patients, with 797 deaths reported annually in the United States.[6] In the developing world, the burden of norovirus infection is much greater, causing 200,000 deaths of children under the age of 5 every year.[5] Currently, no specific treatment or vaccine for norovirus infection is available.[7]

Due to the global prevalence and a variety of problems caused by infectious disease, developing effective vaccines or antimicrobial drugs has become an urgent challenge. Pathogenesis is generally initiated by the specific adhesion of pathogens to host cell surfaces. Microorganisms utilize sugar-binding proteins, which are lectins or adhesins, to specifically recognize carbohydrates, known as glycans, present on host cells.[8] Disruption of carbohydrate-mediated

host-pathogen interactions is one of the most promising strategies to prevent infection. Human milk glycans have been proven to function as soluble receptors that inhibit a variety of pathogens from binding to the host by mimicking endogenous ligands on the host mucosa.[9-11] These glycans hold great promise to become a novel class of antimicrobial agents that can prevent infectious disease.[12] However, due to the structural diversity and complexity of these glycans, the structure-function relationship of many of human milk glycans has not been established, and their inhibitory effects on various pathogens are not well-characterized. Therefore, a high-throughput and efficient technology that can screen the interactions between human milk glycans and multiple pathogens is urgently needed to unravel the role of these glycans in preventing infectious diseases.

1.2 Background

1.2.1 Carbohydrate-mediated host-pathogen interactions

Cell surfaces are covered with a layer of carbohydrates, which possess complex structures and are present in different forms, including glycoproteins, glycolipids, glycosaminoglycans (GAGs) and other glycoconjugates.[13] This layer of carbohydrates plays numerous biological roles related to cellular structure, signal transduction, as well as mediation of host-pathogen interactions (Figure 1.1).[14]

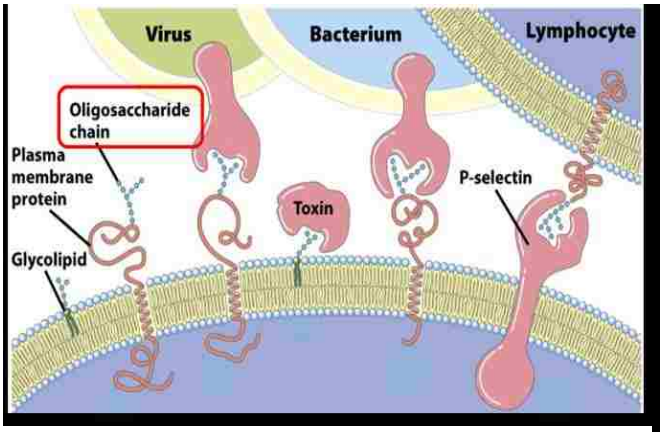

Figure 1.1. The cell surface is covered with a layer of glycans, which play an important role in cell adhesion, immune response and host-pathogen interactions. Adapted from reference (13).

Bacteria and viruses often initiate pathogenesis through their interactions with complex carbohydrates on the host cell surface.[8] The structural complexity of carbohydrates, which originates from the different monosaccharide building blocks and various linking chemistries, determines specific and diverse host-pathogen binding patterns.[12]

Norovirus (NV), a major cause of acute gastroenteritis, recognizes a class of oligosaccharides on epithelial cell surfaces, known as human histo-blood group antigens (HBGAs).[15] The synthesis of HBGA starts with a disaccharide precursor by sequential addition of a monosaccharide. Each step of the synthesis is catalyzed by a glycosyltransferase with specific substrates and linkages.[6] Individuals with secretor gene *FUT2,* which encodes α-1,2-fucosyltransferase, possess HBGAs with α-1,2-linked fucose; while those with Lewis gene *FUT3* (nonsecretors), which encodes α-1,3- or α-1,4-fucosyltransferases, have HBGAs with α-1,3- or 1,4-linked fucose. Previous research has shown that the binding specificity of norovirus depends on the secretor status and blood group type of individuals. 14 strains of norovirus have been found to have 7 binding patterns to different HBGAs.[16] Three norovirus strains (VA387, Norwalk and MOH) only bind to human gastro-duodenal epithelial cells derived from individuals of the secretor phenotype, while strain VA207 binds to the epithelial cells from both secretors and nonscretors.[16] Nonsecretors lack α1,2-fucosyltransferase activity encoded by the *FUT2* gene, which suggests that the α1,2-fucose epitope is essential for the secretor-binding strains. Among the secretor-binding strains, VA387 binds to all secretors (A, B and O blood group types), while Norwalk recognizes A and O and MOH recognizes A and B.[16] This demonstrates that carbohydrate-mediated host-pathogen interactions are highly complicated, making it difficult to identify the specific pathogen receptor and develop effective antimicrobial agents.

The mechanism of HIV transmission also involves glycans on host cell surface. These glycans include sulfated glycolipids and glycosaminoglycans (GAGs) on the surface of colonic and vaginal epithelium and other host cells. GAGs are a diverse class of polysaccharides consisting of repeating disaccharide units that contain at least one deoxyamino sugar. They represent a large number of polymers with significant chemical and structural differences that arise from the patterns of disaccharide building blocks, variable sulfation and overall chain length.[17] Common GAG molecules include heparin, heparan sulfate (HS), chondroitin sulfate (CS), dermatan sulfate (DS) and keratan sulfate (KS).

HIV gains entry into host $CD4^+$ T cells through a multi-step process, including the essential first step of HIV envelope protein gp120 binding to its host cell receptor CD4, the sequential conformational changes in gp120 and the binding of gp120 to the major chemokine co-receptors, CCR5 or CXCR4 on the host cell surface.[18] Previous studies have shown that heparan sulfate on $CD4^+$ T-cell surface participate in this HIV infection process, as evidenced by the reduction of HIV infection after enzymatic treatment of heparan sulfate.[18] For $CD4^-$ host cells, such as epithelial cells on genitourinary tract, GAGs have been proven to be direct binding receptors for HIV, indicating the critical role of GAGs in HIV entry into host cells.[19]

It has been reported that heparan sulfate on host cells interacts with a V3 loop on gp120 and facilitates HIV entry into host cells.[20] Since the V3 loop is positively charged, the interactions between gp120 and polyanionic heparan are regarded as electrostatic interactions.[20] Removal of sulfate groups on heparan reduces the binding of HIV to $CD4^+$ T-cells, further indicating the ionic nature of gp120-heparan interactions and the importance of sulfation in HIV-host receptor interactions.[18]

1.2.2 Human milk glycans and infectious diseases

Breast-feeding has been known as a highly effective and economic strategy for preventing morbidity and mortality in infancy.[11] Previous studies have shown that breastfed infants have a significant lower risk of diarrhea, respiratory infections and other types of infectious disease than their formula-fed peers.[21] This reduced incidence of infectious disease in breastfed infants has been attributed to a variety of components in human milk.[21] In recent decades, human milk glycans have been recognized as one of the anti-infective components.[22] Among a large number of glycans in human milk, fucosylated oligosaccharides and glycoconjugates have been proven to be the active components in preventing diarrhea caused by stable toxins of *Escherichia coli*, *campylobacter* and norovirus.[11] By mimicking endogenous ligands on the host mucosa, these milk glycans function as soluble receptors that inhibit pathogens from binding to the host.

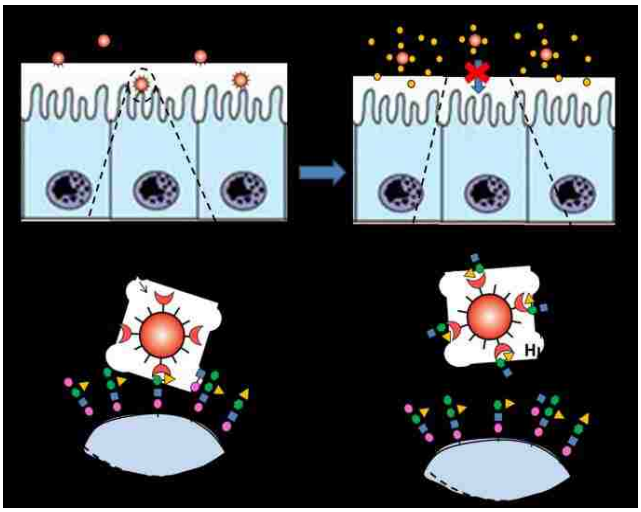

As mentioned in the previous section, norovirus recognizes HBGAs as host receptors and the binding patterns depend on viral genotypes and the structure of HBGAs. (Figure 1.2) Studies by Jiang *et al.* demonstrated that human milk can block binding of norovirus to HBGAs in saliva and the inhibitory specificity is consistent with the binding specificity of norovirus to HBGAs.[10] For instance, milk from secretor mothers blocked VA387 from binding to its host receptors, while milk from nonsecretor mothers blocked the binding of VA207.[10] By separating

human milk into fractions with different molecular weight, Jiang *et al.* further identified a glycosylated component with high molecular weight (1.3-2.0 MDa) that inhibited norovirus binding to HBGAs, and deglycosylation of this fraction induced loss of its inhibitory function.[23] This suggests that a macromolecular carrier conjugated with multiple carbohydrate moieties are required to inhibit norovirus-receptor binding.

In addition to diarrheal disease, human milk has also been proven to protect infants from HIV infection.[24] This anti-viral activity is, in part, attributed to one type of glycans in human milk — GAGs. Previous studies have demonstrated that human milk GAGs can inhibit the binding of the HIV envelope glycoprotein, gp120, to its host cell receptor, CD4.[25] Human milk GAGs are a mixture of several types of GAGs, including dermatan sulfate, heparan sulfate, heparin and chondroitin sulfate. Further research using enzymatic digestion demonstrated that the ability of human milk GAGs to inhibit binding was unaffected by digestion with lytic enzymes specific for heparin, heparan sulfate and dermatan sulfate, but was lost when the milk fraction was treated by the enzyme specific for chondroitin sulfate.[25] This indicates that chondroitin sulfate could be the active component in human milk to inhibit gp120-CD4 interactions.[25]

Human milk glycans are promising anti-viral agents to prevent infectious diseases. However, in order to develop these glycans into anti-infective drugs or vaccines, the detailed structural information of the active human milk components must be clarified and the molecular mechanism of inhibition needs to be elucidated.

1.2.3 Surface plasmon resonance imaging (SPRi)

Surface plasmon resonance (SPR) biosensor is a label-free technology for detecting biomolecular interactions occurring in very close vicinity of a transducer surface.[26] The basic principle and

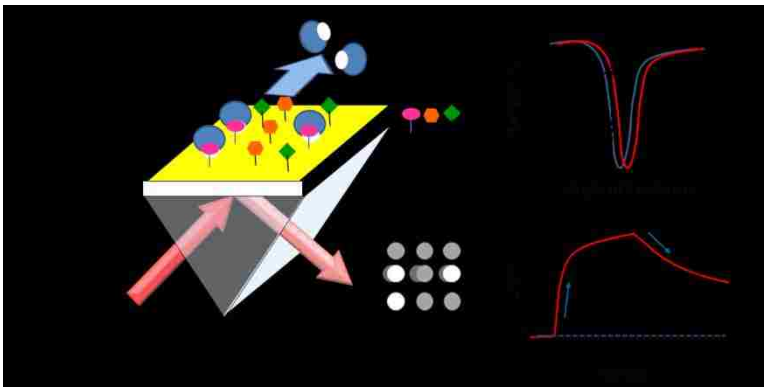

operation of SPR is illustrated in Figure 1.3. In a typical SPR setup, a thin gold film (50-100 nm) is deposited on a glass slide and optically coupled to a glass prism through refractive index matching oil. Surface plasmons are a charge density oscillation at the interface of metal/dielectric media (e.g., gold/air or gold/water interface), which is associated with the evanescent electromagnetic field generated at this interface.[27] When the interface is illuminated by an incident light at certain wavelength and angles under total internal reflection conditions, the light waves are coupled to the oscillation of surface plasmons at the interface, resulting in a minimum in the reflectivity. The angle at which the minimal reflection occurs is denoted as an SPR angle, which is sensitive to the refractive index of the interface. Adsorption of biomolecules on the gold surface changes the interfacial refractive index, causing the shift of the SPR angle. If the SPR angle is fixed, changes in reflectivity can be measured to detect any binding events on the gold surface. Integrating a CCD (charge-coupled device) camera with a traditional SPR instrument, SPR imaging (SPRi) enables direct visualization of binding events.

Compared to traditional fluorescence- or enzyme-labeled methods, SPRi monitors interactions in real-time, maintains the native structure of analyte biomolecules without labeling and provides quantitative binding kinetics. In addition, SPRi can also be used as an inhibition assay to identify the molecules that can inhibit ligand-analyte interactions. Due to these advantages, SPRi has been widely used in drug development, food and environment monitoring, diagnosis and other

biomedical fields.[28-30] In the study of glycomics, carbohydrate-functionalized SPRi chips have been prepared to detect interactions of glycans with a variety of proteins and whole cells, including lectins, enzymes, antibodies and bacteria.[14, 31], [32] SPRi provides valuable information to elucidate the role of carbohydrates in cell-cell adhesion, cell signaling, immune response and host-pathogen interactions.

1.2.4 Strategies for carbohydrate immobilization on biosensor surfaces

To apply SPRi in the study of carbohydrate-mediated biological interactions, reliable and facile strategies for carbohydrate immobilization on gold surface are critically important. A variety of methods have been developed for this purpose. They are generally divided into two categories — non-covalent and covalent immobilization.

Due to the hydrophilic nature of most carbohydrates, it is difficult to non-covalently immobilize carbohydrates on hydrophobic gold surfaces. Modification of natural carbohydrates is necessary to increase their binding strength to gold. One strategy is to introduce a thiol group to one end of a carbohydrate molecule and immobilize carbohydrates on gold through the strong thiol-gold interactions.[33] Another method is to conjugate carbohydrates to a protein carrier (e.g. bovine serum albumin) and deposit the glycoproteins on gold surface through protein-gold hydrophobic interactions.[34]

For covalent immobilization, both activation of gold surface and modification of carbohydrates are required in most cases. As shown in Figure 1.4, an X functional group is introduced to a gold surface, while a Y group is attached to carbohydrate molecules. The reaction between X and Y enables conjugation of carbohydrates on the gold surface.[35] In recent years, a number of X-Y reactive pairs have been developed, including thiol-maleimide (Figure 1.4 b), cyclopentadien-benzoquinone (Figure 1.4 c) and azide-alkyne (Figure 1.4 d) *etc*.[36] These methods involve multiple steps to activate the gold surface and modify the carbohydrates, which are laborious and time consuming. To reduce the burden of carbohydrate modification, introducing an X group that can directly react with natural sugars has been actively explored. One strategy is using hydrazide- or aminooxy-coated surfaces, which are capable of conjugating unmodified sugars at the anomeric position.[37] Another method reported recently is based on photoactivatable functional groups. Upon UV radiation, natural carbohydrates are immobilized onto a solid surface through random bond insertions.[38]

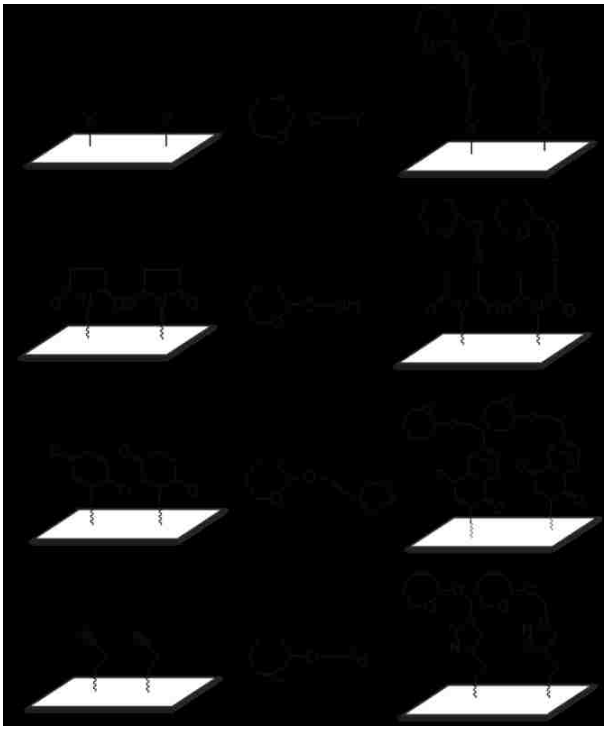

Though numerous strategies for carbohydrate immobilization have been developed, sophisticated chemical synthesis or surface modification is always required, which may not be amenable to

non-synthetic laboratories. In addition, each conjugation method is only suitable for a specific type of molecules (e.g., X-Y reaction pairs), making it difficult to immobilize carbohydrates with various functional groups on one single chip. A versatile and facile strategy for carbohydrate immobilization is needed to advance the study of carbohydrate-mediated interactions.

1.2.5 Carbohydrate microarrays

In addition to immobilization methods, there are other challenges for the biosensing community to study carbohydrate-involved interactions. First, carbohydrates can be very difficult to obtain in large quantities either by isolation from natural sources or by chemical synthesis.[39] Limited access to glycan molecules is a big hindrance to carbohydrate immobilization and binding studies. Furthermore, traditional biosensors usually detect only one or several binding events simultaneously, which is laborious and inefficient if we want to identify specific binding pairs from a large glycan pool (including hundreds or even thousands of different carbohydrates). To overcome these challenges, carbohydrate microarrays have been developed in recent years. Using robotic or manual microarrayers, numerous glycans with various structures can be immobilized on a solid support with miniscule amount of materials.[39] Carbohydrate microarrays enable detecting carbohydrate-macromolecule interactions in a high-throughput manner, significantly improving the efficiency for biomolecular screening.[40] By integrating carbohydrate microarrays with SPRi, hundreds of carbohydrate-protein/cell interactions can be detected in parallel with the added advantage of label-free and real-time analysis.[41]

1.2.6 Silicon photonic microring resonators

Biosensing technologies have become an active research area in recent years due to the urgent need for clinical diagnosis, food and environmental monitoring, drug discovery and basic biomedical research.[42, 43] Most of current biosensors require sophisticated technology, large equipment setup and skilled personnel, which may not be applicable to point-of-care diagnosis, onsite monitoring and detection. Moreover, the high cost of advanced biosensors is a huge barrier for many developing countries. To improve the practicality of biosensors and expand their applications especially in remote areas, more and more efforts have been dedicated to developing portable, low-cost and facile devices for detection.

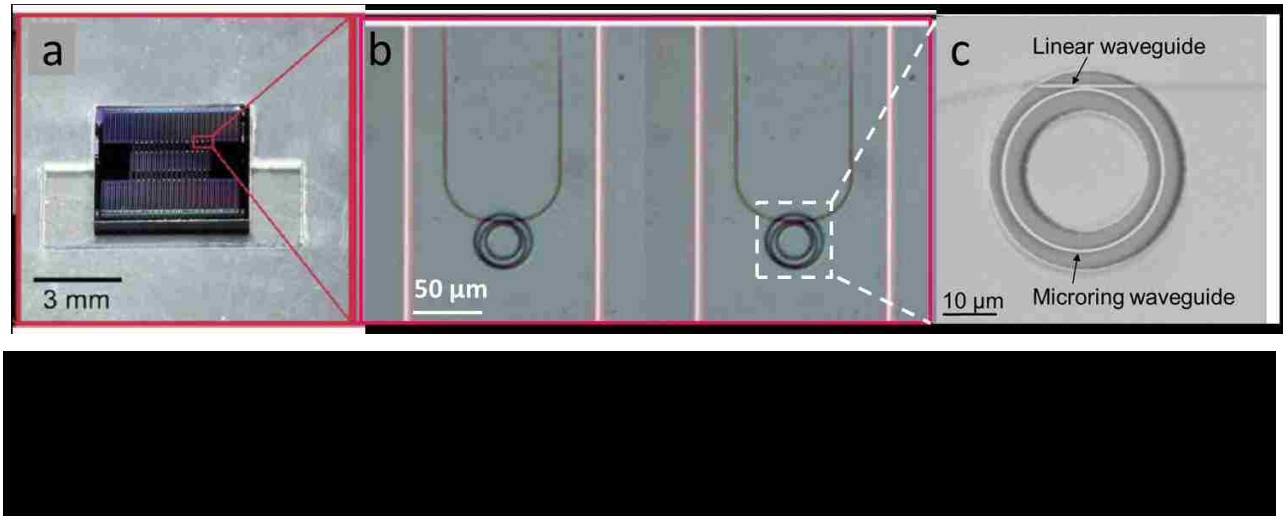

Among the emerging biosensing technologies, silicon photonics – specifically the silicon microring resonator – has gained increasing attention due to demonstrated capabilities in high-sensitive multiplexed detection, chip-scale integration, and the potential of low-cost mass production using existing silicon fabrication processes.[44] The optical microring resonator platform consists of an array of planar ring-shaped silicon waveguides optically coupled to bus waveguides on a silicon oxide insulator. (Figure 1.5)

Propagation of light through narrow waveguides generates an evanescent field, a local region of light 'leakage', which extends a distance of 100–300 nm at the surface of the waveguide. As the microring waveguides and bus waveguides are precisely positioned with a certain distance, evanescent field coupling occurs when the condition in Equation 1.1 is satisfied.[45]

$$2\pi R\eta = \lambda m \tag{1.1}$$

where R is the radius of the microring, η the effective refractive index (RI) of the micro-ring, λ the wavelength, and m is any integer.

Under the resonance conditions, the incident light passing through the input waveguide enters the microring and continuously circulates within the microring structure. A small fraction of the light in the microring escapes into the output waveguide. If we measure the output light intensity as changes in the wavelength of incident light, a deep drop of intensity will be seen at the resonant wavelength. Adsorption of biomolecules on the microring sensors causes small changes in the effective refractive index (η), resulting in a detectable shift in resonance wavelength.[45]

As compared to other label-free biosensors such as SPR, silicon microring resonators have several distinguished advantages. First, the small size of microring resonators enables integration of hundreds or even thousands of resonator sensors on a small silicon chip. Each of the microrings can be addressed individually and used to detect one type of biomolecules, which means thousands of binding events can be detected in parallel.[46] This chip-based assay has great potential to integrate into portable diagnosis devices for point-of-care application. Second, microring resonators can be manufactured in large quantity with minimal cost using mature photolithographic techniques from the silicon industry, which makes it more accessible for use in developing countries.[45]

The feasibility of microring resonators for label-free detection of various biomolecules and cells, including proteins, oligonucleotides and bacteria has been previously demonstrated in the literature.[45-48] Microring resonators hold great promise to become the portable, affordable and high-accurate detection devices in the near future. However, to achieve this goal, several scientific and technical problems must be solved, including biofunctionalization of silicon surface, prevention of non-specific adsorption and design of microfluidic channel.

1.3 Dissertation Overview

The objectives of my PhD research are to develop carbohydrate-functionalized label-free biosensing platforms based on SPRi and silicon photonic microring resonator technologies, apply these platforms to investigate the interactions of human milk glycans with norovirus and HIV, and identify the anti-infective glycans in human milk that can disrupt norovirus/HIV-host cell receptor interactions. Chapters 2 and 3 focus on developing reliable and facile strategies for functionalizing label-free SPRi and microring resonator biosensors. Chapter 4 describes the application of SPR biosensors to characterize norovirus-human milk glycan interactions and the inhibitory activity of these glycans against norovirus-host receptor interactions. Chapter 5 reports the investigation of the anti-HIV activity of human milk glycosaminoglycans by HIV cell culture assays and SPR biosensors. Chapter 6 presents a summary of all the results in this dissertation and a discussion on potential future research directions.

Chapter 2: Developing a Versatile Method for Functionalizing Biosensor Surfaces with Bioactive Glycans

2.1 Abstract

Most of the existing methods to functionalize biosensor surfaces involve multiple steps and laborious work for surface activation and carbohydrate modification. A simple and reliable conjugation method must be developed to facilitate the study of carbohydrate-mediated interactions. In this chapter, we demonstrate the potential of simplified chemistries to fabricate a glycan microarray, utilizing divinyl sulfone (DVS)-modified surfaces for the covalent immobilization of natural and chemically derived carbohydrates, as well as glycoproteins. The bioactivity of the captured glycans was quantitatively examined by surface plasmon resonance imaging (SPRi). Composition and spectroscopic evidence of carbohydrate species on the DVS-modified surface was obtained by X-ray photoelectron spectroscopy (XPS) and time-of-flight secondary ion mass spectrometry (ToF-SIMS), respectively. The site-selective immobilization of glycans based on relative nucleophilicity (reducing sugar vs. amine- and sulfhydryl-derived saccharides) and anomeric configuration was also examined. Our results demonstrate straightforward and reproducible conjugation of a variety of functional biomolecules onto a vinyl sulfone-modified biosensor surface. The simplicity of this method will facilitate the study of human milk glycan-pathogen interactions, and will have a significant impact on glycomics research, as it expands the ability of non-synthetic laboratories to rapidly construct functional glycan microarrays and quantitative biosensors.

2.2 Introduction

Versatile methods for surface modification and bioconjugation are essential to the biosensor and microarray communities. A variety of strategies have been used to achieve non-covalent and covalent attachment of biomolecules on a solid support.[49-54] Non-covalent adsorption is the most straightforward immobilization method, but it is often most suitable for high molecular weight biomolecules (e.g. proteins, DNA).[55] Water-soluble ligands (e.g., sugars, biotin, small peptides) tend to desorb due to weak interactions with the surface and high solubility.[50, 56, 57] As such, covalent bonds between biomolecules and the surface can yield more reliable attachment. For example, carbodiimide chemistries are frequently involved in surface activation to form stable amide/carbamate bonds with biomolecules bearing primary amine groups.[58-62] Isocyanate, epoxy, and acyl chloride groups[63-65], which are highly reactive towards sulfhydryl, amine, and hydroxyl groups present on biomolecues, have also been utilized for surface modification. These reactive groups have expanded the pool of biomolecules that can be immobilized for array, sensor and biomaterial applications. However, the intrinsic moisture sensitivity of most immobilization chemistries requires specialized handling, freshly distilled/dried reagents, anhydrous storage and sophisticated techniques for surface modification—this is neither convenient nor always possible for the end-user or nonchemist.[66, 67]

In the field of glycomics, alternative methods for array fabrication have been proposed to simplify the process of array/biosensor fabrication. These methods have been developed to address the significant synthetic burden associated with traditional glycan array fabrication. For instance, Cummings and colleagues have developed a novel strategy based on the reductive amination of isolated glycans with an amine-functionalized linker for covalent immobilization to N-hydroxysuccinimide and epoxy activated slides.[53, 65] This method is being used by the

Cummings group to perform ‘shotgun glycomics’ to profile glycan structure and biological function using tissue- and cell-specific glycan libraries. Alternate approaches have also been developed based on photoactivatable functional groups.[68, 69] Upon UV radiation, biomolecules are conjugated onto the surface through random bond insertions, resulting in unbiased conjugation. The ultimate aim of these alternative methods for array and biosensor functionalization is to facilitate expansion of the diversity of immobilized glycan, and lower the barrier to enter the field of glycomics research.

Along these lines of simplifying the immobilization of carbohydrates for array/biosensor fabrication, we explore the use of divinyl sulfone (DVS), an efficient, robust, and commercially available homobifunctional linker. Since the 1970’s, DVS has been utilized to conjugate biomolecules to various materials for applications in biotechnology and biomedicine.[58] For instance, chromatographic resins (e.g., Sepharose) have been activated and crosslinked [70] using DVS and conjugated to a variety of ligands (e.g., antigen, enzyme, carbohydrate) for protein affinity purification.[71] DVS has been widely used to couple proteins and carbohydrates to polymers,[72-75] labels for detection (e.g., fluorophores and biotin) [76, 77] and solid supports[77-79] for enzyme recovery, drug delivery and immunoassay development. In addition, vinylsulfone-based chemistries have been used in biosensor and microarray fabrication[80, 81], including applications of N-hydroxysuccinimide-polyethyleneglycol-vinylsulfone, for the construction of DNA and protein microarrays.[82, 83] The versatility of vinylsulfone chemistries has also been extended to include glycoconjugate synthesis to study the biology of carbohydrate-mediated interactions.[84, 85]

Herein we describe a simple two-step method to functionalize hydroxyl-terminated surfaces with unmodified and modified saccharides (thiolated and aminated) as well as proteins and

glycoproteins via a DVS conjugation strategy. The process involves two sequential nucleophilic 1,4-additions (i.e., Michael reactions) in basic solution at ambient temperature, wherein DVS serves as a linchpin between the surface and captured biomolecules. The first step modifies hydroxyl groups present on the surface to generate an activated vinyl sulfone-modified substrate. In the second step, the DVS is reacted with biomolecules bearing sulfhydryl, amino or hydroxyl groups. The functional biomolecules are thus covalently bound to the surface in a site selective manner based on the nucleophilicities of the reactive groups. This strategy enables immobilization of a variety of biomolecules on a single array/chip and simplifies the process for arraying synthetically challenging biomolecules (e.g. carbohydrates) by covalent capture via endogenous nucleophiles.

A variety of analytical and biophysical methods were employed to validate this conjugation strategy. X-ray Photoelectron Spectroscopy (XPS) was used to characterize each surface modification step. Spectroscopic evidence of saccharide-related species on the surface was also obtained by Time-of-Flight Secondary Ion Mass Spectrometry (ToF-SIMS). Surface Plasmon Resonance imaging (SPRi) was used to screen carbohydrate-specific protein binding on the saccharide-functionalized array; lectin binding affinities on unmodified and modified mannose were determined. In addition, Nuclear Magnetic Resonance (NMR) spectroscopy was used to establish the site selectivity of a model coupling reaction between a reducing sugar and ethyl vinyl sulfone, simulating the reaction of free sugars to DVS-modified surfaces. To preserve precious reagents, a manual microarray printer was adapted to fabricate carbohydrate microarrays on SPR gold chips.

2.3 Materials and Methods

2.3.1 Reagents and Materials

All chemical reagents were purchased from Sigma-Aldrich (St. Louis, MO) and Acros Organics (West Chester, PA) and used as received without further purification. Aminopropyl mannoside [86] was provided by Prof. Rodrigo B. Andrade at Temple University. Mannose thiol and oligo(ethylene glycol)$_3$ thiol (OEG thiol) were synthesized as previously described.[40] Bovine serum albumin (BSA) and wheat germ agglutinin (WGA) were purchased from Sigma-Aldrich (St. Louis, MO). Concanavalin A (Con A) was purchased from MP Biomedicals (Solon, OH). RNase A and RNase B were purchased from New England Biolabs (Ipswich, MA). Ricin (RCA_{120}) was purchased from EY Laboratories (San Mateo, CA) and dialyzed overnight against PBS prior to use. Ethanol (200 proof, USP) was purchased from Decon Labs (King of Prussia, PA). Culture-Well Silicone sheets were purchased from Grace Bio-Labs (Bend, OR). SF-10 glass substrates were purchased from SCHOTT Glass Technology (Duryea, PA). Silicon wafers were purchased from Silicon Valley Microelectronics (San Jose, CA). Millipore-filtered water was used for all aqueous solutions and rinsing. Unfunctionalized bare gold SIA Biacore kits were purchased from GE Healthcare Bio-Sciences AB (Uppsala, Sweden).

2.3.2 Preparation of Au substrates

Titanium (2 nm) and gold (45 nm) films were deposited onto cleaned SF-10 glass (18 mm × 18 mm) and silicon wafers (10 mm × 10 mm) for SPRi and surface analysis, respectively. Metal films were prepared via electron beam evaporation at the Washington Technology Center (Seattle, WA).

2.3.3 DVS-modified surfaces

Fresh Au substrates were immersed in 11-mercaptoundecanol (0.1 mM in EtOH) for 2 h at room temperature to form a hydroxyl-terminated self-assembled monolayer surface. The surfaces were dipped in a stirring ethanol bath for 1 min. The cleaned surfaces were dried under a stream of argon for 1 min and then immersed in 10% DVS (v/v, 0.5 M carbonate buffer, pH 11) solution for 1 h at ambient temperature. The DVS-modified surfaces were thoroughly rinsed with ~10 mL water, dried by a stream of argon and stored in the dark at 4 ^{0}C under an inert atmosphere.

2.3.4 Glycan-functionalized surfaces

The DVS-modified surfaces on silicon wafer substrates were immersed in mannose (20% w/v, pH 10 carbonate buffer) solution at ambient temperature for 16 h unless specified. The surfaces were then thoroughly rinsed with ~10 mL water and ~5 mL ethanol, dried under a stream of argon for 1 min and stored in dark at 4^{o}C.

2.3.5 Trifluoroethyl derivation of DVS-activated surface

Trifluoroethyl derivation was carried on in three fluoride reagents bearing hydroxyl, amine, and thiol group respectively. The DVS-modified surfaces on silicon wafer substrates were immersed in aqueous solutions of the trifluoroethyl nucleophile (trifluoroethanol 20% w/v in pH 10 carbonate buffer, trifluoroethanethiol 10mM in pH 7.4 PBS buffer, trifluoroethylamine 10mM in pH 10 carbonate buffer) at ambient temperature for 16 h unless specified. The surfaces were then thoroughly rinsed with ~10 mL water and ~5 mL ethanol, dried under a stream of argon for 1 min and stored in dark at 4 ^{o}C.

2.3.6 Glycan-functionalized arrays

Nine-element silicone masks were placed onto the DVS-modified surfaces. 2 μL of dissolved glycan (pH 10 carbonate buffer for natural glycans, aminated glycans, RNase A, and RNase B and pH 7.4 PBS for thiolated glycans,) was spotted onto each spot. To prevent oxidation of thiolated glycan, 0.5 stoichiometric equivalents of tris(2-carboxyethyl)phosphine (TCEP) were added to the aqueous thiol solutions prior to spotting. The arrays were incubated in a 75% relative humidity chamber. After 16 h incubation, surfaces were immersed in OEG-thiol[87] (1mM in carbonate buffer, pH 8.5) for 2 h to deactivate remaining vinyl sulfone groups, then rinsed with water, dried under a stream of argon and stored at 4 ^{o}C.

2.3.7 XPS analysis

XPS composition data was acquired on a Kratos AXIS Ultra DLD instrument equipped with a monochromatic Al-K X-ray source ($h\nu$ = 1486.6 eV). XPS data were collected at 0^0 take-off angle in the hybrid mode with approximately 10 nm sampling depth. Compositional survey and detailed scans (N 1s, O 1s, and S 2p) were acquired using a pass energy of 80 eV. Three spots on two or more duplicates of samples were analyzed. Reported compositional data were averaged over multiple spots. Data analysis was performed on the CasaXPS software (Casa Software Ltd.).

2.3.8 ToF-SIMS analysis

ToF-SIMS data was acquired using an ION-TOF TOF.SIMS 5-100 system (ION-TOF GmbH, Münster, Germany). Positive spectra were recorded by rastering a pulsed 25 keV Bi^{3+} primary ion source over a (100 × 100) μm^2 area, and keeping the total ion dose below the static limit (i.e., 10^{12} ions/cm^2). The mass resolution ($m/\Delta m$) was typically 6000 at m/z = 27 for all spectra, which

were mass calibrated using the CH_3^+, $C_2H_3^+$, $C_3H_7^+$, and $AuC_2H_4^+$ peaks. Maximum calibration errors were kept below 15 ppm.

2.3.9 Glycan-protein interactions detected by SPR

Glycan-specific protein binding was performed on a SPRimagerII (GWC Technologies). The SPRimagerII was operated at room temperature using a standard flow cell and a peristaltic pump (BioRad-EconoPump) at 100 μL/min. All surfaces were passivated with 0.1% BSA in PBS buffer for 30 min and equilibrated in protein buffers prior to protein binding. HEPES buffer (10 mM HEPES, 150 mM NaCl, 1 mM Ca^{2+} and Mn^{2+}, pH 7.4) was used for Con A binding, PBS (2.7 mM KCl, 137 mM NaCl, 10 mM phosphate, pH 7.4) was used for RCA_{120} and WGA binding. Unless specified, lectins were used at 500 nM. Data acquisition consisted of the averaging of 30 images over a short duration to create an average image. The SPR signal given by the average image (in pixel intensity) was subsequently converted to normalized percentages change in reflectivity according to GWC protocol. Urea (8 M) was used to strip bound proteins and regenerate the array surfaces. For sensorgram acquisition, a 500 μm × 500 μm of the image was selected as the region-of-interest (ROI). For visual clarity, the contrast and brightness of SPR difference image was adjusted by ImageJ software (U. S. National Institutes of Health, Bethesda, MD). Two spots on two or more duplicates of samples were analyzed. Reported changes in SPR reflectivity (Δ%R) were averaged over multiple spots and background subtracted.

Surface performance of the glycan-functionalized chip was carried on a Biacore T100 (LSDF Center for Intracellular Delivery of Biologics). The SPR was operated at room temperature using a syringe pump at 30 μL/min. All saccharide-functionalized surfaces were passivated with 0.1% BSA in PBS buffer for 30 min and equilibrated in protein buffers prior to protein binding. HEPES buffer was used for Con A binding. Glycine (10 mM, pH 2) was used to remove

captured lectin and regenerate the array surfaces; to avoid damaging the microfluidic channels in the Biacore T100, 8.0 M urea was not used for this regeneration step. Data analysis was performed using Biacore evaluation software.

2.3.10 Synthesis of ethylvinyl sulfone mannosides

Ethyl vinyl sulfone (0.67 g, 5.5 mmole) was added to mannose (1 g, 5.5 mmole) in 10 mL buffer (0.5 M sodium carbonate, pH 10), and stirred at room temperature for 16 h. The reaction was concentrated by rotary evaporation and a portion of the resulting solid (containing product and buffer salts) was extracted in a minimal volume of methanol and applied to a silica flash column (methanol : dicholormethane = 2:8). The anomeric mixture of product was separated by preparative thin layer chromatography (isopropanal: methanol: water = 8:2:0.5) to isolate the α and β anomers. The separated fractions were analyzed by ion trap mass spectrometry (Bruker Daltonics, Billerica, MA) and were found to have the same mass ($[M+Na]^+$ m/z 323.2). α-Anomer ^{1}H NMR (500 MHz, D_2O): δ 4.83 (d, J = 1.5 Hz, 1H; H_1), 4.18-4.14 (m, 1H; -O-CH_aH_b-$CH_2SO_2CH_2CH_3$), 3.90-3.83 (m, 3H; H_2, H_{6a}, -O-CH_aH_b-$CH_2SO_2CH_2CH_3$), 3.74-3.71 (m, 1H, H_5), 3.68-3.62 (m, 2H, H_3, H_{6b}), 3.58-3.54 (m, 1H, H_4), 3.41-3.37 (m, 2H, -O-CH_aH_b-$CH_2SO_2CH_2CH_3$), 3.18-3.13 (m, 2H, -O-CH_aH_b-$CH_2SO_2CH_2CH_3$), 1.39-1.36 (t, 3H, -O-CH_aH_b-$CH_2SO_2CH_2CH_3$). ^{13}C NMR (500 MHz, D_2O): δ 100.56 (C_1), 73.76 (C_5), 71.21 (C_3), 70.48 (C_2), 67.01 (C_4), 61.48 (C_6), 60.88 (-O-CH_2-$CH_2SO_2CH_2CH_3$), 51.50 (-O-CH_2-$CH_2SO_2CH_2CH_3$), 48.59 (-O-CH_b-$CH_2SO_2CH_2CH_3$), 5.21 (-O-CH_2-$CH_2SO_2CH_2CH_3$).

2.3.11 Glycan microarray printing

A manual microarrayer (V&P Scientific, Inc., CA) designed for microscopy glass slides was used to print glycan microarrays on DVS-activated surfaces. To adapt this arrayer to gold chips,

the number of pins was reduced and the position of a gold chip on a glass holder was adjusted. RNase B (1 mg/ml) dissolved in pH 10 carbonate buffer containing different concentrations of Tween-20, glycerol and dimethyl sulfoxide were printed. The microarrays were incubated in a 75% relative humidity chamber. After 16 h incubation, surfaces were immersed in BSA solutions (1 mg/ml in pH 8.5 buffer) for 1 h to passivate the surface. The response of printed RNase B to Con A was measured by SPRi.

2.4 Results and Discussion

2.4.1 Surface modification and characterization

The simple stepwise process for DVS-based immobilization of modified and unmodified glycans is illustrated in Scheme 2.1. A hydroxyl-terminated self-assembled monolayer (SAM) on Au was used for DVS modification under alkaline conditions followed by incubation with the sugar. Each surface modification step and subsequent incubation was characterized using XPS to obtain the organic composition (Table 2.1). On the spectrum of SAM-modified surface, carbon, oxygen and sulfur peaks were observed. Due to XPS sulfur signal attenuation by the outermost organic monolayer, the O/S ratio (2.4 ± 0.2) in the SAM-modified surface is higher than the value predicted by stoichiometry (1.0), which is expected.[88, 89] For sequential DVS- and glycan-treated surfaces, a slight excess of sulfur was observed and attributed to the addition of DVS on the surface.[87, 89]

Scheme 2.1. Immobilization of natural sugars as well as amine- and sulfhydryl-derived glycans on the DVS-modified surface.

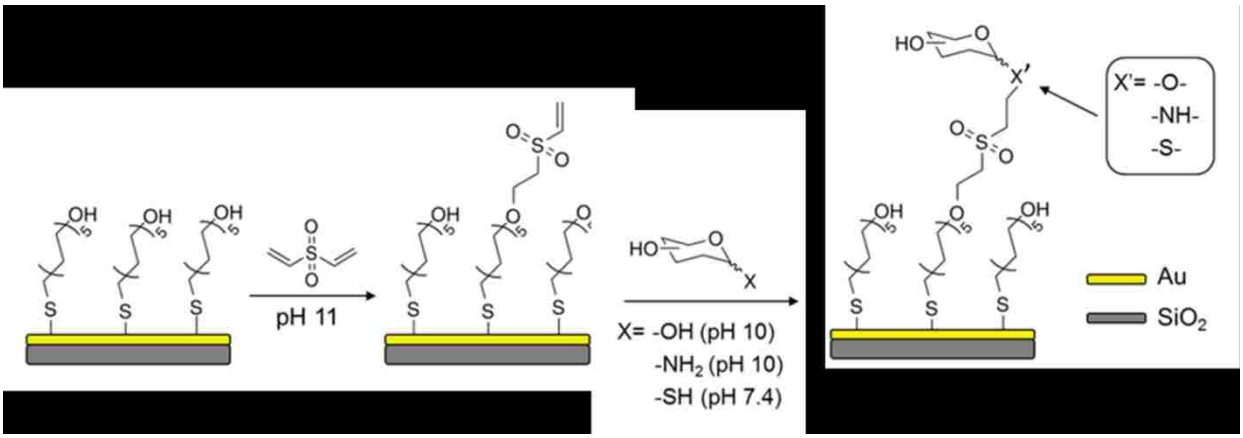

Table 2.1. Comparison of theoretical versus observed XPS composition of modified surfaces.

	SAM (11-mercaptoundecanol)		DVS-modified SAM		Mannose-functionalized SAM via DVS	
	Theoretical	Observed	Theoretical	Observed	Theoretical	Observed
C	84.6	88.2±0.6	75.0	84.3±1.2	65.6	84.9±0.7
O	7.7	8.3±0.6	15.0	12.0±1.0	28.1	10.7±0.5
S	7.7	3.5±0.2	10.0	3.7±0.2	6.3	4.4±0.2

a. DVS/hydroxyl reaction yield is assumed to be 100%;

b. The sequential mannose coupling yield is assumed to be 100%;

c. XPS values represent the averages and standard deviations from at least three spots on two replicates or more.

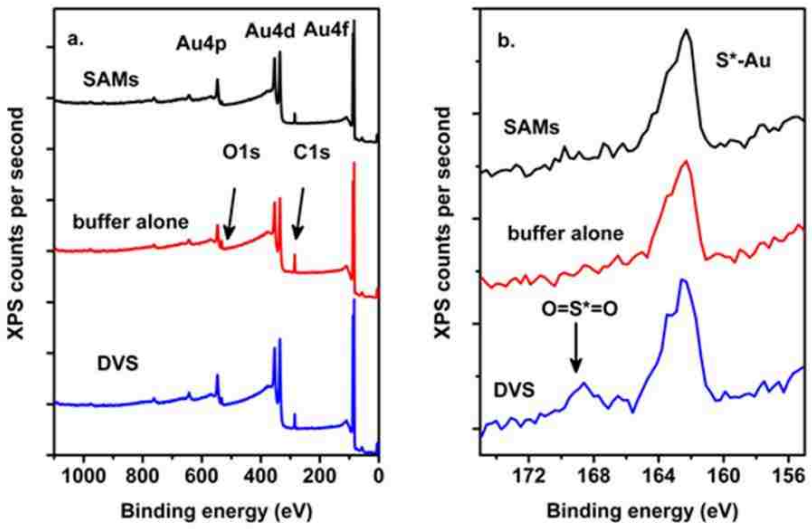

Figure 2.1. XPS spectra (a) wide scan and (b) sulfur 2p scan for hydoxyl-terminated alkane thiol (SAMs), control SAMs treated with buffer (buffer alone), and DVS-modified surface (DVS). The sulfur species at high binding energy (168 eV for oxidized sulfur) [90] indicates that DVS is conjugated to the SAM.

On the XPS detailed sulfur 2p scan spectrum (Figure 2.1), two peaks were observed and assigned to the Au-bound thiol (160 eV) and oxidized sulfur species (168 eV), respectively.[90, 91] To establish that the oxidized sulfur species observed on the DVS-modified SAMs originates from the vinyl sulfone and not from oxidation of the Au-thiol during handling, the SAM was incubated in buffer with and without divinyl sulfone. The absence of an oxidized sulfur signal on the buffer treated control SAM confirmed that oxidation of thiols in the SAM is not observed by XPS. These results suggest that the observed oxidized sulfur species at 168 eV can be attributed to the vinyl sulfone modification of the SAM. The XPS ratio of sulfone to Au-thiol is approximately 1:8. Taking into account signal attenuation due to the monolayer thickness, the DVS coupling efficiency is estimated to be 10%. The XPS results indicated that all surfaces are

of high quality and contain the expected elemental composition with minimal amounts of contamination.

Elemental information obtained by XPS, however, is not sufficient to determine whether carbohydrate is in fact present on the surface. Therefore, to verify the existence of surface-bound glycan, ToF-SIMS was employed to identify molecular fragments unique to immobilized carbohydrate species. Consistent with the reported positive ion fragments, a series of surface species related to saccharides were identified by ToF-SIMS. As illustrated in Figure 2.2, peak 73 ($C_3H_5O_2^+$) is a positive ion fragment characteristic of a pyranose moiety,[92, 93] therefore confirming the presence of mannose on the surface.

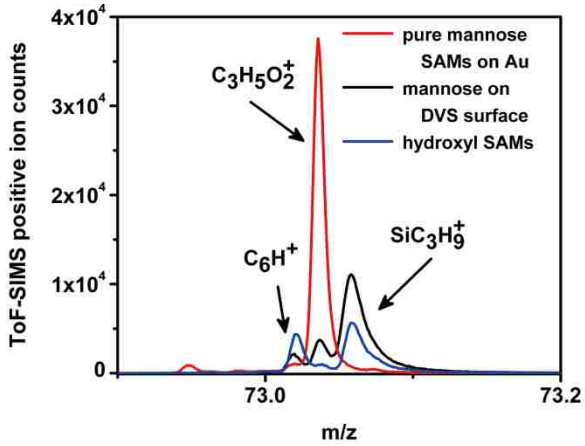

Figure 2.2. ToF-SIMS positive ion spectra of a mannose-functionalized DVS surface, a thiolated-mannose SAM, and a hydroxyl-terminated alkanethiol SAM, indicating the presence of immobilized mannose on the surface (as evidenced by the carbohydrate-associated fragment $C_3H_5O_2^+$ [92, 93]). Two positive ion fragments, C_6H^+ and $SiC_3H_9^+$, are believed to originate from adventitious hydrocarbon and silicone contamination respectively.

2.4.2. Bioactivity of saccharide-functionalized array surface by unmodified saccharides

To assess the bioactivity of DVS immobilized glycoprotein, unmodified mono- and oligosaccharides, a spotted glycan array was fabricated for SPRi binding studies. Solutions of monosaccharides (glucose, mannose, and galactose), oligosaccharides (maltose, lactose, chitobiose, and maltotriose), RNase B and RNase A were included in the spotting array. Carbohydrate-binding proteins concanavalin A (Con A), ricin (RCA_{120}), and wheat germ agglutinin (WGA) were used to screen carbohydrate bioavailability. As shown in Figure 2.3a and 2.3b, those spots treated with mannose, maltotriose, maltose, glucose, and RNase B showed expected SPR signal increases due to Con A binding, whereas the rest of the spots which were immobilized with galactose, lactose, chitobiose, and RNase A did not show appreciable change in reflectivity. RNase B is a glycoprotein modified with highly-branched mannose, while RNase A has the identical peptide sequence but lacks the mannose moiety. These binding results are consistent with the fact that Con A has specific affinity towards α-mannose, α-glucose, maltose (which displays a terminal α-glucose residue) and other mannose-containing glycoproteins, but not towards galactose, lactose, or RNase A. RCA_{120}, a protein toxin, selectively binds to β-galactose and lactose. When a solution of RCA_{120} is passed over the surface, only the spots with galactose and lactose showed changes in SPR reflectivity (Figure 2.3c and 2.3d). Lastly, WGA, which has affinity to chitobiose, was screened on the array. The SPRi results showed expected chitobiose-WGA binding specificity (Figure 2.3e and 2.3f).

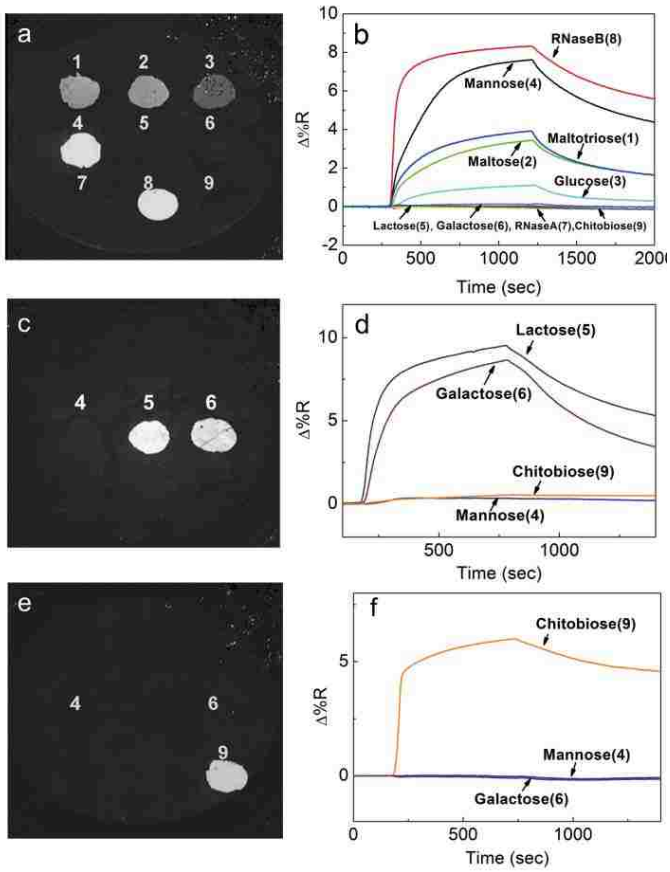

Figure 2.3. SPRi reflectivity images and the corresponding sensorgrams on a spotted glycan array. Glycan bioactivity was established via lectin binding with ConA (a and b), RCA120 (c and d), and WGA (e and f). The 9-element array includes (1) maltotriose, (2) maltose, (3) glucose, (4) mannose, (5) lactose, (6) galactose, (7) RNase A, (8) RNase B, and (9) chitobiose.

By varying glycan immobilization conditions (solution concentration, pH, and incubation time), high protein bioactivity can be achieved; using mannose as an example, Figure 2.4 illustrates the effects of these variables on Con A binding (as measured by SPRi). Compared to the XPS composition study, SPRi binding (Figure 2.4a) showed a dose dependent change as the function of mannose solution concentrations. This can be explained by the fact that SPR is more sensitive to changes of very low concentrations of surface-bound ligand, which cannot be observed

accurately by XPS. SPR measures the response of protein (analyte) binding to the immobilized ligand, which can be easily detected at low ligand density (sub-monolayer). As expected, the protein binding capacity was increased with high concentration of mannose (20 - 30% w/v), alkaline immobilization buffer (pH 10 - 11) and longer incubation time (20 h or more). These results can be used to determine optimal fabrication conditions for printed glycan arrays prepared via DVS capture.

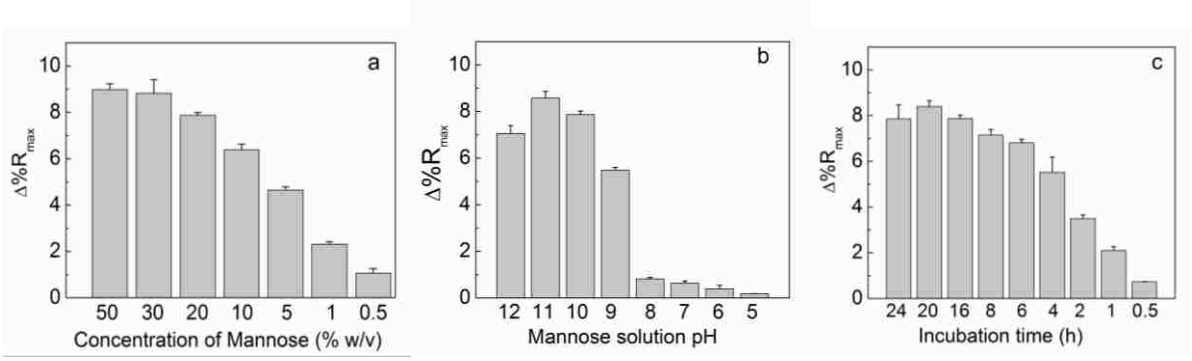

Figure 2.4. Glycan immobilization conditions (free sugar concentration in solution, pH and incubation time) play a significant role in determining the bioactivity of the modified surfaces. Average SPRi ConA response (with standard deviation) to mannose-functionalized array surfaces. (a) pH 10 carbonate buffer, 16 h incubation; (b) 20% w/v mannose, 16 h incubation; (c) 20% mannose, pH 10 carbonate buffer.

During surface activation and glycan functionalization steps by using DVS, it is possible that crosslinking of terminal hydroxyl groups on the alkanol SAM and hydrolysis of vinylsulfone could reduce the coupling efficiency, but it doesn't significantly affect our ability to use the surfaces for glycan conjugation and bioactivity detection. Our results showed that glycan-functionalized surfaces are highly stable and reusable for biosensing experiments. Printed arrays retained 90% of their maximum protein-binding capacity after one hundred continuous binding-

regeneration cycles on SPR (Figure 2.5) or after three months of storage (4 ^{0}C, dark, desiccated). Under the same storage conditions, the unreacted DVS-modified surfaces maintained 90% maximal activity to glycan immobilization after 1 week and 80% after 1 month of storage. These results demonstrate the potential for long-term stability of activated surfaces, greatly simplifying array fabrication by making it possible to create and store activated surfaces.

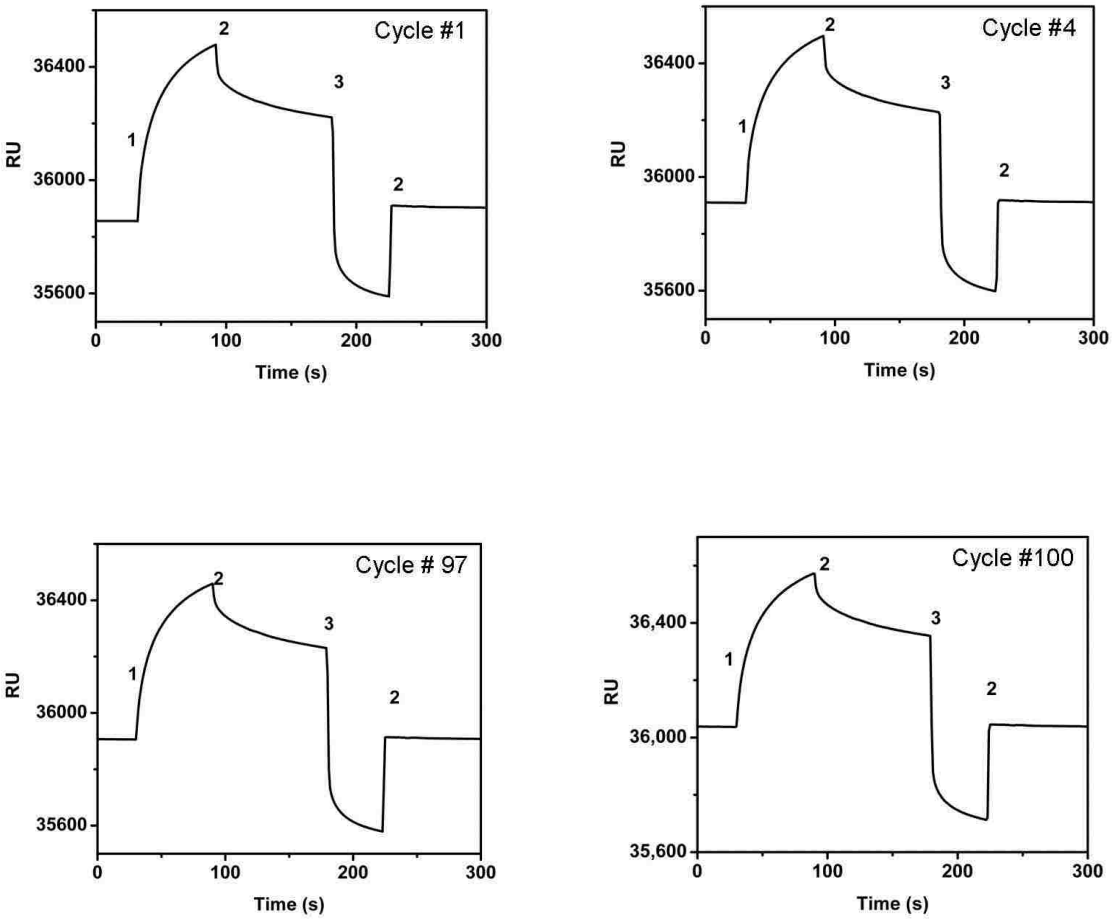

Figure 2.5. Glycan modified surfaces conjugated via DVS chemistries are highly stable to multiple rounds of protein capture and regeneration. Bioacore SPR sensorgrams for 100-cycle lectin binding-regeneration on a mannose-modified Biacore chip. (1) 500 nM ConA, (2) HEPES buffer, and (3) Glycine (10mM, pH 2) for surface regeneration.

DVS is an especially versatile method for surface functionalization, and can easily be adapted to a variety of hydroxyl-bearing substrates.[73, 74] To demonstrate the flexibility of this approach, we have begun to explore a variety of surfaces for DVS modification with great success. For instance, in addition to utilizing hydroxyl-terminated alkane-thiols (11-mercaptoundecanol), DVS immobilization of carbohydrates was also achieved on surfaces bearing hydroxyl-terminated oligo(ethylene glycol) (OEG). Compared to the alkanethiol SAM, we observed lower nonspecific adsorption (Figure 2.6a) and a similar Con A binding profile (Figure 2.6b) on the DVS modified OEG substrate.

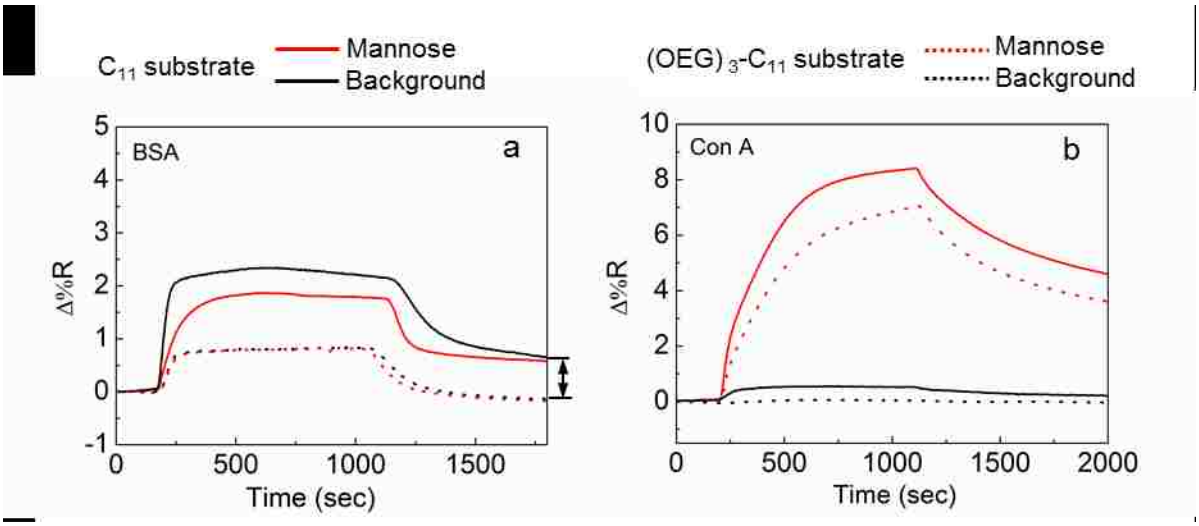

Figure 2.6. SPR sensorgrams (without background subtraction) of non-specific BSA (a) and specific Con A (b) binding to mannose functionalized chips with different underlying chemistries. C_{11} substrate: 11-mercaptoundecanol, $(OEG)_3$-C_{11} substrate: (11-mercaptoundecyl) tri(ethylene glycol). — Mannose, — Background (non-glycan functionalized region) on C_{11} substrate, ····· Mannose, ····· Background on $(OEG)_3$-C_{11} substrate. These results indicate that the $(OEG)_3$-C_{11} SAMs yield surfaces that are more resistant to non-specific protein adsorption, as shown by the difference in non-specific BSA binding in (a).

To investigate Con A non-specific uptake onto inactivated DVS surfaces, we examined Con A binding to a mannose-functionalized chip without prior blocking with BSA (Figure 2.7). The results showed a small refractive index change (~0.5Δ%R) due to Con A non-specific adsorption during the first binding cycle. However, nonspecific uptake was not observed in following cycles.

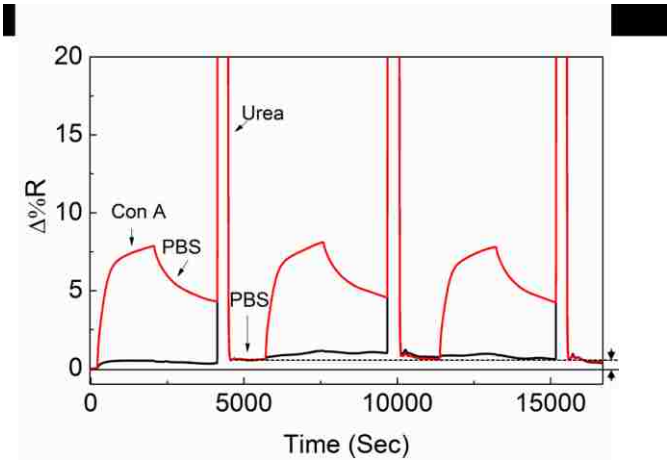

Figure 2.7. SPR sensorgrams (without background subtraction) of Con A binding to an OEG-SH inactivated DVS surface without blocking by BSA. —— Mannose, ——Background (non-glycan functionalized region). During the first Con A binding cycle, the baseline rose ~0.5 Δ%R (indicated by the arrows), which is attributed to Con A nonspecific uptake to the inactivated DVS surface. However, the baseline returned to the initial level in the second and third cycle of Con A binding. These results indicate that there is some nonspecific Con A uptake to the inactivated DVS surface, but after the first binding cycle, only the specific Con A binding is observed on the SPR sensorgram.

2.4.3 Bioactivity of saccharide-functionalized array surfaces

The site selectivity of the 1,4-conjugate addition, or Michael reaction, between biomolecules and the vinyl sulfone moiety of DVS is determined by the nucleophilicity of the pendant functional groups on the biomolecule (i.e., hydroxyl, amino or sulfhydryl).[94-96] In weakly alkaline

solutions, the sulfhydryl and amino groups are more nucleophilic than the hydroxyl.[96] Hence, thiolated and aminated mannoses can be conjugated onto the DVS-modified array surface via their sulfhydryl and amino groups, orienting the bioactive glycan moiety at the array surface. SPRi Con A binding (Figure 2.8) shows that the amine- and thiol-modified mannose exhibited high Con A binding capacity, as they needed lower solution concentration and shorter immobilization time than unmodified mannose. To evaluate the possibility of physical adsorption of mannose species (especially thiolated mannose) on SAM surfaces, unmodified, aminated and thiolated mannoses were spotted on the hydroxyl-terminated SAM without DVS activation. Con A specific binding was not detected on these surfaces (data not shown), further demonstrating the importance of DVS for glycan immobilization.

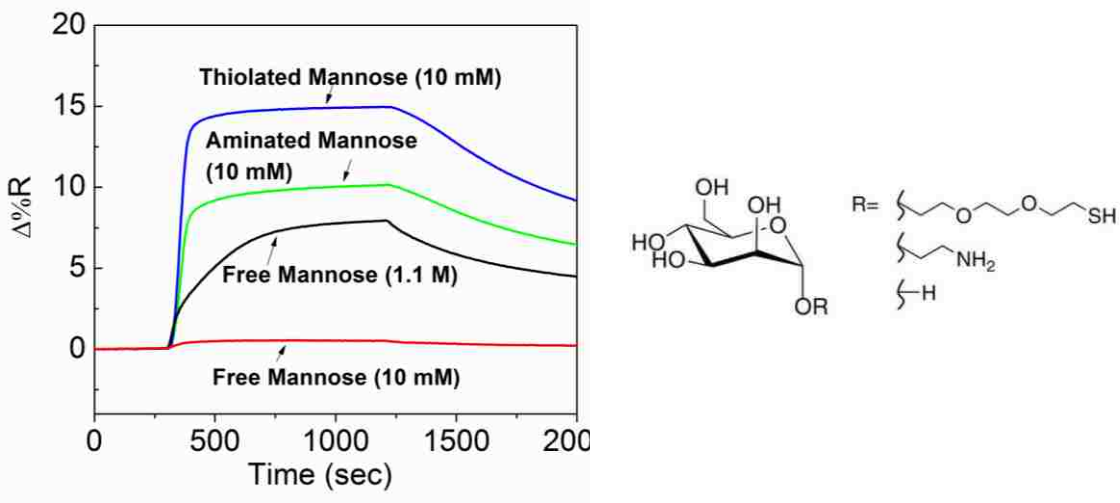

Figure 2.8. SPRi shows that the response of Con A varies as a function of the nucleophile used for conjugation of mannose to the surface.

2.4.4 Unmodified versus modified glycan: A comparison of adsorption isotherm and surface density

To establish the role of thiolated and aminated linker in the bioactivity of DVS-immobilized glycans, the adsorption isotherms of Con A were constructed for surfaces composed of unmodified-, thiolated-, and aminated mannose, and their interactions were analyzed with the Langmuir adsorption model.[97] SPR response at equilibrium was related to Con A concentration according to the following equation, where R_{eq} is the SPR response to Con A with concentration of C at equilibrium and R_{max} is the equilibrium response when C is infinity. [51, 97, 98]

$$\frac{1}{R_{eq}} = \frac{1}{R_{max} K_A} \times \frac{1}{C} + \frac{1}{R_{max}} \tag{2.1}$$

The association constant (K_A) and the maximum response (R_{max}) of Con A binding with unmodified and modified mannose are listed in Table 2.2. These binding parameters indicate that the interaction is greater for the thiolated and aminated mannose, suggesting higher bioactivity – and possibly higher densities – of glycan species on the array surface.[51, 99] Our measured association constants agree with the reported values, $10^5 \cdot M^{-1}$ to $10^6 \cdot M^{-1}$.[33, 98, 100]

Table 2.2. Association constant (K_A) and the maximum binding (R_{max}) of Con A to array surfaces composed of unmodified, thiolated, and animated mannose.

Immobilized mannose	K_A ($10^6 \cdot M^{-1}$)	R_{max}	Δ %R [a]
Unmodified [b]	3.1 ± 0.2	11.0	7.9 ± 0.5
Aminated [c]	7.3 ± 0.5	11.9	9.8 ± 0.3
Thiolated [d]	8.6 ± 0.7	17.7	14.6 ± 0.4

a. Con A 500 nM in HEPES buffer for 50 min flow;
b. 20% (1.1 M), 16 h, pH 10 carbonate buffer;
c. 10 mM, 1h, pH 10 carbonate buffer;
d. 10 mM, 1h, pH 7.4 PBS;
e. SPRi values represent the averages and standard deviations from at least two spots on two replicates or more.

To obtain a more accurate sense of the immobilized surface density of thiol-, amine- and hydroxyl-bearing molecules, DVS-modified surfaces were reacted with trifluoroethanol, trifluoroethanethiol and trifluoroethylamine, and analyzed by XPS (Figure 2.9). The XPS fluorine to oxygen (F/O) ratio obtained from these modified surfaces can be used to establish the density of the trifluoroethane-nucleophile, since the presence of surface-bound fluorine is unique to the trifluoro-species, while oxygen is mainly attributed to hydroxyl-terminated surface. The F/O ratio was determined to be 0.08 ± 0.01 for trifluoroethanol, 0.20 ± 0.06 for trifluoroethanethiol, and 0.19 ± 0.03 for trifluoroethylamine. Based upon a starting density of 4.67 hydroxyls (or less) per nm^2,[101] the estimated density for trifluoroethanol on DVS-modified surface is roughly 0.1 molecule/nm^2, while the stronger amino- and thiol- nucleophiles yielded nearly 0.3 molecules/nm^2. These results, combined with the Con A binding to different functional mannosides (*i.e.* free sugar, aminated and thiolated), suggest that thiolated and aminated biomolecules conjugate more efficiently to DVS and result in a higher surface density, in agreement with the well-established reactivity of these nucleophilic groups.[58]

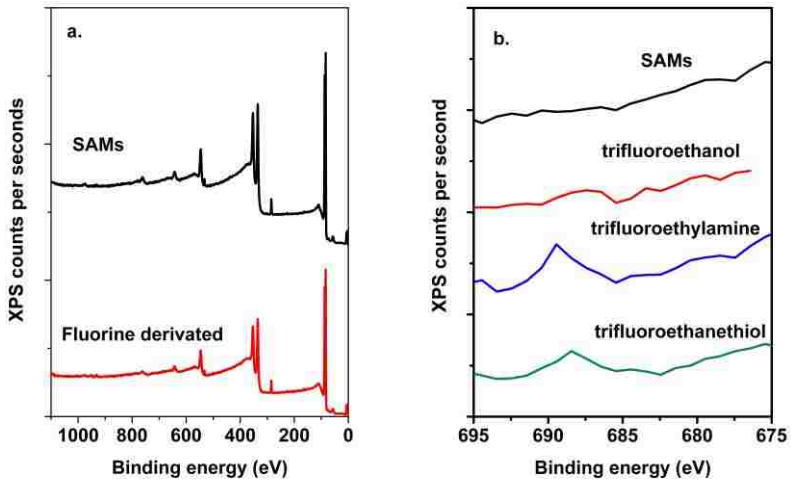

Figure 2.9. XPS (a) wide survey scan and (b) F 1s scan for fluorine-derivated SAMs by trifluoroethanol, trifluoroethylamine, and trifluoroethanethiol.

2.4.5 Vinyl sulfone reaction preference for hydroxyl groups in saccharides

By definition, carbohydrates display multiple hydroxyl groups and reducing sugars present a ratio of the α and β anomeric configuration at equilibrium in solution. Therefore, free sugars may conjugate to the DVS-modified surface via any one of its multiple hydroxyl sites and can exist as both the α- and β- diastereomers, making it necessary to carefully characterize the mode of unmodified carbohydrate-binding to DVS surfaces. To establish reaction sites and the ratio of α- and β- isomers conjugated with vinyl sulfone, proton and carbon NMR spectroscopy were used to examine a model reaction based on the reaction of ethyl vinyl sulfone (EVS) with free mannose (Scheme 2.2). As predicted by the increased nucleophilicity of the anomeric hydroxyl, NMR characterization of the mannose-EVS products suggests that the glycan reacts with EVS predominantly via the anomeric hydroxyl group, resulting in a mixture of α and β products (Figure 2.10). From the ^{1}H NMR spectrum of mannose/EVS reaction products, the peaks at 4.85

ppm and 4.62 ppm are assigned to α- and β- isomers respectively, which is consistent with the reported chemical shift difference (~0.2) between the two anomeric protons.[102] By integration of the area under these two peaks, the ratio of α- and β- isomers is estimated to be 3:1, as predicted by the anomeric effect in aqueous solution. This model reaction suggests that reducing sugars, like mannose, react with the vinyl group on a surface via the more nucleophilic hydroxyl group at its anomeric position (the hemiacetal). In the case of mannose, this reaction showed alpha selectivity, and the resulting immobilized glycan was specifically recognized by Con A.

Scheme 2.2. Model reaction of free mannose with ethylvinyl sulfone (EVS).

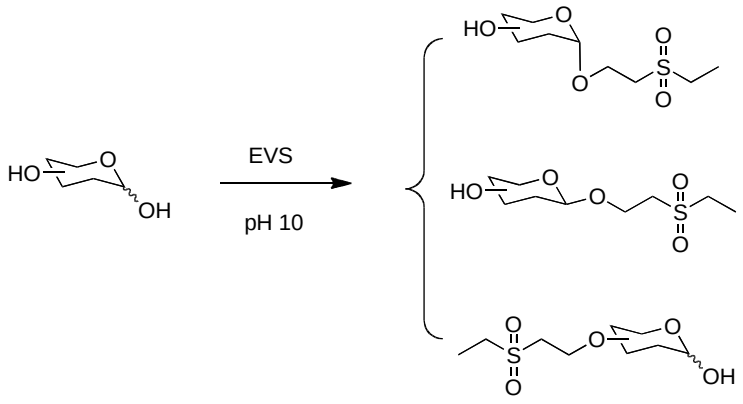

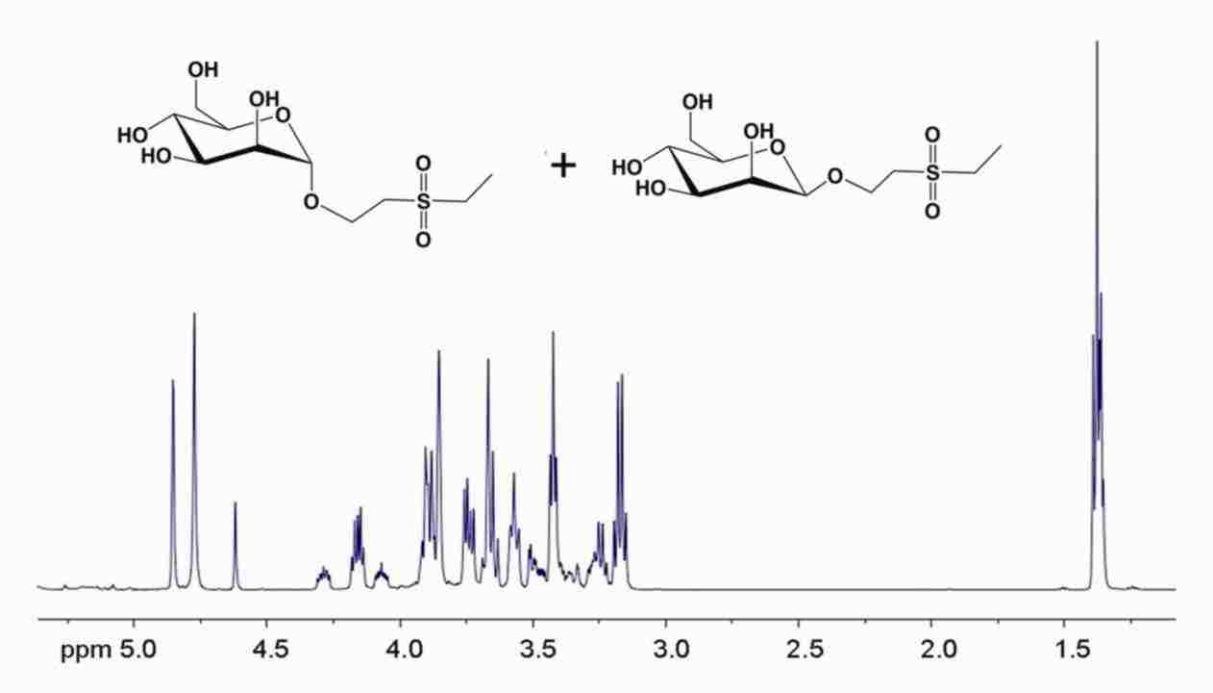

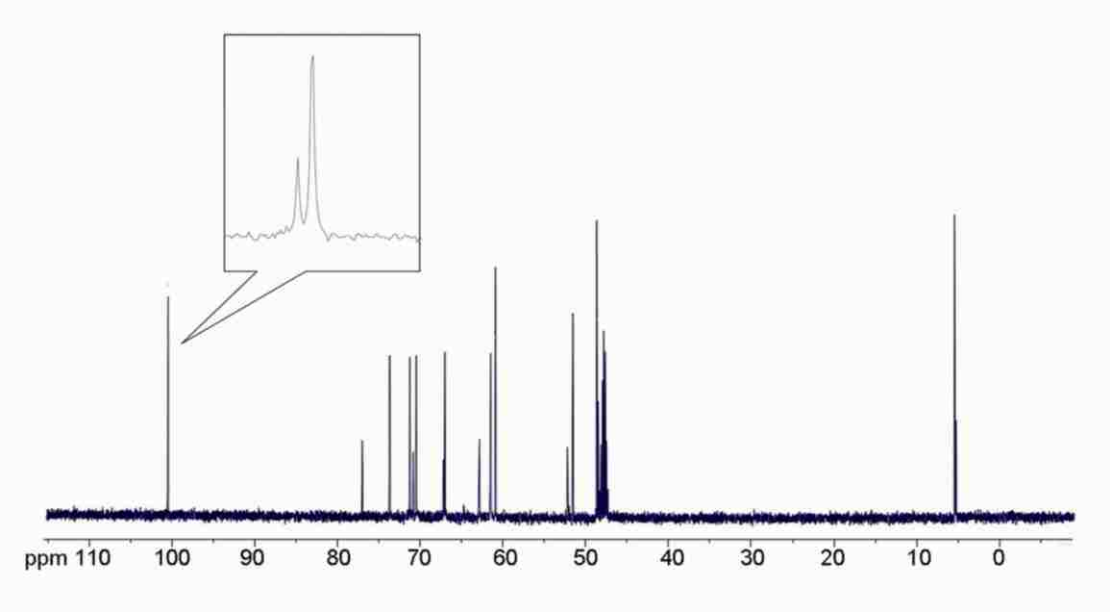

Figure 2.10. ^{1}H and ^{13}C NMR of mannose/EVS reaction products (major fraction), indicating the conjugate contains a mixture of the alpha and beta anomers (α:β = 3:1).

2.4.6 Optimization of glycan microarray printing

The consumption of glycans during immobilization must be minimized in order to preserve precious glycan reagents, as large quantities of pure glycans are difficult to obtain either by separation from natural sources or by chemical synthesis. In this study, a manual microarrayer designed for glass slides was adapted to fabricate carbohydrate microarrays on SPR gold chips. As compared to the 9-element array we used before, this microarrayer enables printing 100 spots on one SPR chip and reduces the printing solution from 2 μl/spot (9-element array) to 10 nl/spot. This microarray could allow detection of 100 binding events in parallel, dramatically increasing the biosensing efficiency.

However, one potential problem of the microarrayer is that printed spots dry very fast during printing, which may deter the chemical reaction between vinylsulfone and nucleophilic groups. To solve this problem, we tested the effects of different printing conditions on the bioactivity of immobilized glycans. Three reagents were added to RNase B solution to reduce evaporation during printing, including Tween-20, glycerol and dimethyl sulfoxide (DMSO). The binding of printed RNase B to Con A was measured by SPRi. The images in Figure 2.11 and 2.12 demonstrate that the printing area of spots with additives is larger than that of buffer alone, and the maximal response to Con A decreases with increases in any of these additives. These results indicate that these additives do not improve the microarray quality, and the buffer solution alone is the best printing condition. The reason for these unexpected results is attributed to the changes in surface tension with added reagents. The glycan density becomes lower when the area of spots increases, resulting in lower binding response. For the spots with buffer alone, they are dried during printing but can be rehydrated after incubating in a humid chamber overnight. Since the reaction still occurs after rehydration, the binding of Con A to the printed RNase B in buffer

alone was detected by SPRi. Therefore, we kept using pH 10 buffer as the printing solution for subsequent experiments.

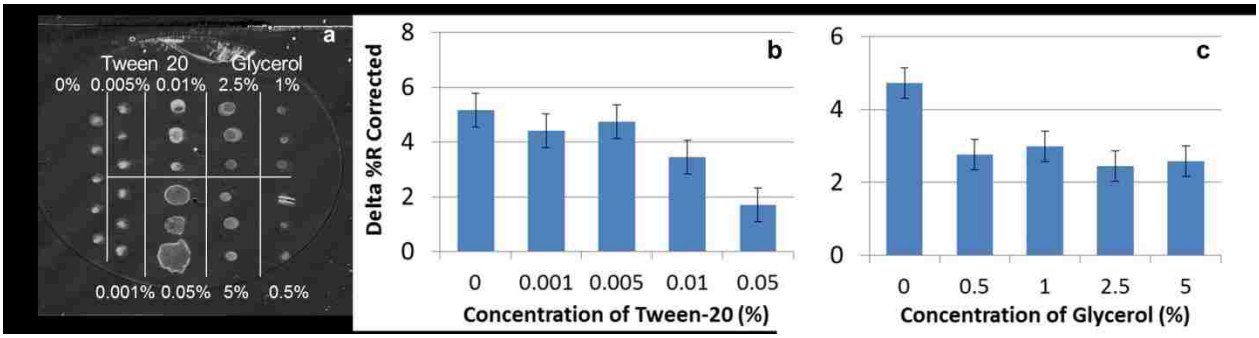

Figure 2.11. (a) SPR image of Con A binding to RNase B on the DVS-activated surface. (b) Maximal Con A response to RNase B as the Tween-20 concentration increases. (c) Maximal Con A response to RNase B as the glycerol concentration increases.

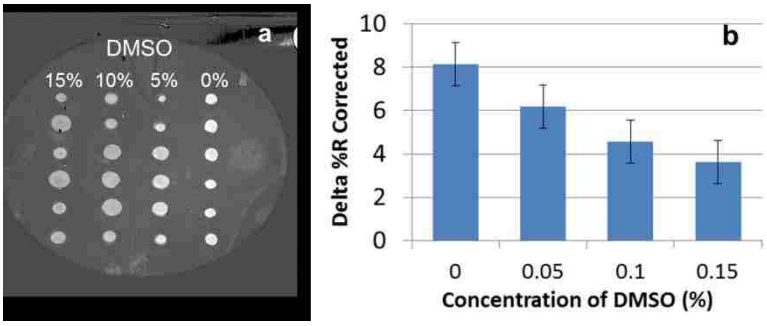

Figure 2.12. (a) SPR image of Con A binding to RNase B on the DVS-activated surface. (b) Maximal Con A response to RNase B as the DMSO concentration increases.

2.5 Conclusions

In this chapter, we demonstrate a simple method to functionalize hydroxyl-terminated surfaces with bioactive glycans and glycoproteins via DVS chemistry. Surface analysis using XPS, ToF-

SIMS and SPRi show that DVS results in covalent immobilization of biomolecules on the activated surface and natural and modified carbohydrates retain their protein-binding specificity. DVS provides a facile method to capture biomolecules with nucleophilic hydroxyl, sulfhydryl or amino groups onto a solid surface, such as biosensors and cellulose for paper-based diagnostics. In the case of the carbohydrate microarray, the direct immobilization of natural sugars dramatically reduces the challenge of glycan modification and will have significant impact on research in the burgeoning field of glycomics by making the array paradigm more amenable to non-synthetic laboratories. The biosensing platform based DVS chemistry will facilitate the study of carbohydrate-mediated host-pathogen interactions.

Chapter 3: A Robust Surface Functionalization Strategy for Silicon Photonic Microring Resonator Biosensors

3.1 Abstract

Silicon photonic microring resonators have established their potential for label-free and low-cost biosensing applications. However, the long-term performance of this optical sensing platform requires robust surface modification and biofunctionalization. In this chapter, we demonstrate a conjugation strategy based on an organophosphonate surface coating and a vinyl sulfone linker to biofunctionalize silicon resonators for biomolecular sensing. To validate this method, a series of glycans, including carbohydrates and glycoconjugates, were immobilized on divinylsulfone (DVS)/organophosphonate-modified microrings and used to characterize carbohydrate-protein and norovirus particle interactions. This biofunctional platform was able to orthogonally detect multiple specific carbohydrate-protein interactions simultaneously. Additionally, the platform was capable of reproducible binding after multiple regenerations by high-salt, high-pH or low-pH solutions and after 1-month storage in ambient conditions. This remarkable stability and durability of the organophosphonate immobilization strategy will facilitate the application of silicon microring resonators in various sensing conditions, prolong their lifetime, and minimize the cost for storage and delivery; these characteristics are requisite for developing biosensors for point-of-care and distributed diagnostics and other biomedical applications. In addition, the platform demonstrated its ability to characterize carbohydrate-mediated host-virus interactions, providing a facile method for discovering new anti-viral agents to prevent infectious disease.

3.2 Introduction

Biosensors allow sensitive and rapid detection of a variety of biomolecular interactions, facilitating basic biomedical research, drug discovery, food and environmental monitoring, and diagnostics.[42, 43] Among the emerging biosensing technologies, silicon photonics – specifically the silicon microring resonator – has gained increasing attention due to demonstrated capabilities in sensitive multiplexed detection, chip-scale integration, and the potential of low-cost mass production using existing silicon fabrication processes.[44, 46, 47, 103] The optical microring resonator platform consists of an array of planar ring-shaped silicon waveguides optically coupled to linear bus waveguides on a silicon oxide insulator. Binding of biomolecules to the ligand-functionalized microring sensor causes small changes in the effective refractive index, resulting in a detectable shift in resonance wavelength.[45] The feasibility of microring resonators for label-free detection of various biomolecules and cells, including proteins, oligonucleotides, and bacteria has been previously demonstrated in the literature.[45, 46]

The dominant strategy for functionalizing silicon devices, including microring resonators, is based on common siloxane chemistries.[47, 48] However, the moisture-sensitivity of silanization and the instability of bound silanes limit the real world use of silicon-based biosensors.[104] The quality of silanized surface coatings strongly depends on the atmospheric moisture content, making standardization and reproducibility difficult.[105] Low surface coverage and hydrolytic instability of silane layers also limit ligand conjugation to, and reproducible detection by, silicon-based biosensors.[104, 106] Furthermore, formation of multi-layer silane networks attenuates the sensitivity and reduces the stability of functional surfaces for biosensing.[107] Therefore, more robust surface functionalization strategies could result in stable and reliable silicon-based biosensors. Recently, organophosphonate self-assembled monolayers (SAMs) have been

employed successfully to modify various inorganic oxide surfaces, such as Al_2O_3[108], TiO_2[109] and SiO_2[110]. The "T-bag" method developed by Hanson et al., involves adsorbing organophosphonic acid to a solid surface, which converts to surface-bound phosphonate at 120-140 ℃.[111, 112] These organophosphonates have superior physicochemical properties. Relative to silanes, phosphonate SAMs can form densely-packed monolayers with higher surface coverage,[111, 112] and are much more stable in both acidic and alkaline solutions.[107, 109, 113] Previous studies have demonstrated the efficacy of phosphonate chemistry in the fabrication of complementary circuits and transistors,[114, 115] modification of DNA biosensors[104, 112] and preparation of cell adhesion substrates.[110, 116, 117] Towards the development of stable and reproducible silicon microring biosensors, we applied organophosphonate SAMs in the modification of this biosensing platform.

The suitability of organophosphonate-modified microring resonators for biosensing applications was demonstrated by examining its ability to detect carbohydrate-mediated host-virus interactions. As we mentioned in previous chapters, carbohydrates play an essential role in various pathogenic processes.[39] Pathogenesis is frequently mediated via the adhesion of pathogens to glycans on the host cell surface. For example, norovirus, a major cause of acute gastroenteritis, recognizes human histo-blood group antigens, which contain well-defined carbohydrate epitopes.[118] Inhibition of these glycan-dependent host-pathogen interactions has been established as a valuable target for drug development. For instance, human milk glycans containing fucosylated carbohydrate moieties can protect infants against diarrhea caused by a variety of bacterial and viral pathogens, including norovirus.[10, 11] These glycans represent a promising new class of anti-microbial agents to prevent infectious disease.[9] The structure and the inhibitory mechanism of many of the human milk glycans are under active investigation.[22]

To meet the urgent need for new anti-infective agents based on human milk glycans, it is necessary to unravel the specific binding patterns between these glycans and pathogens. We propose that the silicon photonic microring resonator provides a versatile label-free and sensitive platform that can advance the study of carbohydrate-mediated host-pathogen interactions.

Herein, an 11-hydroxyundecylphosphonic acid (UDPA) modified silicon microring resonator biosensor was examined for its ability to reproducibly detect glycan-protein/virus interactions. Glycans were immobilized on the organophosphonate-modified sensors via a facile and versatile divinyl sulfone (DVS) conjugation method; DVS can conjugate biomolecules containing nucleophile groups (e.g. hydroxyl, amine and thiol) on hydroxyl-terminated surfaces.[119] In the present study, amine-bearing saccharides and glycoproteins were conjugated to DVS-activated organophosphonates on silicon microrings through an amine-vinyl sulfone. Each surface functionalization step was characterized by X-ray photoelectron spectroscopy (XPS). Time-of-flight secondary ion mass spectrometry (ToF-SIMS) imaging further verified the attachment of a phosphonate film on the silicon microrings. These glycan-functionalized microring resonators were evaluated by their response to well-characterized lectins (glycan-binding proteins); the reproducibility and stability of the bioactive surfaces was subsequently examined under different regeneration and storage conditions. Finally, this biosensing platform was used successfully to screen interactions between glycans and norovirus-like particles, demonstrating the utility of organophosphonate-modified microring resonators for studying carbohydrate-mediated host-virus interactions.

3.3 Materials and Methods

3.3.1 Reagents and Materials

All chemical reagents and bovine serum albumin (BSA) were from Sigma-Aldrich (St. Louis, MO) and were used without further purification. 11-hydroxyundecylphosphonic acid was synthesized as described.[120] Hexafluorobenzamide **1**, mannosyl amino OEG (oligo(ethylene glycol)) **2** and galactosyl amino OEG **3** were provided by Justin Kaplan and Prof. Rodrigo B. Andrade at Temple University. Lacto-N-fucopentaose III-human serum albumin (LNFPIII-HSA, **4**) and H disaccharide-bovine serum albumin (H2-BSA, **5**) were provided by Dr. David Newburg, Boston College. Virus-like particles of norovirus strain VA387 were from Dr. Xi Jiang, Cincinnati Children's Hospital Medical Center. Millipore-filtered water was used for all aqueous solutions and rinsing. Concanavalin A (Con A), Ricinus Communis Agglutinin II (RCA_{60}), Ulex Europaeus Agglutinin I (UEA I) and Lotus Tetragonolobus lectin (LTL) were from Vector Laboratories (Burlingame, CA). Con A was dissolved in HEPES pH 7.4 buffer (10 mM 4-(2-hydroxyethyl)-1-piperazineethanesulfonic acid, 150 mM NaCl, 1 mM $CaCl_2$, 1 mM $MnCl_2$). RCA_{60} and UEA I were dissolved in PBS pH 7.4 buffer (phosphate buffered saline, 10 mM phosphate, 2.7 mM KCl, 137 mM NaCl). LTL was dissolved in HEPES pH 7.5 buffer (10 mM 4-(2-hydroxyethyl)-1-piperazineethanesulfonic acid, 150 mM NaCl, 0.1 mM $CaCl_2$). Culture-well silicone sheets were from Grace Biolaboratories (Bend, OR). Silicon wafers were from Silicon Valley Microelectronics (San Jose, CA).

3.3.2 Silicon microring resonator chips and instrumentation

Silicon microring resonator biosensors and the corresponding analysis instrumentation were manufactured by Genalyte, Inc. (San Diego, CA), as described.[48] Briefly, each biosensor chip

contains an array of 32 individually addressable microring resonators (30 μm in diameter). Of the 32 microring sensors, 24 are exposed for biosensing and 8 are coated with a fluoropolymer-cladding to serve as temperature and vibration reference controls. Figure 1 shows a scanning electron micrograph of a microring and an illustration of the microring cross-section. An external cavity diode laser with a center frequency of 1560 nm was rastered across the biosensor surface to rapidly interrogate individual microring resonators, measuring the resonance wavelength shift for each sensor with ~250 ms time resolution.

3.3.3 Functionalization of the silicon microring resonator chips

Modification with organophosphonic acid. Chips were cleaned by immersion in freshly prepared piranha solution (1:1 30% H_2O_2: 98% H_2SO_4) for 15min, rinsed with water, and dried in a stream of nitrogen. (Caution! Piranha solution is extremely dangerous; it can explode or catch fire when contacted by organic compounds.) Chips were modified with 11-hydroxyundecylphosphonic acid (UDPA) using the "T-BAG" method.[111] Briefly, silicon chips were held vertically by clips and immersed in a 1 mM solution of UDPA in anhydrous tetrahydrofuran. The solvent was allowed to evaporate at room temperature over 3 h, until the level of the solution fell below the silicon chips. The coated silicon chips were transferred to an oven and heated at 120 °C overnight. Following heating, the chips were washed with sonication in 0.5 M K_2CO_3 in 2:1 ethanol/water for 20 min to remove any multilayer UDPA, rinsed with water and dried under a stream of nitrogen.

Immobilization of glycans. Glycan immobilization was accomplished using DVS chemistry.[119] The organophosphonate modified silicon chips were immersed in 10% DVS (v/v, 50 mM carbonate buffer, pH 11) solution for 1 h at ambient temperature. After activation, the silicon chips were rinsed with water and dried by a stream of nitrogen. A silicone mask with four wells

was placed on top of the silicon chips, exposing four biosensing microrings in each well for functionalization. 16 of the 24 biosensing microrings were functionalized with glycans, and the remaining 8 rings were used as BSA-passivated controls. One microliter of each glycan solution (5 mM for **2** and **3**, 0.5 mg/ml for **4** and **5,** Scheme 1) in pH 10 carbonate buffer were spotted into each well and incubated in a 75% relative humidity chamber. After 16 h incubation, solutions in each well were removed, and the chips were immersed in a BSA solution (0.1% w/v, pH 8.5) for 2 h to passivate the surface. Finally, the chips were rinsed with water and dried under a stream of nitrogen. A scheme demonstrating the process of functionalizing a DVS-organophosphonate-modified chip was shown in Scheme 3.1.

Scheme 3.1. Process of functionalizing a DVS-organophosphonate-modified silicon microring chip for detection of glycan-protein/virus particle interactions.

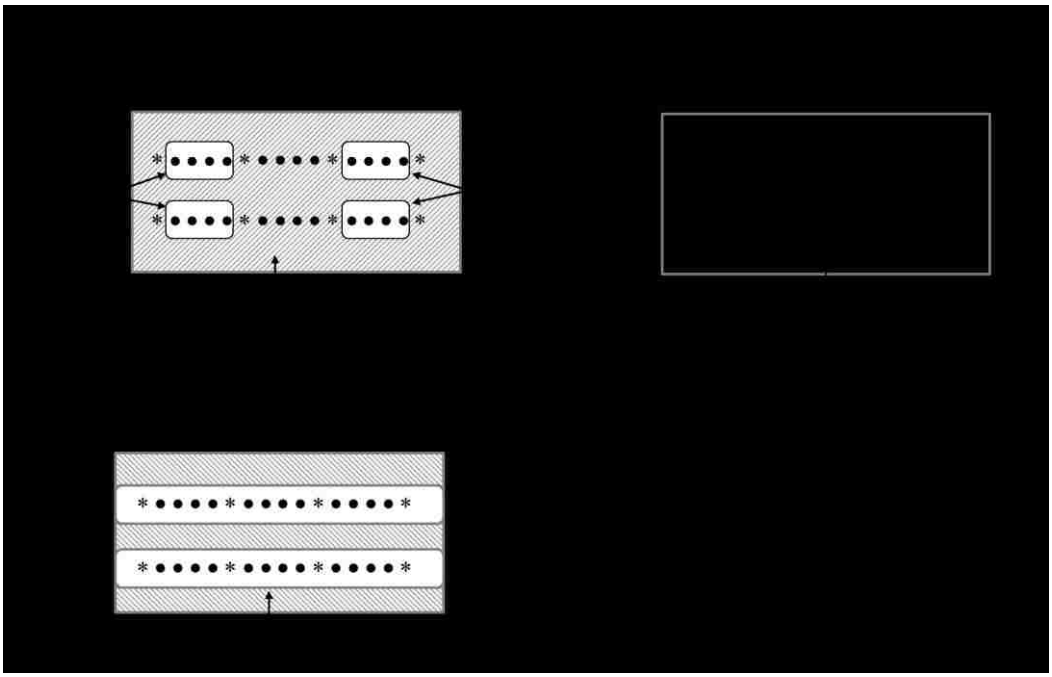

3.3.4 Surface characterization

XPS analysis. To facilitate surface analysis, silicon wafers were cleaned, modified with UDPA and activated by DVS using the same procedure described above. Hexafluorobenzamide **1**, containing six fluorine atoms and a primary amine, was immobilized on the DVS-activated silicon wafer to mimic the glycan immobilization procedure. XPS composition data were acquired on a Kratos AXIS Ultra DLD instrument equipped with a monochromatic Al-Kα X-ray source ($h\nu$ = 1486.6 eV). XPS data were collected at 0° takeoff angle in the hybrid mode with approximately 10 nm sampling depth, using a pass energy of 80 eV. Three spots on two or more duplicate samples were analyzed. Reported compositional data were averaged over multiple spots. Data analysis was performed on the *CasaXPS* software (Casa Software Ltd.).

ToF-SIMS analysis. ToF-SIMS data was acquired on an ION-TOF 5-100 instrument (ION-TOF GmbH, Münster, Germany) equipped with a 25 KV liquid metal ion gun source. Ion images were acquired using Bi^{3+} primary ions in the high current bunched mode (i.e., high mass resolution mode). These images were collected by rastering the beam over a 100 x 100 μm^2 area on the sample surface and keeping the fluence below the SIMS static limit of $1x10^{12}$ ions/cm^2. All images contained 128 x 128 pixels. A low-energy electron beam was used for charge compensation. The mass resolution ($m/\Delta m$) of negative secondary ion spectra was typically between 6000 and 7500 for the m/z = 25 peak. Mass calibration was applied by using CH^-, OH^- and C_2H^- peaks.

3.3.5 Detection of glycan-mediated interactions by organophosphonate-modified silicon microring resonators

Glycan-containing chips, functionalized by the DVS/organophosphonate method, were loaded into a custom two-channel microfluidic flow cell defined by a laser cut gasket (Genalyte, Inc.; San Diego, CA). Negative-pressure syringe pumps were used to draw analyte solutions over the sensor surface. The flow rate was set to 10 μl/min. A typical binding experiment was preceded by flowing buffer solution over the surface for 10 minutes to stabilize the sensor response. Lectins or virus-like particle solutions were passed over the sensor for 20 min, followed by another 20 min of buffer to examine dissociation. After acquisition of association/dissociation curves, regeneration solutions were passed over the analyte-bound surface for 5 minutes, and then buffer solution was flowed over the surface to reestablish the baseline. To validate the bioactivity of the immobilized glycans, a panel of the following lectins were used: Con A (binds to α-linked mannose)[121], RCA_{60} (binds to β-linked galactose)[122], UEA I (binds to α-1,2-linked fucose)[123] and LTL (binds to both α-1,2- and α-1,3-linked fucose)[22]. HEPES pH 7.4 buffer was used for Con A binding, PBS (pH 7.4) was used for RCA_{60} and UEA I binding, and HEPES pH 7.5 buffer was used for LTL binding. Unless otherwise stated, lectins were used at 500 nM. Norovirus particles were used in pH 7.4 PBS at 0.25 μg/ml to 20 μg/ml. Three regeneration solutions were used to strip proteins from lectin-bound chips: 8 M urea; pH 2.0 glycine buffer (10 mM glycine, 160 mM NaCl, HCl was used to adjust pH); and 10 mM NaOH. Virus particle-bound chips were regenerated by 8 M urea. The binding curves are normalized to temperature reference control microrings and referenced to the BSA-passivated microrings to control for thermal effects and non-specific binding. The data are presented as the average ± standard deviation for a set of 4 identical microrings.

3.4 Results and Discussion

3.4.1 Surface modification of silicon microring resonators

The stepwise organophosphonate-based procedure to modify a silicon oxide surface is illustrated in Scheme 3.2, and the glycan modified microring is demonstrated in Figure 3.1. Piranha-cleaned silicon substrates were modified with UDPA using the "T-BAG" method;[111] phosphonate head groups form a tri-dentate bond with silicon oxide on the substrate.[124] As shown in the XPS elemental composition results (Table 3.1), a phosphorous signal was detected on the organophosphonate SAM-modified sample, but was absent in the bare silicon substrate. As compared to previous organophosphonate SAM studies, the relative percentage of phosphorous observed is lower than the reported value (0.8 atom %).[107] However, this result was expected, as we adopted an expedient one-cycle SAM deposition approach, instead of three cycles as previously reported. Using the "T-bag" method, the organophosphonic acid-adsorbed silicon substrates must be heated in order to covalently deposit onto silicon oxide;[124] however, the repeated thermal cycling may cause functional loss of silicon waveguide-based biosensors. Thus, the single-cycle deposition was selected to minimize this possible damage. It has been noted that one-cycle deposition may not be sufficient for 100% surface coverage.[104] But for the purpose of carbohydrate-protein binding studies, a low density organophosphonate film is sufficient for surface modification.[125]

ToF-SIMS imaging analysis was conducted to directly characterize organophosphonate-modified microrings. In the negative ion spectra, we observed Si^-, SiO^- and SiO_2^- peaks as well as the peaks representing organophosphonate fragments, including PO_2^- and PO_3^-. As shown in Figure 3.2, the ring structure of the device is clearly distinguished on the SiO_2^- and PO_3^- ion images. In

combination with the XPS composition analysis, the ToF-SIMS data further verified the successful deposition of organophosphonate onto the silicon microrings.

Scheme 3.2. Functionalization of silicon substrate using 11-hydroxyundecylphosphonic acid (UDPA) and divinyl sulfone (DVS) linking chemistry. The molecules immobilized on silicon microrings include: Hexafluorobenzamide (**1**), mannosyl amino OEG (**2**), galactosyl amino OEG (**3**), LNFPIII-HSA (**4**), H2-BSA (**5**). Abbreviation of carbohydrate residues in **4** and **5** represents: Gal, galactose; Fuc, fucose; GlcNAc, N-acetylglucosamine; Glc, glucose.

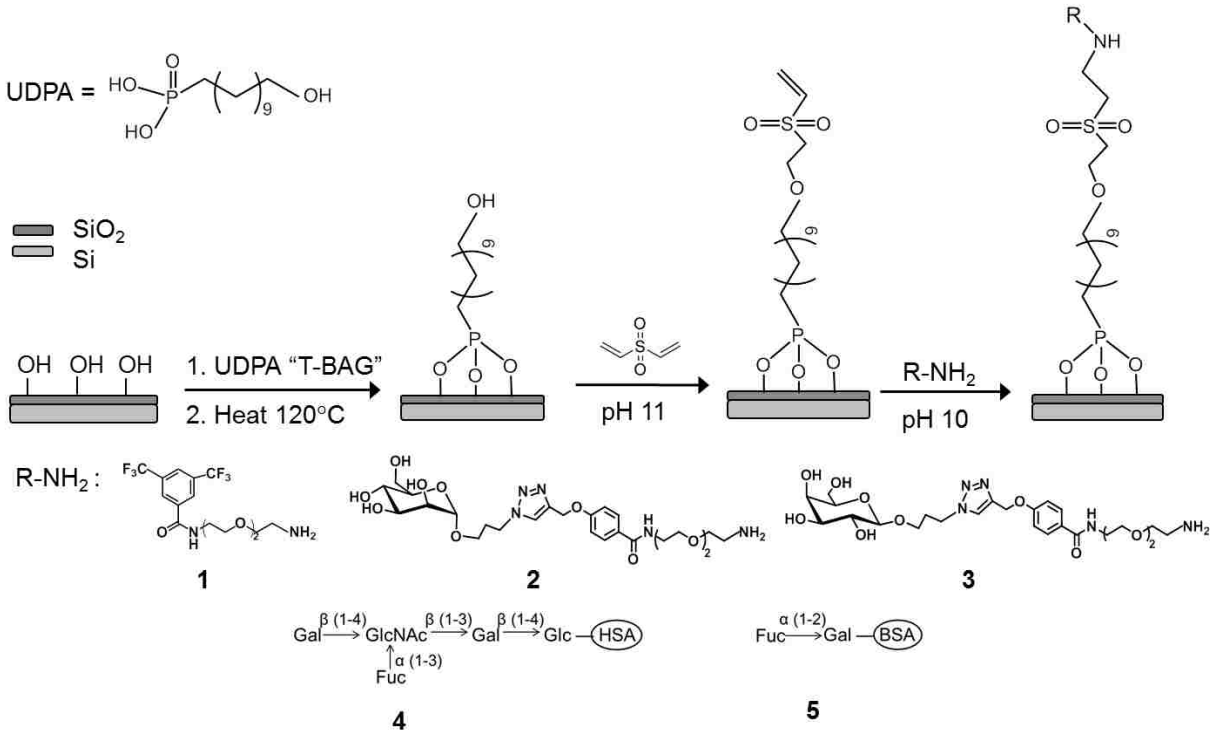

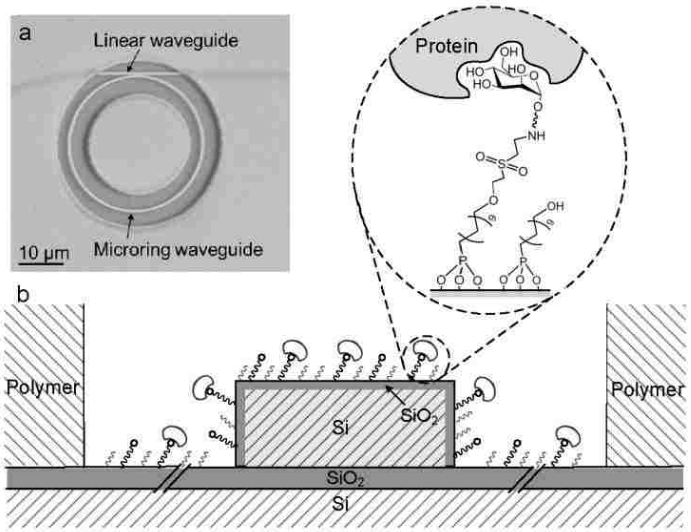

Figure 3.1. (a) SEM image of a microring resonator; (b) Cross-section of a glycan-modified organophosphonate/DVS microring resonator.

Table 3.1. Relative compositions of organophosphonate-functionalized silicon substrates determined by XPS.

	Silicon	PO_3-C_{11}-OH	PO_3-C_{11}-OH + DVS	PO_3-C_{11}-OH + DVS + **1**
Si 2p	48.9 ± 0.8	46.6 ± 0.9	47.4 ± 1.4	33.0 ± 0.3
C 1s	12.4 ± 1.6	20.8 ± 0.4	18.2 ± 1.6	28.4 ± 0.4
O 1s	38.7 ± 0.8	32.5 ± 0.5	34.1 ± 0.4	29.6 ± 0.4
P 2s	n/d	0.3 ± 0.1	0.3 ± 0.1	0.2 ± 0.1
F 1s	n/d	n/d	n/d	6.6 ± 0.5
N 1s	n/d	n/d	n/d	2.2 ± 0.1

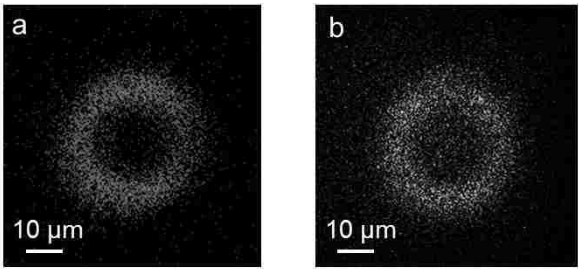

Figure 3.2. ToF-SIMS images of organophosphonate-modified silicon microrings. (a) SiO_2^- ions; (b) PO_3^- ions.

After deposition of the organophosphonate layer, we utilized DVS, a homobifunctional linker, to link one end to the UDPA hydroxyl moiety, and the other end to the amine-bearing monosaccharides and glycoconjugates, thereby fixing them covalently to the silicon microrings. In the XPS spectra, sulfur from the DVS molecule cannot be used for demonstrating the immobilization of DVS on the surface, due to the proximity of S2p peak to the Plasmon peak of silicon. Therefore, we used a fluorine tagged molecule **1** to facilitate characterization. Hexafluorobenzamide **1** with a pendant amino functional group was used to mimic the reaction between amine-bearing glycans and the DVS-activated surface. Following immobilization of **1** on the DVS-activated silicon substrate, fluorine and nitrogen peaks (Table 3.1) appeared with a compositional ratio of 3:1, which is in good agreement with their stoichiometric ratio in one fluorine-tagged molecule. Due to the signal attenuation of phosphorous, which is buried under a long alkane chain, it is difficult to quantify the coupling efficiency of this method. However, based on our previous study on DVS chemistry,[119] we estimated that ~6% of the phosphonate

moieties are functionalized with aminated molecules. Thus, silicon oxide can be functionalized with amine-bearing biomolecules through phosphonate modification and DVS conjugation.

3.4.2 Carbohydrate-protein interactions detected by silicon microring resonators

Two functionalized monosaccharides (mannose **2** and galactose **3**) were immobilized onto DVS/organophosphonate-modified silicon microrings to assess the bioactivity of the functional biosensor. On one sensor chip, four micorings were selectively functionalized with mannose and another four with galactose to realize simultaneous dual detection. The availability of immobilized sugars to ligands was tested by protein-binding experiments. Con A lectin specifically binds to α-mannose[121] while RCA_{60} recognizes β-galactose[122]. When Con A is passed over the sensor surface, only the microrings functionalized with mannose exhibited binding to this lectin while the microrings with galactose did not show a specific response (Figure 3.3(a)). Conversely, in the presence of RCA_{60}, only the microrings functionalized with galactose exhibited a positive response (Figure 3.3(b)). Thus, silicon microring resonators functionalized with bioactive carbohydrates through organophosphonate modification and DVS activation are able to detect specific and multiple binding events on a single chip.

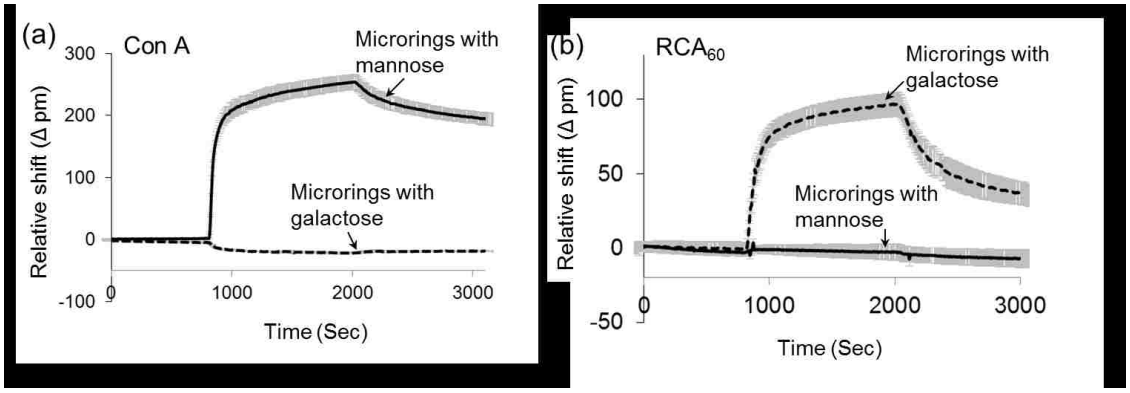

Figure 3.3. Binding response of microrings functionalized with **2** and **3** to (a) Con A and (b) RCA_{60} .

3.4.3 Stability and reproducibility of carbohydrate-modified silicon microring resonators

A robust and reusable biosensing system requires the ability to remove surface-bound analytes (e.g., proteins and cells) after each binding experiment without losing the underlying ligand functionality. Many common regeneration solutions rely on stringent conditions or reagents to disrupt analyte-ligand interactions, including high- or low-pH buffers and high-concentration chaotropic salts, which can damage the ligand-functionalized layer on silicon chips and subsequently deteriorate the performance of the biosensor.[126] To assess the potential degradation of performance after many cycles of use, Con A binding to mannose-functionalized microring resonators was measured after a series of binding-regeneration cycles. Three commonly-used solutions (8M urea, pH 2.0 glycine buffer and 10 mM NaOH), which represent typical high-salt, low-pH and high-pH regeneration conditions, were used to strip surface-bound proteins following analyte capture. The sensing response (maximum relative wavelength shift after 20 min exposure to Con A) of a mannose-functionalized microring sensor was examined after each binding-regeneration cycle. Binding between Con A and immobilized mannose is highly reproducible after the 8 M urea wash (Figure 3.4). After one binding-regeneration cycle, the microring resonator retained ~98% bioactivity (Table 3.2), and after 20 binding-regeneration cycles over 80% of the initial response. Similar binding curves were also obtained after pH 2.0 glycine and 10 mM NaOH regeneration (Figure 3.5). The sensing response remained 88% after regeneration by pH 2.0 glycine and 97% after 10 mM NaOH (Table 3.2). High-pH solutions are frequently required to regenerate whole-cell bound surfaces, and often damage silane-modified surfaces.[109, 127] Remarkably, 10 mM NaOH is not harmful to the organophosphonate-modified sensors.

Long-term stability of the bioactive sensor surface under ambient conditions is critical for the utility of a distributed reusable biosensor. To explore the ability of the biofunctional organophosphonate-modified sensor to retain bioactivity, a mannose-functionalized microring chip was exposed to the atmosphere for 1-month at room temperature and tested for its Con A-binding. The relative response of these stored microring resonators to Con A was ~94% of the original value (Table 3.2).

The organophosphonate layer, already established as a robust modification method for silicon oxide,[110] confers remarkable stability of carbohydrate/organophosphonate-modified sensors towards both concentrated-salt/extreme-pH, and prolonged storage under ambient conditions. The data validate the DVS/organophosphonate approach towards producing biofunctional sensors capable of reproducible detection, prolonged lifetime and adaptability to a variety of experimental conditions. These capabilities support the future application of silicon-based biosensors for point-of-care diagnostics, environmental monitoring and other applications.

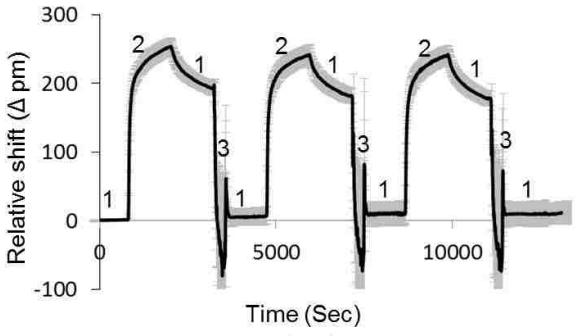

Figure 3.4. Reproducible binding response of the microrings functionalized with mannose to Con A after urea regeneration. 1. HEPES buffer; 2. 500 nM Con A in HEPES; 3. 8 M urea. All data are presented as the average ± standard deviation (n = 4) and are referenced to BSA-passivated microrings.

Table 3.2. Retained bioactivity of the microrings functionalized with mannose to Con A (500 nM) after one binding-regeneration cycle and after 30-day storage at ambient condition.

	After regeneration (day 0)			After
	8M Urea	pH 2.0 glycine	10 mM NaOH	30-day storage[b]
Response retained (%)[a]	98 ± 1	88 ± 2	97 ± 2	94 ± 3

[a.] Normalized to the sensing response before regeneration on day 0.

[b.] Room temperature, exposed to atmosphere.

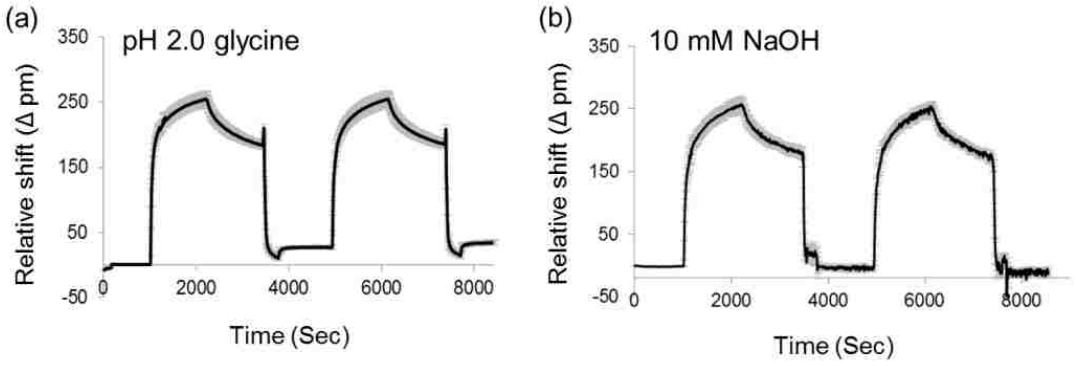

Figure 3.5. Reproducible binding response of the microrings functionalized with mannose to Con A after (a) pH 2.0 glycine and (b) 10 mM NaOH regeneration. The binding curve is presented as the average ± standard deviation (in gray, n = 4) and is referenced to the BSA-passivated microrings.

3.4.4 Glycoconjugate-virus interactions measured by the microring resonator biosensor

The ability of the DVS/organophosphonate microring resonator to measure glycan-virus interactions was evaluated. Carbohydrates on host cell surface are used by many pathogens as

initial recognition and attachment receptors.[14] Human histo-blood group antigens (HBGAs) are complex glycans present on the surface of red blood cells and epithelial cells, or as free antigens in biological fluids.[128] These HBGAs can be recognized by noroviruses, initiating binding and pathogenesis.[7] Previous studies have demonstrated that human milk glycans possessing HBGAs can block the binding of noroviruses to their host-cell receptors.[10] However, the specific molecules in human milk responsible for this anti-infectious activity have not been identified.

To elucidate these norovirus-glycan interactions, the organophosphonate-modified silicon microring resonators were employed to investigate the specificity of norovirus adhesion to select human milk glycans. Virus-like particles constructed from the recombinant outer capsid proteins of norovirus strain VA387 were screened for binding to two neoglycoproteins, LNFPIII-HSA (**4**) and H2-BSA (**5**). The glycoproteins used for this study were prepared from a core albumin protein (human serum or bovine serum, respectively), to which covalently-bound carbohydrate moieties from human milk (lacto-N-fucopentaose III (LNFPIII) and H disaccharide (H2)) are attached. LNFPIII contains α-1,3-linked fucose while H2 possesses α-1,2-linked fucose.[129] Conjugation of these glycoproteins onto the DVS/organophosphonate-modified sensor was accomplished through the reaction between the surface-bound vinyl sulfone and an amine on the protein carriers. Two fucose-binding lectins, UEA I and LTL, were used to evaluate the bioactivity of the immobilized glycoconjugates. UEA I recognizes α-1,2-fucose residues[123] while LTL binds to both α-1,3- and α-1,2-linked fucose residues[22]. As expected, the microrings functionalized with H2-BSA but not LNFPIII-HSA responded to UEA I, while both types of functionalized microrings bound LTL (Figure 3.6 (a) and (b)). Control microrings functionalized with HSA or BSA did not respond to either lectin.

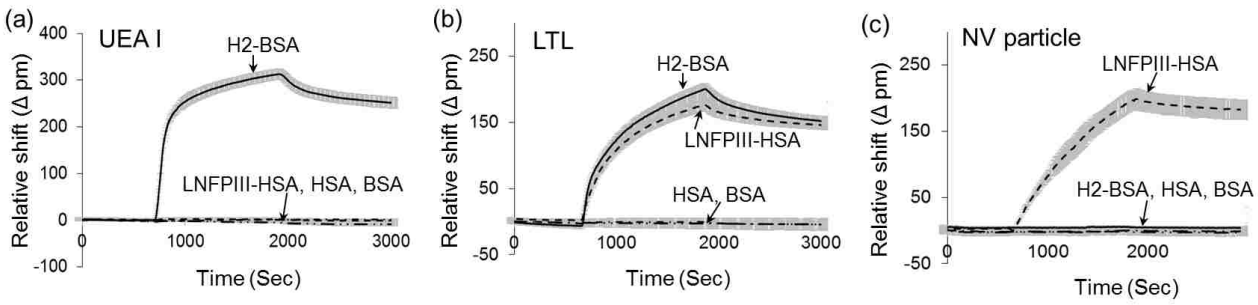

Figure 3.6. Binding response of microring resonators functionalized with H2-BSA, LNFPIII-HSA, HSA and BSA to (a) UEA I (500 nM), (b) LTL (500 nM) and (c) Norovirus (NV) VA387 particles (10 μg/ml). The data are presented as the mean ± standard deviation (n = 4) and are referenced to BSA-passivated microrings.

By presenting glycans on microring resonators, the carbohydrate-functionalized biosensing platform is able to model the host cell surface for characterizing host-virus interactions. The norovirus-like particles used in this study are a complex of 24 protruding domains of VA387 capsid protein, with a total molecular weight of ~850 KDa.[7] The novovirus capsids are organized in octahedral symmetry and exhibit the native virus receptor-binding specificity.[7] Microrings functionalized with LNFPIII-HSA bound to norovirus particles (Figure 3.6 (c)), while microrings with H2-BSA, HSA and BSA showed no binding. Thus, glycan-functionalized microring resonators are able to detect specific binding of norovirus particles to the glycans with LNFPIII moieties.

Glycan-modified biosensors are capable of interrogating carbohydrate-mediated host-pathogen interactions, facilitating the study of fundamental biochemical and molecular mechanisms of

pathogenesis. Antibody-functionalized sensors contrast this approach, where detection is the primary goal of the functional device. The limit of detection (LOD) of antibody-functionalized microring resonators, similar to those used in this study, have been reported in sub-ng/mL range, which is comparable to other label-free biosensors, such as surface plasmon resonance.[130] However, norovirus-glycan binding affinities are several orders of magnitude weaker than antibody-virus binding. As a result, the carbohydrate-functionalized sensors are expected to have only modest LOD. Within the detection range in this study, we observed a linear relationship between the initial slope of binding and the concentration of norovirus particles (Figure 3.7). The experimental LOD for norovirus particles is estimated to be 250 ng/mL, which is sufficient for the analysis of carbohydrate-mediated norovirus binding. However, if detection were the objective, antibody-mediated capture should be employed.

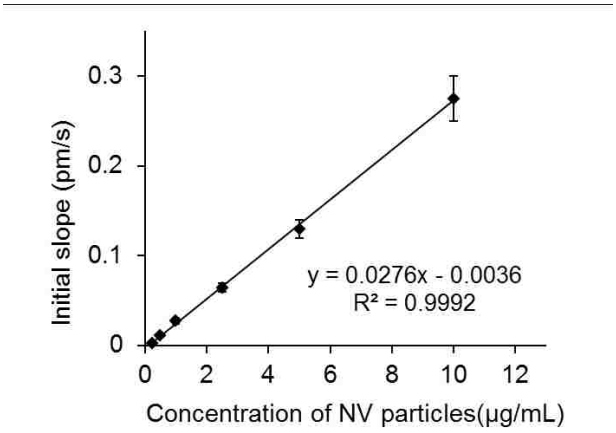

Figure 3.7. Linear curve-fitting of the initial slope of LNFPIII-HSA—norovirus (NV) particle binding curves and the concentration of virus particles. The data are presented as the mean ± standard deviation, n = 4.

3.5 Conclusions

This study demonstrated the versatility of an organophosphonate-based strategy for covalent modification of silicon photonic microring resonators, and validated the capability of this robust biosensing platform for label-free detection of glycan-protein and glycan-virus interactions. Glycans, including monosaccharides and glycoprotein conjugates, were immobilized on organophosphonate-modified microring sensors using a divinyl sulfone (DVS) linking chemistry, and the conjugation strategy was validated by XPS and ToF-SIMS analysis. Using this method, an array of microrings were functionalized with multiple glycans and used to detect simultaneous orthogonal binding events. This organophosphonate-modified biosensing platform exhibited remarkable stability and reproducibility after concentrated salt, high- and low-pH regeneration and long-term storage in ambient conditions. The robustness of this surface functionalization method could be useful to advance silicon microring resonators towards practical applications as portable and reusable devices and also facilitate multiplexed detection of biomolecules and cells for drug discovery, environmental monitoring as well as basic biomedical research. This study presents the first example of using organophosphonate-modified microring resonators to characterize glycan-virus particle interactions, demonstrating the potential of this platform for screening carbohydrate-mediated host-pathogen interactions and discovering new carbohydrate-based prophylactics and therapeutics.

Chapter 4: Characterization of the Anti-viral Activity of Human Milk Glycans against Norovirus-Host Receptor Interactions

4.1 Abstract

Human milk glycans are promising inhibitors against norovirus infection. However, the detailed structures of these glycans and their interactions with norovirus have not been well characterized. In this chapter, we employed the surface plasmon resonance (SPR) biosensor and glycan microarrays to identify the glycans that bind to different strains of norovirus (VA387 and Norwalk) and examined their inhibitory effects on norovirus-host receptor interactions. The results demonstrate that the VA387 strain binds to two types of glycoconjugates, while the Norwalk strain interacts with a different set of glycoconjugates and oligosaccharides. Furthermore, the results from SPR competitive binding assays indicate that several norovirus-binding glycans are able to inhibit norovirus-host receptor interactions. The structures of these anti-viral glycans vary between two norovirus strains. A glycoconjugate with multiple carbohydrate moieties is required for VA387-host receptor inhibition, whereas both oligosaccharides and glycoconjugates are able to inhibit Norwalk-host receptor binding. Our findings from this chapter provide useful information for designing glycan-based agents to prevent norovirus-caused diarrheal disease.

4.2 Introduction

Norovirus has been known as a leading cause of acute gastroenteritis.[131] It affects over 20 million people of all ages every year in the United States.[5] Due to the lack of specific treatment or vaccine, norovirus infection results in severe illness or death among infants, the elderly and immunocompromised patients.[6, 132] In recent years, extensive studies have been focused on understanding the mechanism of norovirus infection and developing anti-viral drugs.[131-135] Previous studies have demonstrated that norovirus initiates pathogenesis through the adhesion of their capsid proteins to the host receptors, which are histo-blood group antigens (HBGAs) on the mucosal surface of the host gastrointestinal tract.[6] As the structures of HBGAs vary among individuals with different blood types and secretor statuses, various strains of norovirus demonstrate a wide spectrum of binding specificities to their host receptors.[16, 118, 134] For instance, the Norwalk strain recognizes A and O secretors, but not B secretors and nonsecretors; while the VA387 strain binds to all A, B and O secretors.[16] Based on these mechanism studies, researchers have focused on developing strategies to disrupt norovirus-HBGA interactions in order to prevent norovirus infection.[7]

As HBGAs contain complex carbohydrate structures, a variety of compounds bearing HBGAs or similar oligosaccharide structures have been synthesized and tested for their inhibition against norovirus-host receptor interactions.[136-138] However, the complexity of chemical synthesis and potential side effects of artificial compounds limit the application of these agents as real anti-viral drugs. In recent years, more and more efforts have been focused on developing norovirus inhibitors from natural resources. Human milk glycans are one of the natural anti-norovirus agents discovered recently. Human milk is rich in fucosylated glycans, which have analogous structures to HBGAs.[11] Previous studies have reported that the glycosylated components in

human milk can bind to norovirus, thus blocking the adhesion of norovirus to HBGAs in saliva.[10, 23, 139] By separating human milk into fractions with different molecular weight, Jiang *et al.* further demonstrated that a glycosylated component with high molecular weight (1.3-2.0 $\times 10^6$ Da) inhibited norovirus binding to HBGAs.[23] Deglycosylation of this fraction induced loss of its inhibitory function.[23] This study suggests that both the carbohydrate moiety and high molecular weight carrier are required to inhibit norovirus-receptor binding. However, given the complex structures of hundreds of glycans in human milk, it has been challenging to identify the structures of the active glycans that are responsible for norovirus inhibition.

In this chapter, we employed a high-throughput biosensing platform consisting of a surface plasmon resonance imaging (SPRi) biosensor and glycan microarrays to unravel the binding specificities of two norovirus strains to a panel of glycans presenting human milk carbohydrate epitopes. SPR is a label-free biosensor for detecting biomolecular interactions occurring at a metal/dielectric interface (e.g., gold/water).[140] Without tedious procedures for labeling analytes, SPR can provide direct binding results as well as inhibitory information with high sensitivity and selectivity.[141] To apply SPR in characterizing carbohydrate-norovirus interactions, a glycan microarray containing all the molecules of interest were printed on one SPR chip via a divinylsulfone (DVS)-based immobilization method.[119, 124, 142] Two of the most common strains of norovirus (VA387 and Norwalk) were screened in this study. Using direct SPR binding assays, the specific glycans that bind to either of the norovirus strains were identified. Furthermore, the inhibitory activity of some glycans against norovirus-host receptor interactions was characterized by SPR competitive binding assays. This study provides valuable information for understanding the inhibitory mechanism of human milk glycans, and demonstrates the potential of using the

norovirus-binding glycans as anti-viral drugs or food additives to protect people from norovirus infection.

4.3 Materials and Methods

4.3.1 Reagents and Materials

All chemical reagents and bovine serum albumin (BSA) were from Sigma-Aldrich (St. Louis, MO) and were used without further purification. *Lotus Tetragonolobus* lectin (LTL) and *Ricinus Communis* Agglutinin I (RCA_{120}) were from Vector Laboratories (Burlingame, CA). All neoglycoproteins were prepared[143] by Dr. Vladimir Piskarev, INEOS, Moscow, Russia: lacto-N-fucopentaose III-human serum albumin (LNFP III-HSA), H disaccharide-bovine serum albumin (H2-BSA), lacto-N-tetraose-BSA (LNT-BSA), Lactose-BSA (Lac-BSA), Lacto-N-fucopentaose I-BSA (LNFP I-BSA), Lacto-N-neodifucohexaose I-BSA (LNnDFH I-BSA), Lacto-N-difucohexaose I-BSA (LNDFH I-BSA), 2'-Fucosyllactose-BSA (2'FL-BSA). Glycine-oligosaccharide derivatives (H2-Gly, 2'FL-Gly, 3'-Fucosyllactose (3'FL)-Gly, LNT-Gly, lacto-N-*neo*tetraose (LNnT)-Gly, Lac-Gly, LNFP I-Gly, LNFP III-Gly, LNDFH I-Gly, lacto-N-fucopentaose II (LNFP II)-Gly, lactodifucotetraose (LDFT)-Gly, and difucosyllacto-N-hexaose(a) (DFLNHa)-Gly were synthesized[144] by Drs. Leonid M. Likhosherstov, Olga S. Novikova, and Vladimir E. Piskarev, Russian Academy of Sciences, Moscow, Russia. Free 2'FL was synthesized by Glycosyn, Inc. (Medford, MA). Virus-like particles of norovirus strains (VA387 and Norwalk) and biotin-polyacryamide (PAA)-blood group antigen (A, B and H3) conjugates were provided by Dr. Xi Jiang, Cincinnati Children's Hospital Medical Center, OH. The procedure to derive virus-like particles was described previously.[7]

4.3.2 Functionalization of SPR chips with human milk glycans

DVS chemistry. SPR gold chips were functionalized with 11-mercaptoundecanol and activated with DVS, as described in section 2.3.3. Human milk glycoproteins (1 mg/ml) and oligosaccharide-glycine derivatives were dissolved in pH 10 carbonate buffer and printed on the DVS-activated SPR chip using a manual microarrayer (V&P Scientific, Inc., CA). The printed chip was incubated in a 75% relative humidity chamber overnight. After incubation, the chip was immersed in BSA solutions (1 mg/ml in pH 8.5 buffer) for 1 h to passivate the surface, subsequently rinsed with water and dried under a stream of nitrogen.

Biotin-streptavidin method. To immobilize biotin-PAA-blood group antigens on the SPR chip surface, a biotin-streptavidin sandwich method was used. SPR gold chips were immersed in a biotin-BSA (0.1 mg/ml, PBS pH 7.4) solution for 2 h, then rinsed with water and dried under a stream of nitrogen. Streptavidin (50 μg/ml in PBS pH 7.4) solution was spread on the biotin-BSA-modified chip and incubated for 1 h. The chip was rinsed with water and dried under a stream of nitrogen. A(tri)-, B(tri)- and H3(tri)saccharide-PAA-biotin (0.1 mg/ml, PBS pH 7.4) were printed on biotin-BSA-streptavidin-modified chips using the manual microarrayer and incubated overnight. The carbohydrate-modified chip was passivated with BSA-biotin (0.1 mg/ml, PBS pH 7.4) for 1 h, rinsed with water and dried under a stream of nitrogen.

4.3.3 Validating the bioactivity of immobilized glycans by SPRi

Glycan-specific protein binding was performed on a SPRimagerII (GWC Technologies). The SPRimagerII was operated at room temperature using a standard flow cell and a peristaltic pump (BioRad-EconoPump) at 100 μL/min. Fucose-binding lectin LTL in HEPES buffer (10 mM 4-(2-hydroxyethyl)-1-piperazineethanesulfonic acid, 150 mM NaCl, 0.1 mM $CaCl_2$) was used at 2 μM,

and galactose-binding lectin RCA120 in PBS buffer (phosphate buffered saline, 10 mM phosphate, 2.7 mM KCl, 137 mM NaCl) was used at 500 nM. Anti-lewis a and anti-lewis b antibodies in PBS were used at a dilution of 1:200. In a typical binding experiment, a buffer solution was first flowed over the glycan-functionalized surface for ~10 minutes to stabilize the baseline signal, followed by passing a lectin/antibody solution over the surface for 5~8 minutes. Then the buffer solution was flowed onto the surface again for dissociation for another 10 minutes. 8 M urea was used to regenerate protein-bound surfaces. All the binding curves were normalized by subtracting the background signal, represented by the area modified with BSA.

4.3.4 Detection of human milk glycan-norovirus particle interactions by SPRi

After verifying the bioactivity of the immobilized glycans, two strains of norovirus particles (VA387 and Norwalk strains) were flowed sequentially over the sensor surface to test their binding to the immobilized glycans. Bound norovirus was stripped from the surface between each run using 8M urea. The norovirus particles were dissolved in PBS pH 7.4 at 10 μg/ml, unless otherwise specified. The SPRi procedure for norovirus binding is the same as that for lectin binding. All of the binding curves were normalized by subtracting the background signal, represented by the area modified with BSA.

4.3.5 Characterizing the inhibition of human milk glycans against norovirus-host receptor interactions

2'FL-BSA (10 μM), BSA (10 μM) and free 2'FL oligosaccharide (10 mM) were mixed with VA387 virus particles (10 μg/ml). LNFP I-BSA (1 μM), BSA (1 μM) and free 2'FL oligosaccharide (10 mM) were mixed with Norwalk virus particles (10 μg/ml). The norovirus-glycan/BSA mixtures were incubated for half an hour at room temperature, and subsequently

passed over the glycan-functionalized SPR chip. The response of the mixed solutions to the immobilized glycans was compared with that of the solution containing norovirus particles alone.

4.4 Results

4.4.1 Bioactivity of the immobilized glycans

Human milk contains a large family of glycans with various carbohydrate structures, either in the form of glycoconjugates or oligosaccharides.[11] To identify the smallest carbohydrate moieties that are responsible for norovirus inhibition, we selected the simplest and most common carbohydrate moieties in human milk (Table 4.1). These carbohydrates were either conjugated to proteins (-BSA, -HSA conjugates) or modified with a glycine residue (-Gly derivatives) to represent different structures of glycans in human milk. A divinylsulfone (DVS)-based biofunctionalization method was used to capture these glycans onto 11-mercaptoundecanol-modified gold chips via a vinylsulfone-amine reaction.[119] To preserve precious glycans and enable simultaneous analysis, a microarray containing all the glycans was printed onto one SPR chip using a manual microarrayer.

Table 4.1. Structures of carbohydrate moieties.

Lac (-BSA, -Gly)	H2 (-BSA)	2'FL (-BSA, -Gly)
LNT (-BSA,-Gly)	LNnT (-Gly)	
3'FL (-Gly)	LDFT (-Gly)	
LNFP I (-BSA, -Gly)	LNFP II (-Gly)	
LNFP III (-HSA, -Gly)	LNDFH I (-BSA, -Gly)	
LNnDFH I (-BSA)	DFLNHa (-Gly)	

Fuc: fucose, Gal: galactose, Glc: glucose, GlcNAc: N-Acetylglucosamine, GalNAc: N-Acetylgalactosamine, -BSA: carbohydrate-bovine serum albumin conjugates, -HSA: carbohydrate-human serum albumin conjugates, -Gly: carbohydrate-glycine derivatives

Two carbohydrate-binding proteins (lectins), lotus tetragonolobus lectin (LTL) and Ricinus Communis Agglutinin I (RCA_{120}) were employed to evaluate the bioactivity of the immobilized glycans. LTL recognizes both α-1,2- and α-1,3-fucose residues,[22] while RCA_{120} binds to terminal β-galactose residue.[122] When LTL was flowed over the glycan-microarray surface, most of the glycans bearing fucose residues showed specific binding response (Figures 4.1a and b), indicating that these glycans were successfully immobilized on the SPR surface and retained their bioactivity. However, three carbohydrates with fucose residues (LNFP I, LNFP II and LNDFH I) in the form of BSA conjugates and/or glycine derivatives did not exhibit strong specific response to LTL. Previous study has reported that LTL has strong specificity to the fucose linked to Gal-β(1,4)-GlcNAc, but not to that linked to Gal-β(1,3)-GlcNAc.[22] Therefore,

it is reasonable that we detected LTL binding to the fucosylated glycans with Gal-β(1,4)-Glc (e.g., 2'FL) or Gal-β(1,4)-GlcNAc (e.g., LNnDFH I), but not to LNFP I, LNFP II and LNDFH I, which contain Gal-β(1,3)-GlcNAc core structure.

We further used the monoclonal antibodies specific for Lewis a (LNFP II) and Lewis b (LNDFH I) antigens to verify the activity of the remaining fucosylated glycans. As we expected, LNFP II and LNDFH I exhibited specific response to anti-Lewis a and anti-Lewis b antibodies respectively (Figure 4.2), suggesting that LNFP II and LNDFH I retained their bioactivity on the surface. Due to the structural similarities between LNFP I and LNDFH I, the glycans containing LNFP I also showed binding to the antibody specific for Lewis b antigen (LNDFH I) (Figure 4.2). Previous studies by Jiang *et al.* [16] reported the same binding pattern of anti-Lewis b antibody to LNDFH I and LNFP I, indicating that the binding of LNFP I to the anti-Lewis b antibody detected in this study is specific. This antibody-binding result proved that LNFP I-Gly and LNFP I-BSA also retained bioactivities on the sensor surface.

For the glycans that only contain the core carbohydrate structures without fucose modification, RCA_{120} was used to test their bioactivity. As shown in Figures 4.1 c and d, glycans containing terminal β-galactose (LNT, LNnT and Lac) showed strong binding to RCA_{120}, verifying the availability of these glycans on the surface. It should be noted that some of the fucosylated glycans also demonstrated weak bindings to RCA_{120} (as shown by the curves under LNT-Gly in Figure 4.1c). This could be attributed to weak binding affinity of RCA_{120} to the terminal galactose or fucose residues in these glycan structures.[145]

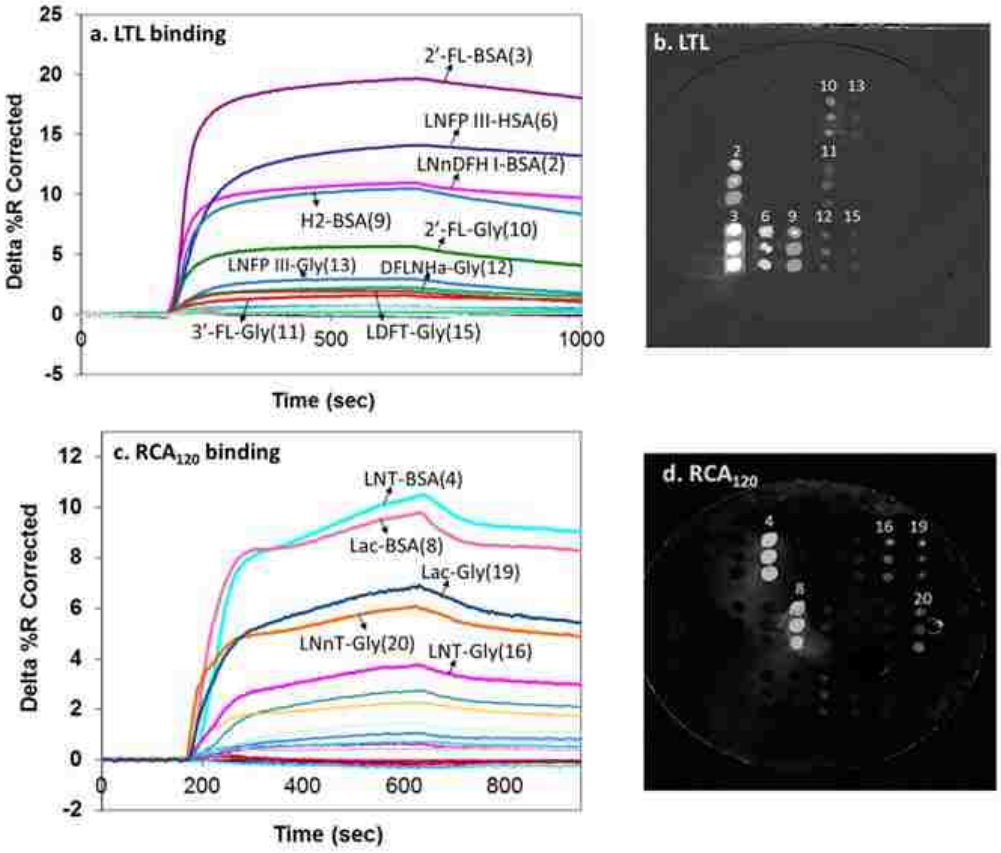

Figure 4.1. SPR sensorgrams and images of LTL (a, b) and RCA_{120} (c, d) binding to the immobilized glycans. All curves are referenced to the negative control, represented by the BSA-passivated area on the SPR chip.

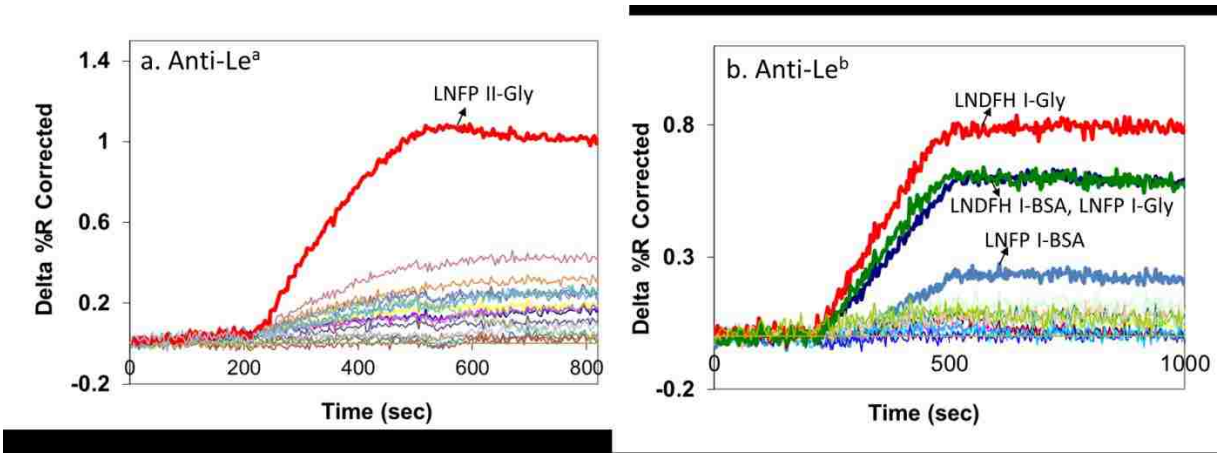

Figure 4.2. SPR sensorgrams of monoclonal antibodies binding to the immobilized glycans. (a) Monoclonal antibody for Lewis a (LNFP II). (b) Monoclonal antibody for Lewis b (LNDFH I). All curves are referenced to the negative control, represented by the BSA-passivated area on the SPR chip.

4.4.2 Norovirus-glycan interactions

The norovirus-like particles used in this study are recombinant complexes of 24 protruding domains of norovirus capsid proteins, with a total molecular weight of ~850 KDa.[132] The norovirus capsids are organized in octahedral symmetry and exhibit the native virus receptor-binding specificity.[7] Two strains of norovirus particles, VA387 and Norwalk, were tested in this study. As shown in Figure 4.3 a and b, the VA387 strain binds to two glycoproteins (LNFP III-HSA and 2'FL-BSA), but not to the other glycans on the surface. Specifically, the oligosaccharides LNFP III-Gly and 2'FL-Gly, which contain the same terminal carbohydrate moieties as LNFP III-HSA and 2'FL-BSA, did not bind to VA387. Compared to VA387, the Norwalk strain binds to a different set of glycans (Figure 4.3 b and d). These Norwalk-binding glycans include LNFP I and LNDFH I in the form of glycoproteins and oligosaccharides, and also several other carbohydrate-glycine derivatives (2'FL-Gly, LDFT-Gly and DFLNHa-Gly).

These norovirus binding results suggest that the VA387 and Norwalk strains have different glycan-binding patterns.

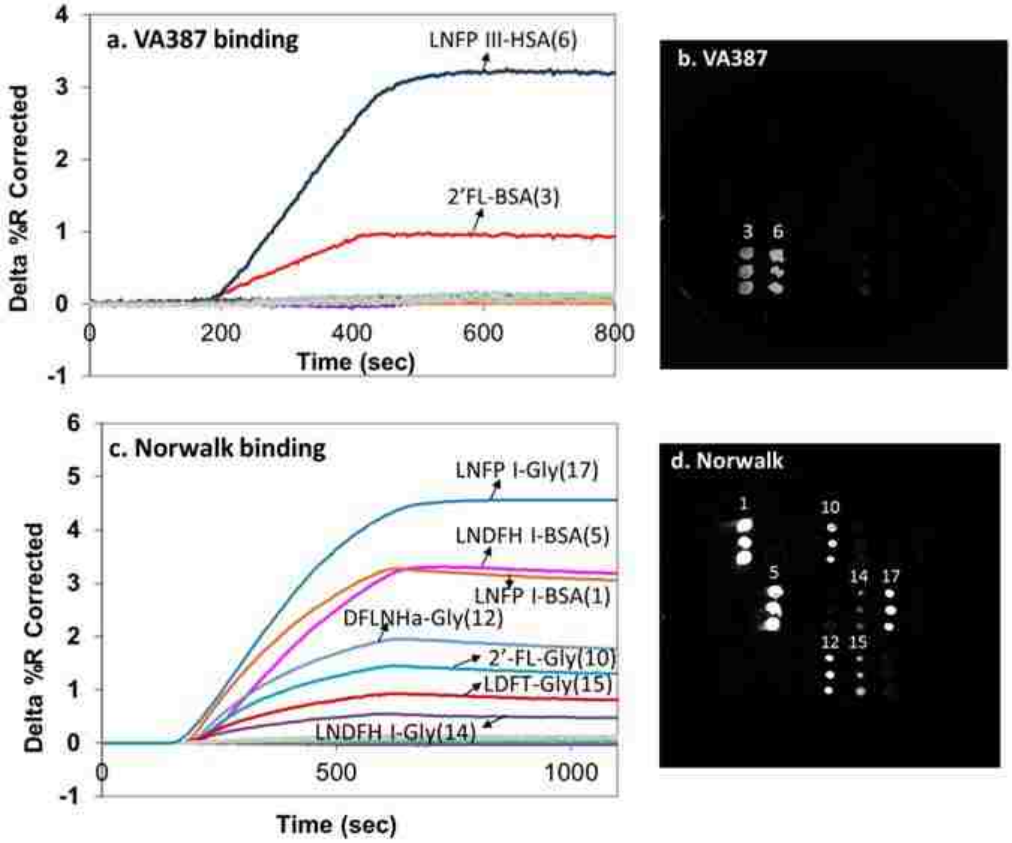

Figure 4.3. SPR sensorgrams and images of norovirus VA387 (a, b) and Norwalk (c, d) particles binding to the immobilized glycans. All curves are referenced to the negative control, represented by the BSA-passivated area on the SPR chip.

4.4.3 Inhibitory activity of human milk glycans against norovirus-host cell receptor interactions

After identifying the glycans that bind to VA387 and Norwalk strains, we further evaluated the inhibitory effects of some glycans on norovirus-host receptor interactions. Human histo-blood

group antigens (HBGAs) have been known as the host receptors for norovirus.[132] To facilitate immobilization and simultaneous analysis, we modified half of a bare gold chip with streptavidin and subsequently printed biotinylated HBGAs onto the streptavidin-functionalized surface. On the other half of the bare gold chip, four glycoproteins (including LNFP III-HSA, 2'FL-BSA, LNFP I-BSA and LNDFH I-BSA) that have specific binding to VA387 or Norwalk were directly immobilized onto the gold surface via hydrophobic interaction.

As 2'FL and LNFP I are the two most abundant fucosylated oligosaccharides in human milk and they showed specific binding to VA387 and/or Norwalk,[11] we selectively investigated the inhibitory activity of these two carbohydrates (in the form of free oligosaccharides and/or glycoconjugates) against norovirus-HBGA interactions. Using SPR competitive binding assays, we compared the binding of norovirus alone and norovirus-glycan mixtures to the functionalized gold surface. As shown in Figure 4.4, the binding of VA387 to the immobilized human milk glycans and its host receptors (H3 and B antigens) was significantly reduced by 2'FL-BSA, but not affected by free 2'FL oligosaccharide or BSA. On the contrary, the binding of Norwalk to the glycoproteins and the host receptors (H3 and A antigens) was almost abolished by both free 2'FL and LNFP I-BSA, but not BSA (Figure 4.5). These results indicate that the glycans that bind to VA387 or Norwalk are able to inhibit the binding of these norovirus strains to their host receptors.

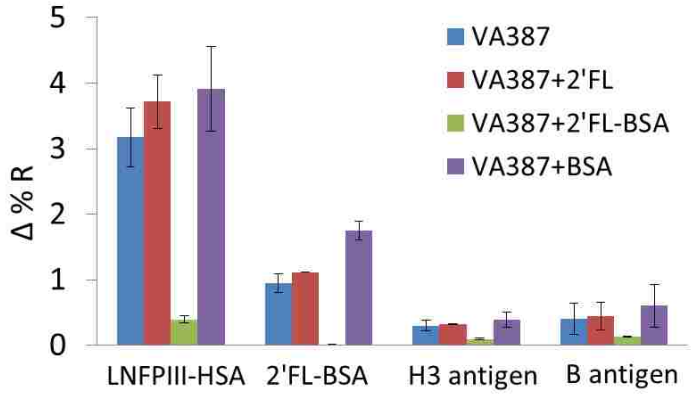

Figure 4.4. SPR responses of the immobilized glycans to VA387 (10 μg/ml, ~12 nM), VA387(10 μg/ml) with 2'FL (10 mM), VA387 (10 μg/ml) with 2'FL-BSA (10 μM), and VA387 (10 μg/ml) with BSA (10 μM). Δ%R is the maximal SPR response after flow of the solutions containing VA387 alone or VA387-human milk glycans mixtures for 5 minutes.

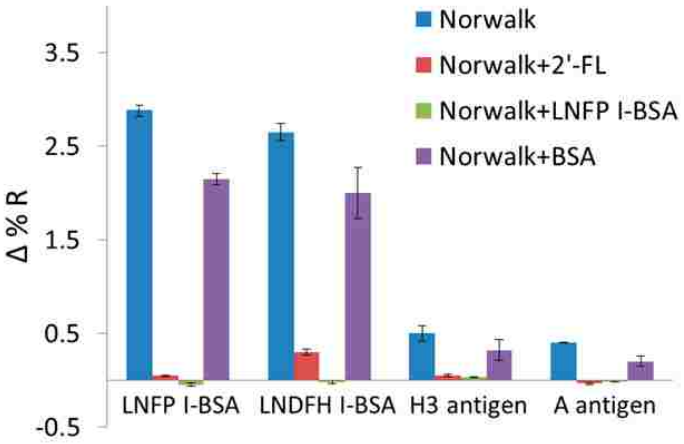

Figure 4.5. SPR responses of the immobilized glycans to Norwalk (10 μg/ml, ~12 nM), Norwalk (10 μg/ml) with 2'FL (10 mM), Norwalk (10 μg/ml) with LNFP I-BSA (1 μM), and Norwalk (10 μg/ml) with BSA (1 μM). Δ%R is the maximal SPR response after flow of the solutions containing Norwalk alone or Norwalk-human milk glycans mixtures for 5 minutes.

4.5 Discussion

Human milk glycans have been proven to protect infants against diarrheal diseases caused by a variety of pathogens, including *campylobacter*, stable toxin of *E.coli* and norovirus.[11] These glycans act as soluble receptors that inhibit pathogens from binding to host cell receptors.[11] Previous studies demonstrated that the glycosylated components in human milk are the major molecules that can bind to norovirus and subsequently inhibit norovirus-host receptor interactions.[10] However, the structures of these anti-norovirus glycans have not been fully elucidated. In this study, we selected a group of glycans with various structures and investigated their bindings to two norovirus strains (VA387 and Norwalk). This group of glycans cover the most common carbohydrate structures in human milk, including the simplest core structures (LNT, LNnT and Lac), fucosylated glycans with one fucose residue (LNFP I, LNFP II, LNFP III, 2'FL and 3'FL), glycans with two fucose residues (LNDFH I, LNnDFH I, LDFT) and the more complex branched structure (DFLNHa). In addition, for some of the carbohydrate moieties, we employed both glycoconjugate- and oligosaccharide-forms. The glycoconjugates (BSA/HSA conjugates) contain multiple carbohydrate moieties on one protein molecule, while the oligosaccharides are single carbohydrate moieties. As these two forms of carbohydrates coexist in human milk, it is critical to understand which form of carbohydrates is responsible for norovirus inhibition.

Using lectins and specific antibodies, we first verified the bioactivity of these glycans on the SPR surface. After the bioactivity tests, we further performed norovirus-binding experiments. From the glycan-VA387 binding results, we summarized several characteristics of VA387 binding specificity. First, the glycans that bind to VA387 must be fucosylated, as the non-fucosylated glycans (e.g., LNT-BSA, Lac-BSA) did not demonstrate response to VA387. Second, among the

fucosylated glycans, VA387 recognizes the glycans with a core structure of Gal-β(1,4)-GlcNAc (e.g., LNFP III-HSA) and Gal-β(1,4)-Glc (e.g., 2'FL-BSA), but not the glycans with a core structure of Gal-β(1,3)-GlcNAc (e.g., LNFP I-BSA and LNDFH I-BSA). Third, these two glycans 2'FL and LNFP III must be present in the form of glycoproteins, as the oligosaccharides 2'FL-Gly and LNFP III-Gly did not demonstrate response to VA387. Previous reports from Jiang *et al*. have demonstrated that only the glycoconjugates with high molecular weight in human milk can inhibit VA387-receptor binding.[23] Our finding further confirmed the importance of a macromolecular carrier in VA387 recognition. Since glycoproteins have higher carbohydrate densities than oligosaccharides on the biosensor surface, the strong binding affinity of VA387 to glycoproteins could be due to the multivalent interactions between VA387 and glycoproteins.[146, 147] It is worth noting that the specific binding of VA387 to LNFP III-HSA detected in this study was not observed in previous work by Jiang *et al*.[6, 16] As Jiang's studies used enzyme-linked immunosorbent assays to detect norovirus binding, the surface density of carbohydrate moieties on the assay surface might be different from that of our SPR assays, which may cause different binding results.

Compared to VA387, the Norwalk strain demonstrated a different glycan-binding pattern. It showed strong binding to LNFP I (H type 1) and LNDFH I (Lewis b) in the form of oligosaccharides and glycoproteins, which are consistent with previous reports.[134, 148] In addition, it also recognized 2'FL and LDFT, which contain a different core structure from LNFP I and LNDFH I. These results suggest that Norwalk has broader binding specificities than VA387 and it does not require a macromolecular carrier for carbohydrate recognition. It should be noted that Norwalk binds to 2'FL-Gly but not 2'FL-BSA, which is the opposite of VA387. This could be attributed to the difference of the carbohydrate moieties on 2'FL-BSA and 2'FL-

Gly. 2'FL-BSA was synthesized via reductive amination, during which the ring structure of the terminal glucose residue on 2'FL trisaccharide was opened. 2'FL-Gly was modified at the glucose end via Kochetkov Amination, which maintained the ring structure of glucose.[149] Therefore, 2'FL-BSA contains only an intact disaccharide (Fuc-α(1,2)-Gal), while 2'FL-Gly has a trisaccharide 2'FL moiety. Based on this structural difference and the binding results, we conclude that the smallest carbohydrate moiety that Norwalk recognizes must be a trisaccharide (2'FL), but not the terminal disaccharide structure (Fuc-α(1,2)-Gal).

The competitive binding studies demonstrated the inhibitory effects of different glycans on norovirus-host receptor interactions. The results suggest that only the glycoprotein 2'FL-BSA can inhibit the binding of VA387 to its host receptors (B and H3 antigens) and two VA387-binders (2'FL-BSA and LNFP III-HSA), while free 2'FL, even with a molar concentration of thousands of times higher than that of VA387 particles, cannot inhibit VA387 binding to its host receptors. It should be noted that A antigen has been reported as a VA387 receptor,[16, 128] but we did not detect a strong specific response of A antigen to the VA387 particles in our experiments. This might be due to the low surface density of A antigen immobilized on the SPR chip. The inhibition results together with the direct binding data confirm that a glycoconjugate presenting multiple carbohydrate moieties is required for VA387 binding and inhibition.

In contrast, both free 2'FL and LNFP I-BSA blocked the binding of Norwalk to its host receptors (A and H3 antigens) and two Norwalk-binding glycans (LNFP I-BSA and LNDFH I-BSA), suggesting that a large molecular carrier is not critical for its binding and inhibition. The reason that the inhibitor structures vary between VA387 and Norwalk could be attributed to the differences in the capsid proteins of these two norovirus strains and their binding affinities to specific carbohydrates.[30]

4.6 Conclusions

This study identified the structures of glycans that bind to norovirus VA387 or Norwalk and confirmed the inhibitory effects of some of the glycans on norovirus-host receptor interactions. The results indicate that the glycan structures required for inhibiting VA387 or Norwalk-host receptor interactions are quite different. For VA387, a glycoconjugate with multiple carbohydrate moieties is necessary to achieve strong binding and inhibition; whereas for Norwalk, either oligosaccharides or glycoconjugates possess the capability of binding and inhibition. These results suggest that both the carbohydrate moieties and the presentation of carbohydrates on a large molecular carrier must be considered together for the design of anti-norovirus agents. The glycan structures identified in this study have great potential to be used as drugs or food additives to combat norovirus infection.

Chapter 5: Investigating the Inhibitory Mechanism of Glycosaminoglycans in Human Milk against HIV Infection

5.1 Abstract

Glycosaminoglycans (GAGs) in human milk are a large family of molecules with diverse polysaccharide structures. While they have been proven to inhibit HIV entry into host cells, the detailed inhibitory mechanism of GAGs against HIV infection has not been elucidated. Furthermore, the specific GAG molecules that elicit anti-HIV activity have not been identified. To address these questions, we investigated the interaction of human milk GAGs with HIV and host cell receptors in this chapter. The inhibitory activity of crude human milk GAGs against HIV-mediated infection was confirmed by HIV cell-based assays. The specific binding of crude human milk GAGs to HIV envelope protein gp120 and HIV host receptor CD4 was detected by SPR biosensors. In addition, the inhibitory activity of human milk GAGs against gp120-CD4 interaction was evaluated via SPR competitive binding assays. The results suggest that human milk GAGs are involved in HIV gp120-host cell interactions, but their inhibitory activity is not due to the disruption of gp120-CD4 interaction. To identify the specific anti-HIV GAGs in human milk, we further explored the strategy to immobilize GAGs on the biosensor surface. The optimized conjugation method developed in this chapter could be applied in future binding studies to identify the smallest GAG moieties that are responsible for the inhibition of HIV infection.

5.2 Introduction

Vertical transmission of HIV from an infected mother to her child remains a serious risk for breast-fed infants.[150] Previous studies have identified both HIV-carrying cells and cell-free HIV in the human milk from HIV-positive mothers.[151] Taken alone, these results imply that breast-feeding is not a beneficial option for the infected mother-child pairs. However, a randomized trial involving 1200 HIV-positive women demonstrated that the cumulative incidence of infant death was significantly lower in the breast-fed group than the formula-fed one.[152] This study also found that the HIV transmission rate with "exclusive breast-feeding" at 6 months was much lower than that with "formula-breast mixed feeding",[153] indicating that although maternal milk can be a source of virus transmission to the newborn, it also contains protective substances that can inhibit viral infection in infants.

Glycosaminolycans (GAGs) have been reported as one of the protective agents in human milk that can inhibit HIV entry to host cells.[25] One study has shown that human milk GAGs can inhibit HIV envelop glycoprotein gp120 binding to its host receptor CD4, suggesting that GAGs play an important role in the initial adhesion process.[25] Using enzyme digestion method, one type of GAG — chondroitin sulfate has been identified as the active anti-viral component.[25] However, the mechanism of GAG-mediated HIV inhibition is unclear, as other studies reported that GAGs, such as heparan sulfate, inhibit the binding of gp120 to HIV coreceptors (CCR5) other than CD4.[154] Removal of sulfate groups abolished the anti-HIV ability of heparan sulfate, indicating the importance of sulfation in the inhibition process. Another detailed study further demonstrated that the co-recepter binding site on gp120 that binds to heparan sulfate is positively charged, highlighting the electrostatic nature of gp120-heparan sulfate interactions. [20]

Although previous studies demonstrated that GAGs are promising anti-HIV agents, the structures of human milk GAGs as well as their inhibitory mechanism have not been clearly identified. In this chapter, the anti-HIV activity of crude GAG samples from human milk was tested using *in vitro* HIV cell-based assays and SPR biosensors. The results suggested that human milk GAGs inhibit HIV entry to host cells, but this anti-HIV activity may not be due to the disruption of interactions between gp120 and CD4 receptor. Furthermore, the strategies we explored to immobilize GAGs on SPR biosensors will be useful for future binding studies to identify the specific structures of GAGs that inhibit HIV-host receptor interactions.

5.3 Materials and Methods

5.3.1 Materials

All chemical reagents were purchased from Sigma-Aldrich (St. Louis, MO) and Acros Organics (West Chester, PA) and used as received without further purification. Crude human milk GAGs were provided by Dr. David Newburg from Boston College, Drs. Mao Yang and Joseph Zaia from Boston University. Antithrombin III was a gift from Dr. Joseph Zaia from Boston University.

5.3.2 Anti-HIV activity assay

The assay utilized for this study measures neutralization in TZM-bl cells as a function of a reduction in Tat-induced luciferase (Luc) reporter gene expression after a single round of virus infection. TZM-bl is a HeLa cell clone that was engineered to express CD4 and CCR5 and contains integrated reporter genes for firefly luciferase, permitting sensitive and accurate measurements of infection.[155] Expression of the reporter genes is induced by viral Tat protein soon after infection. Luciferase activity is quantified by luminescence and is directly

proportional to the number of infectious virus particles present in the initial inoculum. TZM-bl cells (5000 cells/well) were incubated with crude human milk GAGs (provided by Dr. David Newburg, Boston College) at various concentrations (0.016 – 250 μg/ml) for 1 h and subsequently added with virus (approximate 300 $TCID_{50}$ (50% Tissue Culture Infective Dose) per well). After 48 hours of incubation, the luciferase assay was performed. Luciferase expression measured in relative light units was calculated for the infectious inhibition by each sample. The percentage of inhibition was normalized to the relative light units obtained for cells grown in the absence of virus as the background of 0% infectivity and for cells infected with virus in the absence of drug as the 100% infectivity. The IC_{50} values of GAGs against the HIV-1 isolate were calculated using GraphPad Prism. No cytotoxicity was observed as the increase in cell confluency, indicating normal cell viability of TZM-bl cells. This experiment was performed by Dr. Thanyanan Chaowanachan in Dr. Kim Woodrow's lab.

5.3.3 Biacore SPR binding experiments

The binding of human milk GAGs (provided by Dr. Mao Yang, Boston University) to gp120 and CD4 was characterized by surface plasmon resonance (Biacore SPR T100, GE Healthcare). To immobilize proteins on SPR sensor chips, a CM4 chip with carboxyl terminal groups was first activated by 0.2 M N-ethyl-N'-(diethylaminopropyl)-carbodiimide (EDC) and 0.05 M N-hydroxysuccimide (NHS) at 5 μl/min. After 7-minute flow of NHS/EDC, gp120 (50 μg/ml in10 mM acetate buffer, pH 4.8), CD4 (10 μg/ml in10 mM acetate buffer, pH 4.8) and bovine serum albumin (BSA, 50 μg/ml in10 mM acetate buffer, pH 4.8) were directed into three separate channels on the NHS-activated chip for 10 minutes. Then, 1 M ethanolamine (pH 8.5) was injected over all the channels on the chip for 7 minutes to quench the unreacted NHS. To detect direct binding, solutions of GAGs (12.5 μM), gp120 (200 nM) or CD4 (200 nM) (in HEPES with

0.005% Tween 20, pH 7.4) flowed over the functionalized sensor chip at a flow rate of 30 μl/min. The chips were regenerated by 1-min injection of 10 mM HCl. For competitive binding assays, GAGs were mixed with gp120 or CD4 and incubated for half an hour at room temperature. Then, the mixtures were injected over the functionalized chip at a flow rate of 30 μl/min. All of the resulting sensorgrams were referenced to a negative control, BSA-functionalized channel.

5.3.4 Immobilizing GAGs onto SPR chips

Divinyl sulfone (DVS) chemistry. The procedure used to immobilize GAGs onto SPR chips via DVS chemistry was similar to the method described in section 2.3.3. Briefly, SPR gold chips were functionalized with 11-mercaptoundecanol (0.1 mM in ethanol, 24 h incubation) and activated with 10% DVS (v/v, 0.5 M carbonate buffer, pH 11, 1 h incubation) solution at ambient temperature. Heparin (dissolved in pH 10 carbonate buffer, 5 mg/ml ~ 50 mg/ml) was printed onto the DVS-activated SPR chip using a manual microarrayer (V&P Scientific, Inc., CA). After overnight incubation in a humid chamber (75% relative humidity), the chip was rinsed with BSA (0.1 mg/ml, PBS) and water. Then the chip was immersed in BSA (0.1 mg/ml, PBS) for 1 h, rinsed with water and dried with nitrogen.

Hydrazide chemistry. SPR gold chips were functionalized with 11-mercaptoundecanoic acid (0.1 mM in ethanol, 24 h incubation), and subsequently activated with 2 mg/ml 1-Ethyl-3-[3-dimethylaminopropyl] carbodiimide hydrochloride (EDC) and 1 mg/ml adipic acid dihydrazide (in DMSO, 6 h incubation). The hydrazide-activated chip was rinsed with ethanol and dried with nitrogen. Heparin (dissolved in water or pH 10 buffer, 0.05 mg/ml ~ 5 mg/ml) was printed on the hydrazide-activated chip using a manual microarrayer. After overnight incubation in a humid chamber, the chip was immersed in BSA (0.1 mg/ml, PBS) for 1 h, rinsed with water and dried with nitrogen.

5.3.5 Validating the bioactivity of immobilized heparin

Heparin-protein binding was performed using surface plasmon resonance imaging (SPRimagerII, GWC Technologies). The SPRimagerII was operated at room temperature using a standard flow cell and a peristaltic pump (BioRad-EconoPump) at 100 μL/min. Antithrombin III was used at 5 μM in PBS (phosphate buffered saline, 10 mM phosphate, 2.7 mM KCl, 137 mM NaCl, pH 7.4). In a typical binding experiment, PBS was first directed over the heparin-functionalized surface for ~5 minutes to stabilize the baseline signal, followed by passing antithrombin III over the surface for ~5 minutes. Then PBS was passed over the surface again for dissociation for another 5 minutes. 8 M urea was used to regenerate protein-bound surfaces. All the binding curves were normalized by subtracting the background signal, represented by the area modified with BSA.

5.4 Results and Discussion

5.4.1 Anti-HIV activity of crude human milk GAGs

Crude human milk GAGs are a mixture of GAG molecules with different polysaccharide structures. To get a general assessment of the anti-HIV potency of GAGs in human milk, a cell culture assay was performed. Two batches of GAGs isolated from pooled human milk demonstrated inhibition against HIV entry to host cells (Figure 5.1). The IC_{50} values are comparable to the physiological level of GAGs in human milk. This result verified that the GAGs from human milk can inhibit HIV infection. However, the entry of HIV into host $CD4^+$ T cells is a complicated process, including the essential first step of HIV envelope protein gp120 binding to its host cell receptor CD4, the sequential conformational changes in gp120 and the binding of gp120 to the major chemokine co-receptors, CCR5 or CXCR4 on the host cell surface.[18] To date, it is unknown how human milk GAGs interrupt these HIV-host cell

interactions. In addition, crude human milk GAGs contain various GAG molecules with different backbone saccharide structures as well as different degrees of sulfation, making it unclear which subset of human milk GAGs is the active anti-HIV component.

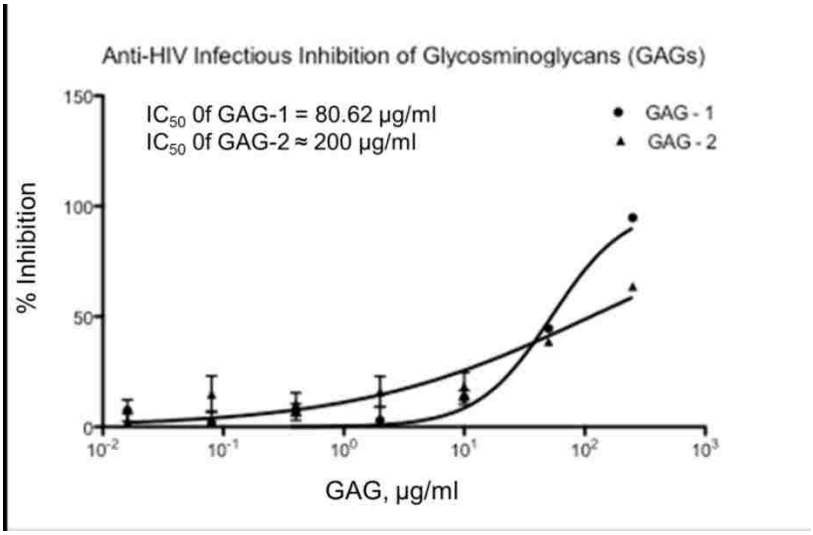

Figure 5.1. Inhibition of human milk GAGs against infection of HIV-1 to TZM-bl cells. GAG-1 and GAG-2 are two batches of GAGs isolated from pooled human milk. Figure by courtesy of Dr. Thanyanan Chaowanachan in Dr. Kim Woodrow's laboratory.

5.4.2 Characterization of gp120-CD4-human milk GAG interactions by SPR

To further understand the inhibitory mechanism of GAGs against HIV infection, SPR binding assays were used to detect the specific interactions between HIV envelope glycoprotein gp120 and HIV host receptor CD4. Gp120 and CD4 were immobilized onto the surface of Biacore CM4 chips via NHS/EDC chemistry. A representative immobilization sensorgram is shown in Figure 5.2. CM4 chips were covered with a layer of carboxymethylated dextran, which can prevent nonspecific adsorption and also provide many carboxyl groups for conjugation. To test the bioactivity of the immobilized proteins, free gp120 and CD4 solutions flowed over the functionalized chip surface. As shown in Figure 5.3, the immobilized gp120 and CD4

demonstrated specific binding to free CD4 and gp120 respectively, indicating that these two proteins were successfully immobilized on the chip and retained their bioactivity.

Figure 5.2. SPR sensorgram of immobilizing proteins onto CM4 chips. NHS (0.05 M), EDC (0.2 M), CD4 (10 μg/ml in10 mM acetate buffer, pH 4.8), gp120 (50 μg/ml in10 mM acetate buffer, pH 4.8) and ethanolamine (1 M, pH 8.5).

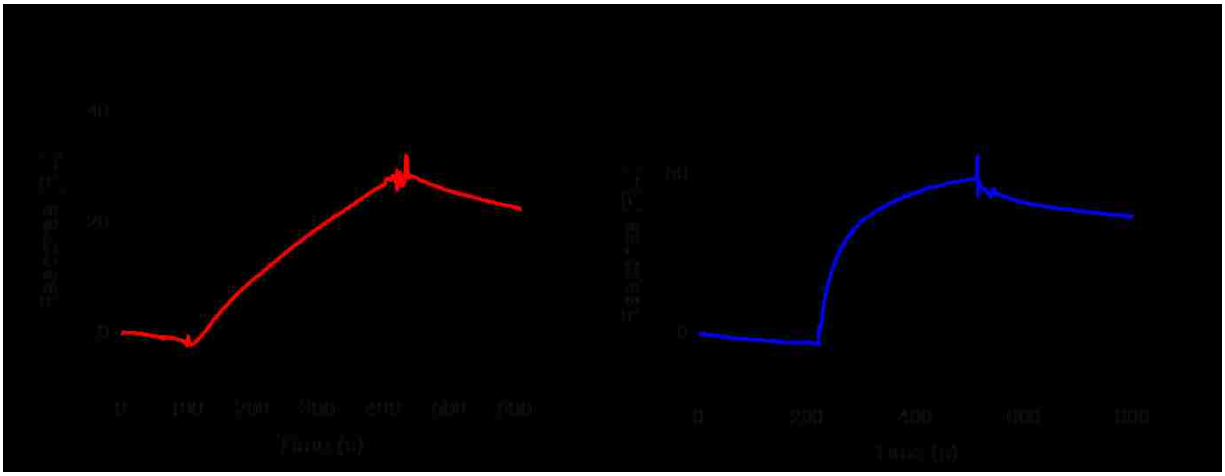

Figure 5.3. SPR sensorgrams of gp120-CD4 binding. (a) Gp120 binds to the surface functionalized with CD4. (b) CD4 binds to the surface functionalized with gp120. The sensorgrams were normalized to the negative control, the BSA-functionalized surface.

To investigate the binding of human milk GAGs to gp120 and CD4, crude GAG samples separated from human milk were flowed over the functionalized chips. The SPR results showed that GAGs bind to both gp120 and CD4 (Figure 5.4), suggesting that GAGs are involved in HIV gp120-CD4 interactions. However, the direct binding experiments cannot explain how GAGs function in the gp120-CD4 binding process. Thus, SPR competitive binding assays were performed. As shown in Figure 5.5, SPR response of gp120-CD4 binding did not decrease with the addition of GAGs. The mixtures of gp120-GAGs and CD4-GAGs exhibited a little higher binding than gp120 or CD4 alone. These results indicate that the human milk GAGs used in this study do not act as inhibitors to prevent gp120-CD4 binding. Similar to our findings, previous research reported that heparan sulfate, one type of GAG, did not inhibit gp120-CD4 interactions, but inhibited gp120 binding to HIV co-receptors CCR5 or CSCR4.[129] Through studies at the molecular level, several other publications demonstrated that gp120 underwent a conformational change after binding to CD4, exposing specific domains on gp120 that bind to HIV co-receptors.[154, 156, 157] As these specific domains on gp120 also have affinity to GAGs, the interaction between gp120 and HIV co-receptors may be inhibited by the competitive binding of gp120 to GAGs. Based on our results and previous studies, we believe that human milk GAGs may block the binding of gp120 to HIV co-receptors instead of HIV primary receptor CD4.

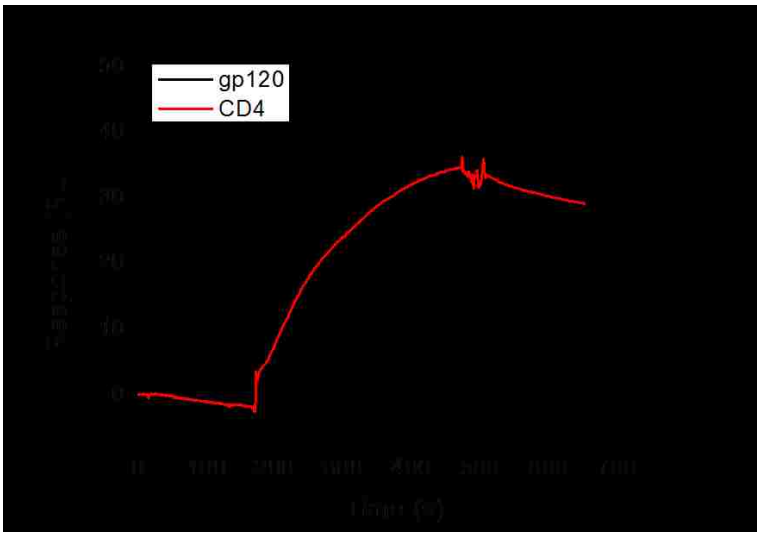

Figure 5.4. SPR sensorgrams demonstrating binding of crude GAGs from human milk to the immobilized gp120 and CD4. The sensorgrams were normalized to the negative control, the BSA-functionalized surface.

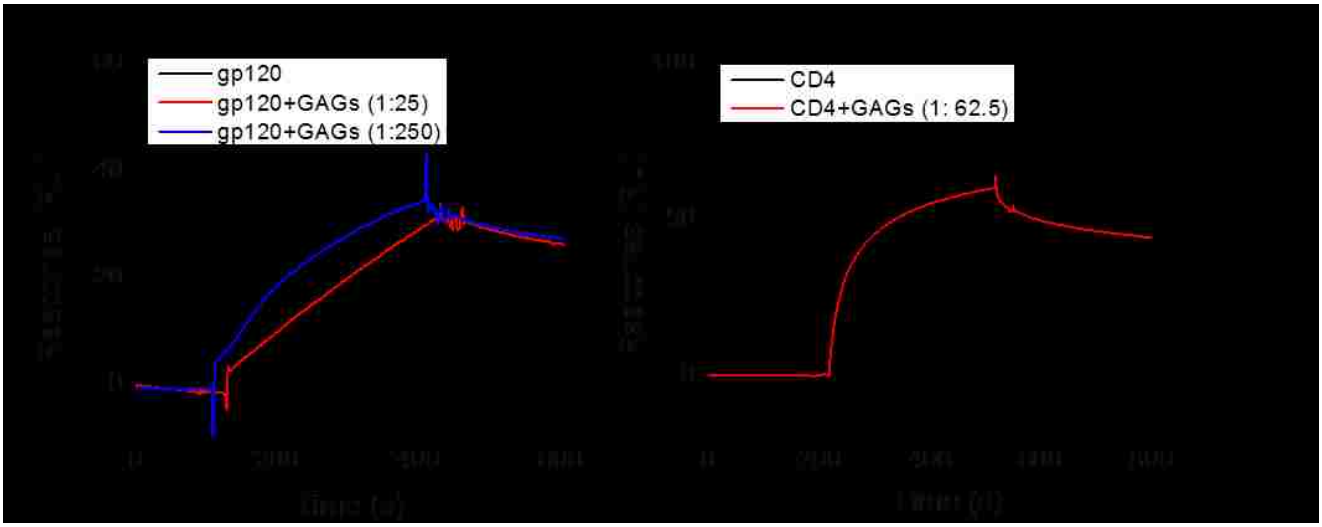

Figure 5.5. SPR competitive binding sensorgrams. (a) Binding of gp120 and gp120-GAG mixtures to the CD4-functionalized surface. The molar ratios of gp120 to GAGs are 1:25 (red) and 1:250 (blue). (b) Binding of CD4 and CD4-GAG mixture to the gp120-functionalized surface. The molar ratio of CD4 to GAGs is 1:62.5. All sensorgrams were normalized to the negative control, the BSA-functionalized surface.

5.4.3 Optimizing conditions for fabricating GAG microarrays

To further understand the mechanism of GAG-gp120 interactions and identify the smallest GAG moieties that are responsible for HIV inhibition, a glycan microarray consisting of purified human milk GAGs and depolymerized GAG fragments is desirable. Before testing precious human milk GAG samples, we first optimized conditions using commercial heparin from porcine intestinal mucosa.

Several conjugation chemistries were investigated for heparin immobilization. DVS chemistry had been successfully applied in immobilizing different carbohydrates on SPR chips in previous chapters. The DVS approach can conjugate unmodified, aminated and thiolated carbohydrates onto a solid surface. Since GAG molecules contain free hydroxyl groups and may also have free amine groups, we first tested the feasibility of using DVS chemistry to fabricate GAG microarrays. A heparin-binding protein, antithrombin III, was used to validate the bioactivity of heparin on SPR chips. As shown in Figure 4.6, the heparin immobilized on the DVS-activated SPR chip exhibited a dose-dependent binding response to antithrombin III. With the lowest concentration of heparin (5 mg/ml), the binding curve is barely above the baseline, which indicates that the response of heparin may not be detectable if we further lower the concentration of heparin. Due to limited quantities of GAG reagents we can obtain, it is not feasible to prepare 5 mg/ml GAG solutions for multiple binding studies. Therefore, other immobilization strategies must be investigated in order to further lower the concentration of heparin for immobilization.

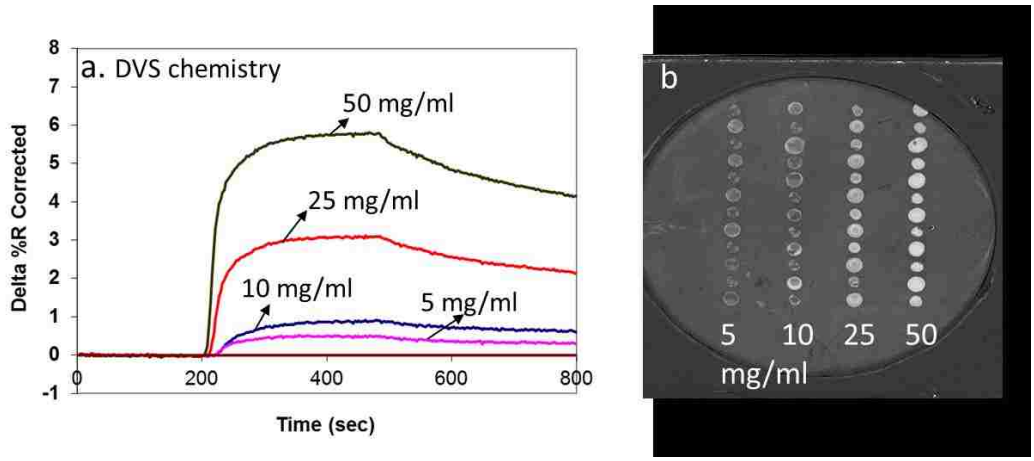

Figure 5.6. SPR sensorgram (a) and image (b) of antithrombin III binding to the heparin immobilized on DVS-activated surface. On the image (b), four columns represent four concentrations of heparin solutions during immobilization. From left to right, the concentrations of heparin are 5 mg/ml, 10 mg/ml, 25 mg/ml, 50 mg/ml, in pH 10 sodium carbonate buffer.

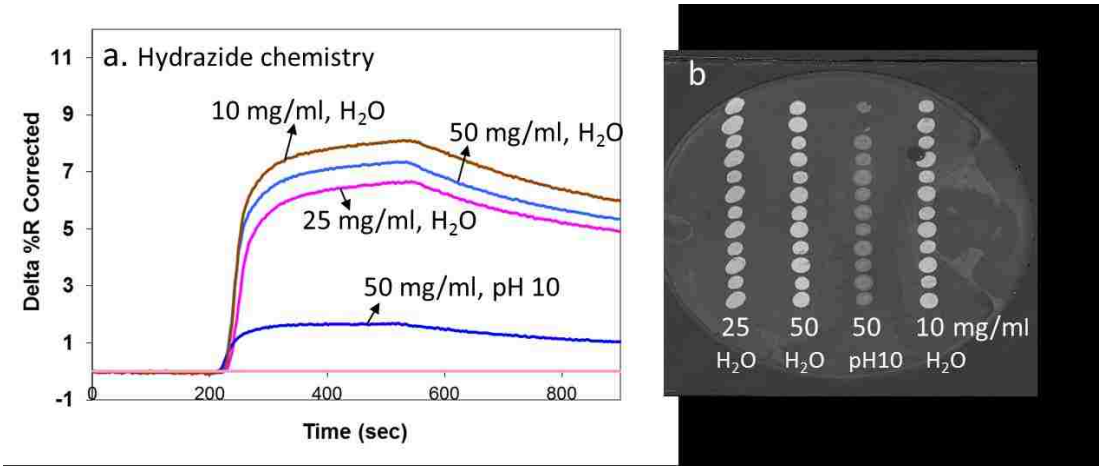

Figure 5.7. SPR sensorgram (a) and image (b) of antithrombin III binding to the heparin immobilized on the hydrazide-activated surface. On the image (b), four columns represent four conditions during immobilization. From left to right, the concentrations of heparin are 25 mg/ml in water, 50 mg/ml in water, 50 mg/ml in pH 10 sodium carbonate buffer, 10 mg/ml in water.

Hydrazide chemistries have been widely used for immobilizing unmodified and oxidized carbohydrates onto solid surfaces.[25] In this method, solid surfaces are activated with hydrazide molecules, and carbohydrates are conjugated to the surface through the reaction of hydrazide with the aldehyde at the reducing end or the oxidized unit of carbohydrates. Using a bifunctional linker adipic dihydrazide, Zhi *et al.* activated an 11-mecaptoundecanoic acid-modified gold surface and conjugated heparin oligosaccharides for protein-binding studies.[5] To test the feasibility of this dihydrazide method in functionalizing SPR chips, we immobilized the commercial heparin and measured their binding to antithrombin III. The SPR sensorgram and image in Figure 5.7 demonstrate that heparin was successfully immobilized on the hydrazide-activated surface, evidenced by their binding to antithrombin III. By varying the concentration of heparin in water (10 mg/ml ~ 50 mg/ml), we did not observe a big difference in antithrombin III binding activity, indicating that the surface density of heparin is saturated at 10 mg/ml. On the contrary, for the DVS-activated surface, the response of heparin with 10 mg/ml has much lower response than that with 50 mg/ml. (Figure 5.6) Through a direct comparison of the SPR response of heparin (10 mg/ml) immobilized on the hydrazide- and DVS-activated surfaces, we found that the heparin conjugated via hydrazide chemistry has a much higher binding capacity than that using DVS chemistry. These results suggest that hydrazide chemistry is a more efficient method than DVS chemistry for heparin conjugation. In addition, hydrazide chemistry works at neutral pH, and the reaction efficiency decreases at basic conditions (e.g., pH 10) (Figure 5.7). Moreover, DVS chemistry requires alkaline conditions for conjugation,[119] which may depolymerize heparin molecules.[158] Therefore, hydrazide chemistry is superior to DVS chemistry to retain the intact structure of heparin.

In order to find the lowest concentration of heparin that can be used for hydrazide chemistry, we investigated the binding of heparin with further diluted concentrations. As shown in Figure 5.8, the heparin with 0.05 mg/ml showed obvious binding response to antithrombin III, but the response was hard to differentiate from the baseline at the concentration of 0.01 mg/ml. Thus, ~0.05 mg/ml is the lowest concentration of heparin that we can use to immobilize heparin on the hydrazide-activated surface, which is 100-fold lower than that used for DVS chemistry. Considering the small volume of reagents needed for microarray printing (10 nl/spot), the consumption of GAGs used for immobilization on hydrazide-activated SPR chips can be lowered to sub-nanogram quantity, which is a reasonable value that we can use for multiple binding studies.

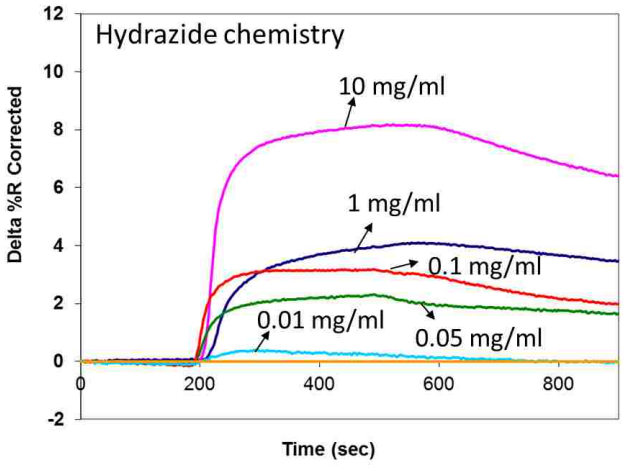

Figure 5.8. SPR sensorgram of antithrombin III binding to the heparin immobilized on hydrazide-activated surface. The arrows indicate different concentrations of heparin in water.

5.5 Conclusions

In this chapter, we verified the anti-HIV activity of human milk GAGs using HIV cell-based assays and investigated the inhibitory mechanism of crude human milk GAGs by the SPR biosensor. The direct SPR binding results suggest that GAGs are involved in HIV gp120-host receptor interactions. However, the inhibition of GAGs against gp120-CD4 was not detected in the SPR competitive binding assays, indicating that the anti-HIV activity of GAGs may not be due to the interruption of gp120-CD4 binding. Further studies are needed to investigate whether GAGs can inhibit gp120 binding to other HIV co-receptors. In addition to studying the mechanism of GAG-HIV-host receptor interactions, it is important to identify the specific GAG molecules in human milk that are responsible for HIV inhibition. To facilitate simultaneous screening of various GAG molecules that bind to gp120, a glycan microarray integrated with SPR biosensors was fabricated and the conditions for microarray printing were optimized. The SPR binding results demonstrate that heparin can be successfully immobilized on both DVS- and hydrazide-activated surfaces while retaining bioactivity. Compared to DVS chemistry, the hydrazide-based method requires a lower concentration of heparin and neutral pH for immobilization, which minimizes the consumption of precious GAG molecules as well as protects GAGs from depolymerization in acidic or alkaline conditions. These optimized methods will be useful for future application of the SPR microarray biosensor toward determining the smallest GAG moieties that prevent HIV infection.

Chapter 6: Overall Conclusions and Future Studies

6.1 Conclusions

In this dissertation, we have established glycan-functionalized label-free biosensing platforms and applied these platforms to investigate human milk glycan interactions with norovirus and HIV. Specifically, we have attained the following research goals:

First, a versatile and facile strategy has been established to functionalize surface plasmon resonance (SPR) biosensors with bioactive carbohydrates. This strategy enables immobilization of unmodified glycans and other biomolecules bearing amine and thiol groups on a divinylsulfone (DVS)-activated surface, dramatically reduces the burden of carbohydrate modification and enlarges the pool of biomolecules that can be conjugated on one biosensor chip. By integrating microarrays with SPR biosensors, we were able to print ~100 glycan spots on one SPR chip with minimal consumption of reagents, which could reserve precious glycans and facilitate parallel binding analysis.

Second, a robust surface functionalization strategy based on organophosphonate and DVS chemistry has been successfully applied in the modification of silicon photonic microring resonantor biosensors. This method overcomes the problems of silane-based strategies for silicon modification, such as instability and moisture-sensitivity. The organophosphonate/DVS-modified microring resonators demonstrated high stability and durability in reproducible detection of carbohydrate-protein interactions. They can withstand harsh regeneration conditions by high-salt, high-pH or low-pH solutions and long-term storage under ambient conditions. These superior properties of the organophosphonate-based method will facilitate the application

of silicon microring resonators in screening carbohydrate-mediated host-pathogen interactions, point-of-care diagnostics and environmental monitoring.

Third, human milk glycans that can bind to norovirus have been identified and the inhibitory activity of these glycans against norovirus-host receptor bindings has been characterized by SPR biosensors. The binding results suggest that different norovirus strains recognize specific glycan structures. The VA387 norovirus strain binds to two neoglycoproteins but not to oligosaccharides. The Norwalk strain binds to a different set of glycans including both neoglycoproteins and oligosaccharides. These results indicate that both the carbohydrate moieties and their presentations (glycoproteins or oligosaccharides) must be considered when designing anti-norovirus agents.

Forth, the anti-HIV activity of human milk glycosyaminoglycans (GAGs) was confirmed by HIV cell-based assays and the mechanism of GAGs against HIV infection was investigated by SPR biosensors. The results demonstrate that human milk GAGs bind to HIV envelope protein gp120 and HIV host receptor CD4, indicating that GAGs are involved in HIV-host cell interactions. However, the inhibition of GAGs against gp120-CD4 interactions was not observed in this study, which suggests that GAGs may act as inhibitors against other gp120-host receptor interactions (*e.g.*, CCR5 and CXCR4), but not gp120-CD4 interaction. To facilitate further identification of the GAG moieties that inhibit HIV, a strategy for immobilizing GAGs on sensor surfaces was explored. The optimized immobilization procedure for GAGs can be applied in future studies on gp120 binding to various human milk GAG molecules.

6.2 Future Studies

While this dissertation identified glycans that bind to norovirus and explored the inhibitory mechanism of human milk GAGs against HIV infection, further studies are needed in order to fully characterize the anti-infective glycans in human milk. For example, the inhibition capacity of different glycans against norovirus needs to be quantified in order to select the most potent glycan inhibitor for each strain of norovirus. A series of SPR competitive binding experiments could be used to quantify the half maximal inhibitory concentration (IC_{50}) for each glycan. This value would be an important indicator for assessing the inhibitory potency of different glycans. In addition, the number of carbohydrate moieties per neoglycoprotein should be characterized by mass spectrometry. This structural information would be useful for the design and synthesis of anti-norovirus glycans.

For the studies on human milk GAG-HIV interactions, SPRi and silicon photonic biosensors could be used to identify the smallest GAG moieties that bind to HIV gp120. We could screen the binding of gp120 to various GAG samples from human milk, including purified GAG molecules and fragmented GAG oligosaccharides. The identified GAG structures would serve as guidance for the synthesis of GAG-based anti-HIV agents. Furthermore, the inhibition of human milk GAGs against gp120-HIV co-receptor (CCR5 or CXCR4) interactions could be investigated using SPR competitive binding assays. The inhibitory results would clarify the anti-HIV mechanism of human milk GAGs and would advance the development of glycan-based agents to prevent HIV infection.

Appendix A: Characterizing the Inhibitory Ability of Glycopolymers in Blocking Carbohydrate-Protein Interactions

Introduction

Carbohydrate-protein interactions play important roles in many biological processes, including cell-cell adhesion, signaling and host-pathogen interactions.[57] However, a single interaction between a carbohydrate and a protein is usually very weak; dissociation constants, K_d, are typically 10^{-3}-10^{-6} M.[159] To enhance these carbohydrate-involved interactions, many biological systems utilize multiple simultaneous molecular contacts, which are known as multivalent binding.[160] For example, bacteria and viruses attach to host cells through the interactions of pathogenic proteins with multiple carbohydrate receptors on the cell surface.[161] A complex of multiple antibodies with mannose residues can activate macrophages by interacting with mannose receptors on the surface of a macrophage in a multivalent manner, while a single antibody cannot induce a response by the macrophage.[162] These critical characteristics of carbohydrate-protein interactions have been investigated extensively in recent years, and have been employed as a novel target for drug delivery and therapeutics.

Glycopolymers, which are synthetic polymers with pendant carbohydrate moieties attached to their backbone structures, are one of the multivalent carbohydrate molecules used as drug delivery target vectors.[163] They can effectively interact with the carbohydrate receptors on the targeted cells, increasing the efficiency of drug delivery as well as reducing the side effects of drugs.[164] In collaboration with Dr. Patrick Stayton in UW Bioengineering, our lab synthesized mannose-conjugated polymers used as a targeting vector for delivering drugs to macrophages. To characterize the binding capacity of the mannose-polymer with mannose-binding proteins, I

examined the inhibition of these polymers to mannose-Con A interactions by SPRi biosensor. This work provided fundamental information about the binding characteristics of mannose-polymer with a lectin, which will advance the development of glycopolymer-based drug delivery system.

Experiments

Mannose-functionalized SPR chip

A bare gold SIA Biacore chip (GE Healthcare Bio-Sciences AB, Uppsala, Sweden) was immersed in 11-mercaptoundecanol (0.1 mM in ethanol) for 2 h at room temperature to form a hydroxyl-terminated self-assembled monolayer surface. The chip was cleaned with ethanol, dried in a stream of nitrogen, and then immersed in 10% DVS (v/v, 0.5 M carbonate buffer, pH 11) solution for 1 h at ambient temperature. After being cleaned with water and dried with a stream of nitrogen, the DVS-activated chip was mounted on a Biacore T100 SPR instrument. 1 mM aminopropyl mannose (0.1 M pH 10 carbonate buffer) flowed over one of the channels on the chip at 1 μl/min for 2 h. Then 1 mg/ml BSA (pH 8.5 carbonate buffer) was passed over the channel functionalized with mannose and a control channel without functionalization to deactivate the surface at 1 μl/min for 2 h. After deactivation, the chip was washed with HEPES buffer (10 mM HEPES, 150 mM NaCl, 1 mM Ca^{2+} and Mn^{2+}, pH 7.4) and ready for Con A binding test.

SPR competitive binding assay

Con A (500 nM in HEPES) was mixed with mannose-polymer (synthesized by Dr. Eun-Ho Song, Dan Ratner lab) or α-methyl mannoside (Sigma-Aldrich, St. Louis, MO) with different concentrations and incubated for 1 h at room temperature. The concentration of mannose

polymer was used from 0 to 5 μM, and α-methyl mannoside was from 0 to 1 mM. Each of the mixture solutions passed over the mannose-functionalized surface for 5 minutes, followed by HEPES buffer wash for 5 minutues and 8 M urea regeneration for 1 minute.

Calculation of IC_{50}

IC_{50} is the concentration of inhibitor that yields 50% of the maximal mannose-Con A binding response. To calculate this value, the maximal SPR response of mannose to a series of Con A-inhibitor mixtures was measured and plotted on a log scale of the concentration of mixtures. The plotted curves were fit with equation A1, which is analogous to a four-parameter logistic model.[165]

$$\Delta\%R = \Delta\%R_{\min} + \frac{\Delta\%R_{\max} - \Delta\%R_{\min}}{1 + ([A]/IC_{50})^{b}} \quad \text{(A1)}$$

where $\Delta\%R_{\max}$ and $\Delta\%R_{\min}$ are asymptotic signal values determined from the regression analysis, [*A*] is the Con A mixture solution concentration, *b* is fitting parameter. When $b = 1$, the equation reduces to the Langmuir isotherm.

Results and Discussion

The inhibition of mannose-polymer to mannose-Con A interactions

The mannose-polymer (MW = 11.4 KD) contains 35-40 mannose residues on one polymer chain. The structure of the polymer is shown in Figure A1(a). The IC_{50} value of this mannose-polymer was calculated to be 115 nM (Figure A2(a)), which is much smaller than the value of α-methyl mannoside (448 μM, (Figure A2(b)). These results demonstrated that the inhibitory efficiency of mannose-polymer to mannose-Con A binding is much higher than that of a single mannose

molecule, indicating that the mannose-polymer interact with Con A in a multivalent manner and significantly enhance the binding capacity of mannose to this lectin.

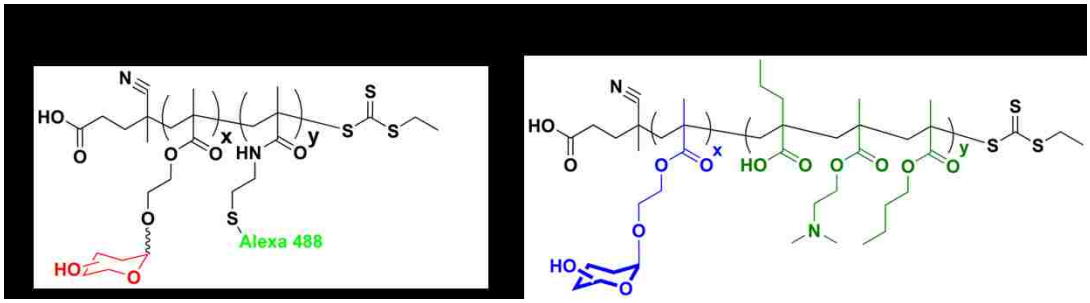

Figure A1. Structures of mannose polymer (a) and mannose-di-block polymer (b).

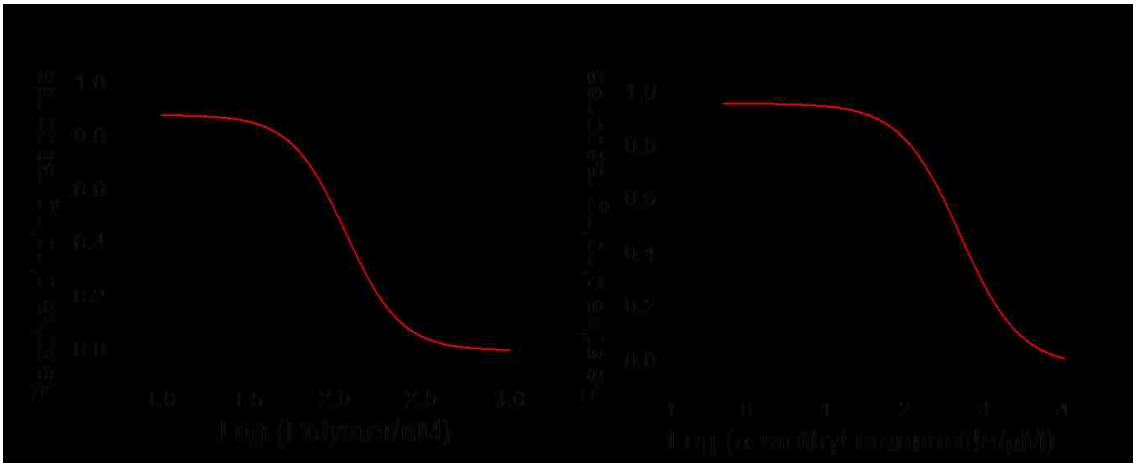

Figure A2. Curve-fitting of the inhibition assays. (a) Mannose-polymer; (b) α-Methyl mannoside.

The inhibition of mannose-di-blockpolymer to mannose-Con A interactions

A targeted drug delivery system must have three functions — targeting, conjugation of drugs and facilitating drugs to escape from the endosome. The mannose-polymer acts as the targeting vector to mannose-receptors on macrophages. However, it must be conjugated with other polymer blocks to fulfill the other functions of the drug delivery system. In part of this project, a polymer block was added to the mannose polymer chain to facilitate endosome escape. The structure of this di-block polymer is shown in Figure A1(b). The tertiary amine on this polymer will become positively charged in low-pH environment of endosome, helping the drug-conjugate escape this organelle.

The di-block polymer can form a micelle structure in aqueous solutions, which may restrict the mannose-polymer chain and influence its targeting ability. To test this effect of the second block on the mannose-polymer block, SPR competitive assays were performed to evaluate the IC_{50} of this di-block polymer. As shown in Figure A3, the di-block polymer exhibited inhibition to mannose-Con A interactions. The IC_{50} value of the di-block polymer is one magnitude higher than that of the mannose-polymer but lower than that of α-methyl mannoside. These results suggest that formation of di-block polymers reduces the binding capacity of mannose-polymer with Con A due to the steric restriction of polymer chains. However, the di-block polymer still possesses relatively high binding ability to Con A, as compared to α-methyl mannoside. This indicates that the multivalent interactions still exist between the di-block polymer and Con A, which may be adequate for targeting mannose-receptors on macrophages.

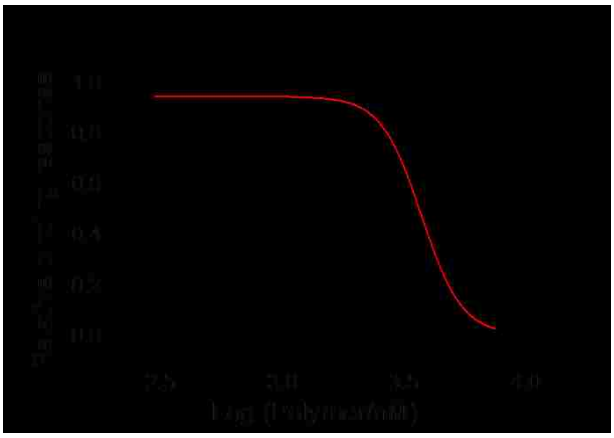

Figure A3. Curve-fitting of the inhibition assay of mannose-di-blockpolymer.

Conclusions

Using SPR competitive binding assays, we demonstrated that the mannose-polymer had much higher binding capacity to a mannose-binding protein Con A than α-methyl mannoside. After conjugation with a second block polymer, the lectin-binding capacity of the mannose-polymer decreased but still showed higher binding ability than a single mannoside molecule. The binding characteristics of the mannose-polymer demonstrated in this study will facilitate the design of a drug-delivery system targeting the mannose-receptors on macrophages. In addition, the inhibitory ability of the mannose-polymer indicates its potential as an inhibitor to prevent infection of particular pathogens, which use mannose residues on the host cell surfaces as receptors.

Appendix B: Biofunctional Paper via Covalent Modification of Cellulose

Abstract

Paper-based analytical devices are the subject of growing interest for the development of low-cost point-of-care diagnostics, environmental monitoring technologies, and research tools for limited-resource settings. However, there are limited chemistries available for the conjugation of biomolecules to cellulose for use in biomedical applications. Divinyl sulfone (DVS) chemistry was demonstrated to covalently immobilize small molecules, proteins and DNA onto the hydroxyl groups of cellulose membranes through nucleophilic addition. Assays on modified cellulose using protein-carbohydrate and protein-glycoprotein interactions and oligonucleotide hybridization showed that bioactivity of the functionalized membranes was specific, dose-dependent, and stable over a long period of time. Use of an inkjet printer to form patterns of biomolecules on DVS-activated cellulose illustrates the adaptability of the DVS functionalization technique to pattern sophisticated designs, with potential applications in cellulose-based lateral flow devices.

Introduction

Lateral flow (LF) has been widely used for the operation of assays in commercial and research applications, particularly as an ideal solution for self-powered, rapid fluid flow in low-cost, distributed diagnostic needs.[166-168] For instance, nitrocellulose-based diagnostic strips employ LF for the transport of solutions over immobilized biomolecules (often antibodies) for analyte

detection.[169] Cellulose, a cheaper and non-hazardous alternative to nitrocellulose, has also recently attracted interest as a LF-based diagnostic platform for low-resource settings.[56, 170-172] Advantages of cellulose include extremely low production cost, portability, durability and excellent wicking ability of aqueous solutions via capillary action. Various cellulose-based diagnostic designs have been introduced, such as microfluidic paper analytical devices (μPADs), 2D-shaped LF strips, and thread-based networks.[172-175] These designs vary in sophistication but typically feature isolated channels that wick aqueous solution to a test site; many operate multiple channels simultaneously to demonstrate multiplexing potential. For example, the simple branched design of the μPAD allows a drop of reagent to be transported via capillary action to multiple test sites, yielding colorimetric readouts within minutes. The low-cost and timely convenience demonstrated by the μPAD is a major advantage to operating diagnostics on cellulosic materials. However, further development of diagnostic devices on cellulose is limited by the need for a reliable strategy to immobilize bioactive molecules and impart selective and specific function to cellulose.

Physical adsorption is the simplest strategy for biomolecule immobilization onto solid substrates. In particular, immobilization of proteins onto supports such as polyvinylidene difluoride (PVDF) and nitrocellulose is well-documented.[176-178] While proteins do interact with slightly anionic cellulose,[179] physical adsorption is unlikely to be effective for biomolecules without cationic character, as they are less firmly bound and easily washed off. This is especially relevant when considering immobilization of small molecule ligands such as carbohydrates, as well as nucleic acids.

Recently, significant attention has been directed towards the chemical modification of cellulose for biomolecule functionalization. For example, carbonyldiimidazole and 1-cyano-4-

dimethylaminopyridinium tetrafluoroborate were used by Stollner. et al to immobilize glucose oxidase and a glycated pentapeptide onto a cellulose dialysis membrane to form part of an immunosensor.[180] The Nahar group has developed a UV-based activation strategy using 1-fluoro-2-nitro-4-azidobenzene to generate nitrenes from the azido group and subsequently immobilize unmodified carbohydrates and proteins to the cellulose.[181, 182] In a case of industrial interest, several methods for immobilizing invertase on Granocel cellulose carriers (e.g., NH_2-Granocel generated with pentaethylenehexamine, 1-chloro-2,3-expoxypropane sodium borohydride) have been explored to increase the enzyme activity.[183] Kong et al. presented an epichlorohydrin method for coupling DNA aptamers to cellulose beads to form an immunoadsorbent that could remove anti-DNA antibodies from the plasma of systemic lupus erythematosus patients.[184] Immobilized DNA has also been demonstrated to detect ATP by Su et al.; they used sodium periodate to generate aldehyde groups on cellulose that could then bind DNA aptamers.[185]

While the aforementioned covalent biomolecular immobilization strategies have successfully demonstrated the potential for chemical modification of cellulose, they are not without their limitations. Most methods require multiple modification steps, involve flammable and hazardous solvents, and are suitable only for specific classes of biomolecules. Therefore, a simple and versatile technique to immobilize a variety of biomolecules onto cellulose is highly desirable. To achieve this aim, we report the use of divinyl sulfone (DVS) in a simple, two-step method for the covalent modification of cellulose with an assortment of biomolecules. The homobifunctional DVS molecule contains two electrophilic vinyl groups which exhibit cross-linking activity with nucleophiles.[186] It has been reported to cross-link agarose to increase enzyme-adsorption, and to modify sepharose with mannose to form an adsorbent for a mannose-binding protein.[187, 188] In

particular, Fornstedt et al. utilized DVS cross-linking ability to generate D-mannose-substituted sepharose to capture and purify a *Vicia ervilia*-derived lectin. Recently, our laboratory has used DVS to functionalize hydroxyl-terminated gold surfaces with glycans for biosensing applications.[119] Cellulose, which contains many hydroxyl groups on its backbone, presents an ideal surface for functionalization. The chemical strategy involves the nucleophilic addition of one of the vinyl groups to the cellulose backbone. Application of nucleophile-bearing biomolecules, either by spotting or inkjet printing, to the remaining unreacted vinyl groups covalently attaches the biomolecules to the cellulose backbone. The chemical theory and our experimental protocol are summarized in Scheme B1.

In this work, we report the functionalization of DVS-activated cellulose with unmodified and modified carbohydrates, a glycoprotein, and DNA. Assays for these biomolecules using carbohydrate-protein interactions and oligonucleotide hybridization indicate that they are specifically immobilized onto the activated membrane. The functionalized membranes also exhibit dose-dependent probe detection and stability to prolonged storage. Furthermore, we demonstrate that this DVS-based functionalization strategy is amenable to the patterning of biomolecules with an inkjet printer using an existing bioprinting technique.

Scheme B1. (a) Chemical theory for the activation and functionalization of cellulose polymers. (b) Schematic illustration of the experimental protocol. (c) Examples of patterns of immobilized carbohydrates visualized by fluorometric probe, scale Bar: 1 cm.

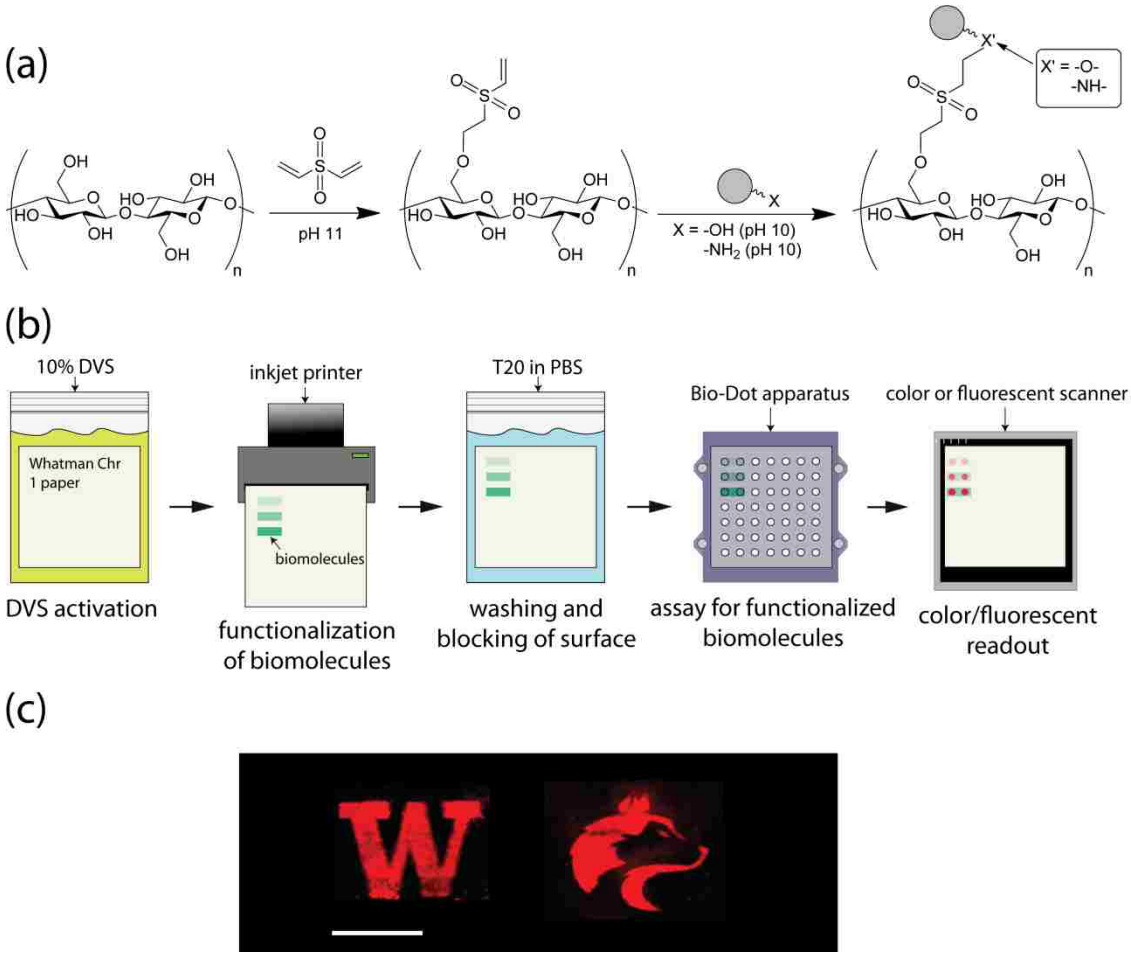

Experiment Section

Materials and Reagents

Chr 1 Chromatography paper (Whatman) was purchased from Sigma-Aldrich, St. Louis, MO. 97% DVS stabilized with 0.05% hydroquinone was purchased from Alfa Aesar, Ward Hill, MA.

D-(+)-Mannose, D-(+)-Galactose, D-(+)-Maltose, D-(+)-Glucose and D-(+)-Lactose, and Sucrose >98% pure powder were purchased from Sigma-Aldrich, St. Louis, MO). Aminopropyl mannoside, aminopropyl galactose, and hexafluorobenzamide were provided by Justin Kaplan and Prof. Rodrigo B. Andrade at Temple University (synthesis details are provided in the Supporting Information). Horseradish peroxidase (HRP)-labeled Concanavalin A (Con A-HRP) was purchased from Sigma-Aldrich, St. Louis, MO. HRP-labeled Ricinus communis (RCA_{120}-HRP) was purchased from EY Laboratories, San Mateo, CA. Dylight 649 amine-reactive dye was purchased from Thermo Fisher Scientific, Rockford, IL. RNase B was purchased from New England Biolabs, Ipswich, MA. PBS buffer (2.7 mM KCl, 137 mM NaCl, 10 mM phosphate, pH 7.4) and HEPES buffer (10 mM HEPES, 150 mM NaCl, 1 mM Ca^{2+} and Mn^{2+}, pH 7.4) were prepared in the lab. Two oligonucleotide sequences were purchased from Invitrogen Corporation, Carlsbad, CA. The sequences are detailed in Table B1:

Table B1. Oligonucleotide Sequences and Modifications

	5' modification	Sequence	3' modification
A	$-NH_2$	CTGAACGGTAGCAT CTTGAC	None
A'	$-NH_2$	GTCAAGATGCTACC GTTCAG	None

DVS Activation of Cellulose Membrane

A 10% DVS (v/v, 0.1 M sodium carbonate, pH 11) solution was used to chemically activate the cellulose membranes; 0.1 M sodium carbonate buffer alone served as a control. 12.0 x 9.0 cm sheets of Chr 1 paper were immersed in either 20 mL 10% DVS solution or in buffer alone, incubated in separate 400 mL-capacity plastic zip-bags, and agitated for 2 h on a rocking shaker.

Following the incubation, the DVS-activated and control membranes were removed from the bags and rinsed in a plastic tray with 100 mL Millipore-purified deionized water three times. These membranes were dried for 2 h in ambient conditions. In cases where the activated membranes were stored, they were either placed in aluminum foil in ambient conditions to protect from light and dust, or in a dry, nitrogen-filled plastic box.

Functionalization of DVS-activated Cellulose Membrane

Free reducing sugars and aminopropyl glycosides were dissolved in 50 mM sodium carbonate buffer (pH 10) at varying concentrations ranging from 1 to 1100 mM. The glycoprotein RNase B was dissolved at 7 mM in PBS. Oligonucleotides were dissolved at either 0.1 or 1 mM in PBS. 2 μL volumes of these biomolecule solutions were spotted on the activated and control-treated membranes in a 96-well grid format using a custom-made 96-well microplate template. The spotted sheets were placed in a 75% relative humidity (RH) box at room temperature to react overnight. The sheets were then immersed in 20 mL PBS-T (0.05% w/v Tween® 20 in PBS) for 1 h in plastic zip-bags to block the rest of the surface and wash off unbound biomolecules.

Inkjet Functionalization of DVS-activated Cellulose Membranes with Galactose

To functionalize patterns of free galactose on the DVS-activated cellulose membrane, an Epson R280 printer was modified using a method recently presented by James Wong and Barry Lutz. We devised a bioprinting solution composed of 10% w/v galactose, 40% w/v sucrose and 5% w/v TWEEN® 20 in 0.1 M pH 10 sodium carbonate buffer. Prior to printing the solution, 5 mL of a priming solution composed of 50% w/v sucrose and 5% w/v TWEEN® 20 in Millipore-purified water was passed through the printhead via a syringe. The printed sheet was placed in the 75% RH box to react overnight.

Tensile Strength Characterization of Modified and Unmodified Cellulose

Untreated and DVS+ membranes were tested for their tensile strength using a universal testing machine at the University of Washington Paper Science and Engineering Laboratory. 12.0 cm x 3.0 cm sheets of the membranes were affixed onto the two grips of the machine and pulled until the sample experienced necking. The maximum of the stress-strain curve was defined as the tensile strength.

Surface Characterization of Modified Cellulose Membrane

XPS composition data of the cellulose membranes were acquired on a Surface Science Instruments S-probe spectrometer equipped with a monochromatic Al-Kα ray source (hν = 1486.6 eV). Data were collected at 55° take-off angle in the hybrid mode with approximately 5 nm sampling depth, using a pass energy of 150 eV. Three spots for each sample were analyzed. The reported data were averaged over multiple spots. Analysis was performed on the Service Physics ESCA2000 A analysis software (Bend, OR). To facilitate analysis, an aminated F-tag (hexafluorobenzamide, see supporting information) in 0.1 M pH 10 sodium carbonate buffer was used to mimic the reaction of an amino-bearing sugar with DVS-activated cellulose.

To prepare the membranes for SEM, samples of the DVS and control membranes were coated with 5 nm of a gold-palladium alloy with an SPI Module™ sputter coater. SEM micrographs of the membranes were acquired with an FEI Sirion SEM at the University of Washington Nanotechnology User Facility, detecting secondary electron emission, using a spot size of 3 and a 10 kV beam accelerating voltage.

Preparation of Labeled Carbohydrate-Binding Protein Probes

Horseradish peroxidase (HRP)-labeled and Dylight 649-labeled carbohydrate-binding proteins (lectins) were employed to detect unmodified and modified carbohydrates and glycoproteins on the functionalized membrane. Con A-HRP in HEPES-T (0.05% TWEEN® 20 w/v in HEPES) interacts with immobilized mannose, maltose, glucose, aminated mannose, and RNase B. RCA_{120}-HRP in PBS-T interacts with immobilized galactose, lactose, and aminopropyl galactose. For fluorescent detection, Con A and RCA_{120} lectins were labeled with Dylight 649 amine-reactive dye. Dylight 649 containing an NHS ester functional group was added to the lectins in the appropriate buffer (e.g., Con A in HEPES), incubated in an orbital shaker for 1 h at room temperature, and dialyzed for 16 h against the appropriate buffer (e.g., Dylight 649-labeled Con A against HEPES) to remove unreacted fluor.

Preparation of Labeled Nucleotide Probes

Dylight 649-labeled oligonucleotides in hybridization buffer (0.3 M NaCl, 20 mM phosphate, 2 mM EDTA, 0.6 M sodium dodecyl sulfate) were employed to detect immobilized DNA. Both the target and complementary probe sequence were labeled with Dylight 649 on their 5' ends, using the same labeling technique as described for Con A and RCA_{120}.

Detection of Immobilized Biomolecules via Carbohydrate-Binding or Hybridization

Assays of the activated and functionalized cellulose membranes were operated on the Bio-Dot apparatus (Bio-Rad laboratories, Hercules, CA). Reagents were added successively to the sheets; each reagent was vacuumed through at 5.0 in Hg pressure before addition of the next reagent (see Figure S1 for more detail on the Bio-Dot setup). 100 µL/well of PBS was first added to rehydrate the sheet. 200 µL/well of probe solution was added and vacuumed through, and the membrane was incubated for 10 minutes to allow the probes to bind to the immobilized biomolecules. Then 1200 µL/well of washing buffer (0.05% w/v TWEEN® 20, 0.1% w/v BSA

in PBS) was vacuumed through to wash off unbound probes and block the rest of the surface. When an HRP-labeled probe was incubated, 100 μL/well of tetramethylbenzidine (TMB, Gaithersburg, MD) was added and vacuumed through to obtain a colorimetric readout (the reaction between HRP and TMB produces a blue colored substrate which is apparent on the paper); the color developed in approximately one minute. The sheet was then scanned on a Canon LiDE 600F desktop scanner (Canon Inc., Lake Success, NY). When Dylight-labeled probe was used, the sheet was scanned after the washing step on a Storm 865 system (GE Healthcare Bio-Sciences Corp., Piscataway, NJ) to obtain a fluorometric readout.

Analysis of Assayed Membrane

Scanned colorimetric intensities were grayscaled, inverted, and analyzed with ImageJ (NIH, Bethesda, MD). Circular regions of interest (ROIs) defined by the approximately 0.45 cm-diameter wells of the Bio-Dot apparatus, were analyzed for the Integrated Density (ID) (additional details on ROI selction can be found in the Supporting Information). Scanned fluorometric intensities were analyzed with ImageQuant TL (GE Healthcare) with circular ROIs (also defined by the Bio-Dot wells) for fluorescent intensity. Mean IDs, fluorescent intensities, and standard deviations for spots immobilized with the same biomolecule were calculated in Microsoft Excel. When appropriate, Student's t-tests were employed at $p = 0.05$ to determine whether intensities of spots on DVS-activated membranes were statistically higher than the background on DVS-activated membranes and corresponding spots on control-treated membranes.

Results and Discussion

Surface Characterization

XPS surface analysis was performed to verify DVS-activation and functionalization procedures. As shown in the XPS elemental composition results (Table B2), only carbon and oxygen was detected at the interface of unmodified cellulose membranes. After DVS-activation, the appearance of a sulfur signal in the XPS spectrum indicates that DVS successfully modified the cellulose substrate. A fluorine-containing aminated probe (F-tag) was used to mimic the reaction of amino-bearing biomolecules with DVS+ cellulose (see Scheme S1 for the structure of this F-tag). After application of the F-tag, fluorine could be observed by XPS on the DVS-activated (DVS+) membrane. Based on the quotient of the observed F/S ratio by the theoretical maximum F/S ratio (each DVS bound to cellulose binds with one F-tag), 19% of the DVS molecules reacted. On the unmodified membrane that was treated only with the buffer (DVS-) and spotted with F-tag, no fluorine was detected, which demonstrates the dependence on DVS for immobilization to the cellulose substrate. This data validated the ability of the DVS conjugation strategy to covalently immobilize amine-bearing molecules on DVS-activated paper.

Table B2. Relative Compositions of Functionalized Cellulose Determined by XPS

	Cellulose	Cellulose + DVS	Cellulose + DVS + F-tag	Cellulose + F-tag
C 1s	57.7 ± 0.2	58.6 ± 0.6	56.9 ± 0.1	58.0 ± 1.6
O 1s	42.3 ± 0.2	40.0 ± 0.8	40.5 ± 0.3	42.0 ± 1.6
S 2p	n/d	1.4 ± 0.2	1.2 ± 0.3	n/d
F 1s	n/d	n/d	1.4 ± 0.2	n/d

SEM micrographs illustrate the morphology of DVS+ cellulose compared with the DVS- control membrane. No apparent difference in morphology or fibrosity was observed between the two samples at magnifications ranging from 32x to 500x. A comparison of the micrographs at 500x is depicted in Figure B1. These morphologic similarities suggest that DVS modification results in

little to no alteration of the physical characteristics of cellulose fibers as a result of DVS cross-linking. These results suggest that DVS-modification will have no undesirable impact on the capillarity and LF suitability of the DVS-activated cellulose membranes. Tensile strength measurements of modified and unmodified cellulose showed a modest change in the material properties of the paper, with a decrease in tensile strength from 49.4 N/m^2 (DVS-) to 33.7 N/m^2 (DVS+). However, the modified paper demonstrated no significant difference under routine handling, printing, and assay development.

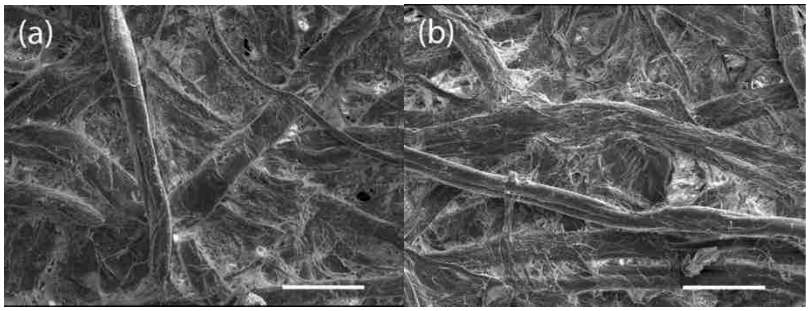

Figure B1. SEM micrographs at 500x magnification of cellulose membranes: (a) DVS- cellulose membrane (b) DVS+ cellulose membrane. Scale bar: 50 μm (Photo credit, Lauren Cummings).

Detection of Carbohydrate-Protein Interactions

Colorimetric and fluorometric assays were employed to examine the bioactivity of the immobilized carbohydrates and glycoprotein on DVS+ membrane. The results of the colorimetric assay in Figure B2 show the binding response of two lectins to DVS-immobilized glycans vs. non-specifically absorbed glycans. On the DVS+ papers, ricin (RCA_{120}) exhibited specific binding to the carbohydrates containing a β-galactose moiety (including aminopropyl galactose, galactose, and lactose), but no response to glycans with mannose residues (including mannose and RNaseB, Figure B2a). By contrast, Con A only shows binding to Con A-specific

glycans (including mannose, glucose, maltose and RNase B, Figure B2b). On the control membrane (DVS-) both lectins show minimal non-specific binding to the glycans physically adsorbed on the surface. These results demonstrate that cellulose paper can be functionalized with bioactive carbohydrates for detecting specific carbohydrate-protein interactions.

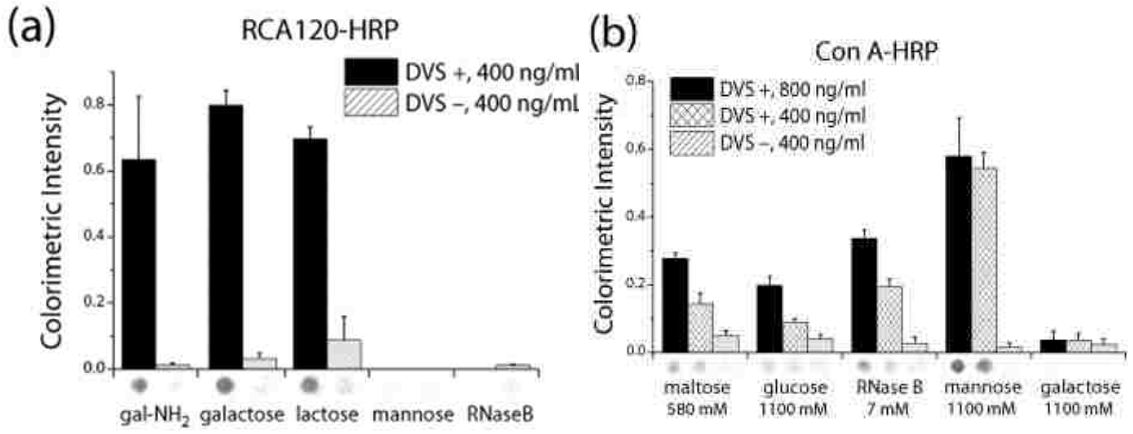

Figure B2. (a) Galactose (1100 mM), lactose (292 mM) and aminopropyl galactose (gal-NH_2, 10 mM) were probed with 400 ng/mL RCA_{120}-HRP; glycan bioactivity was observed on the DVS+ membrane but not on the DVS- membrane. There was no signal from the mannose (1100 mM) and RNase B (7 mM) spots, which is expected since they do not specifically interact with RCA120. (b) Maltose (580 mM), glucose (1100 mM), RNase B (7 mM), and mannose (1100 mM) were bound by Con A-HRP on the DVS+ membrane but not the DVS-. Galactose was not detected, which is expected since it does not specifically interact with Con A. Representative pairs of colorimetric spots from the membranes appear below each corresponding pair of intensity bars (data were averaged over 6 spots for each carbohydrate).

Dose-dependent responses from the galactose-RCA_{120} and mannose-Con A interactions were observed when varying the concentration of both lectins. For RCA_{120}-HRP, response saturated at approximately 500 ng/mL (4.8 nM), with the response of the lowest concentration tested (100 ng/mL, or 0.96 nM) well above background (Figure B3a). For Con A-HRP, response saturated at

approximately 1000 ng/mL (9.6 nM), while the limit of detection (LOD) was determined to be 10 ng/mL (96 pM) (Figure B3b).

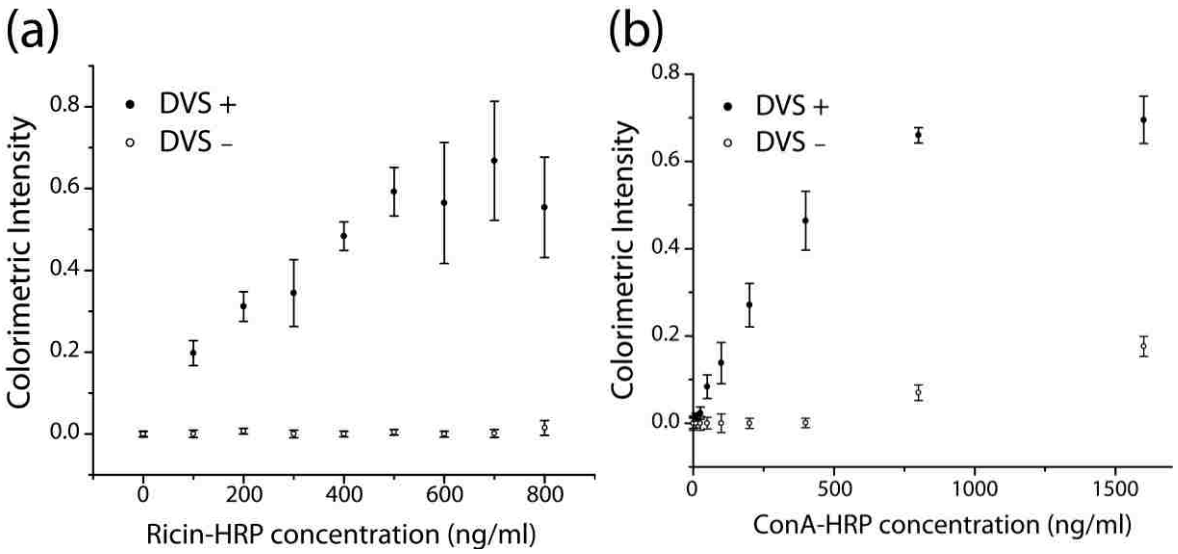

Figure B3. (a) Dose-dependent response of the RCA_{120}-HRP-galactose interaction on DVS-activated cellulose functionalized with 555 mM galactose, for increasing RCA_{120}-HRP concentrations. Response saturated at approximately 500 ng/mL, (4.8 nM), while the lowest signal was approximately 0.96 nM. (b) Dose-dependent response of the Con A-HRP-mannose interaction saturated at approximately 1000 ng/mL (96 nM), while the limit of detection was determined to be 10 ng (96 pM).

Analysis of fluorometric assays for immobilized carbohydrates and glycoprotein demonstrate the same specific binding observed in the colorimetric analysis. Figure B4 depicts specific binding of aminopropyl mannoside, mannose and galactose (negative control) by Dylight 649-labeled Con A. As previously observed, amino-modified glycans show significantly higher conjugation efficiency, as indicated by their increased bioactivity at a given immobilization concentration.[119]

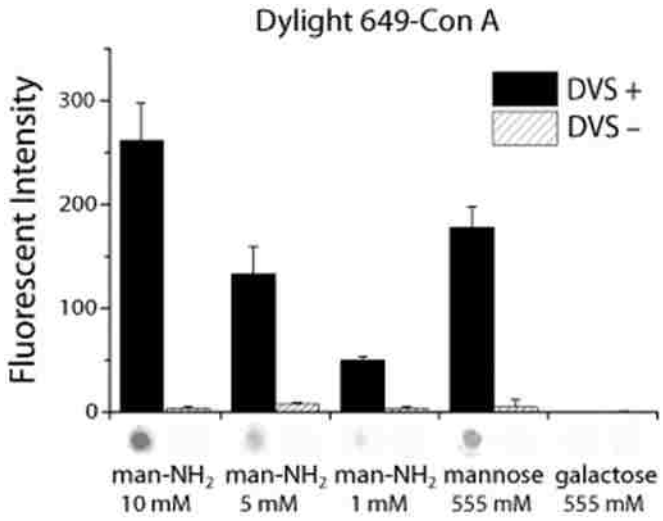

Figure B4. Aminopropyl mannoside (man-NH_2) and mannose were probed with 50 nM Dylight 649-labeled Con A; bioactivity was observed on the DVS+ membrane but not on the DVS- membrane. There was no signal from the galactose spots, which is expected since the sugar does not specifically interact with Con A. Representative pairs of fluorometric spots from the membranes appear below each corresponding pair of intensity bars (data were averaged over 6 spots for each carbohydrate).

Both the colorimetric and fluorometric assays demonstrate that DVS-modified cellulose paper is suitable for conjugation of carbohydrates and analysis of biological interactions using various means of detection. DVS-activated cellulose is a versatile substrate that can be functionalized with various biomolecules bearing nucleophiles for different detection purposes.

Detection of DNA Oligonucleotide Hybridization

Nucleic acid tests (NATs) are significant in clinical diagnostics for their ability to sense pathogens, by detecting the genetic material of viruses and bacteria. The development of NATs in a lab-on-a-chip or paper-based format for low-resource settings has received recent and considerable attention. [56, 167, 185] To demonstrate the suitability of DVS-modified cellulose for

DNA detection, we performed a simple hybridization assay. We observed specific binding of a labeled sequence (A') to the immobilized sequence (A) on DVS+ membranes (Figure B5a). A labeled non-complementary sequence (A) was incubated as a negative control on both the DVS+ and DVS- membranes, and it showed no binding to the immobilized sequence (A) on either membrane. In a separate experiment, a dose-dependent response of the DNA-functionalized membrane was observed by varying the concentration of the probing sequence (A') (Figure B5b). We observed a significant signal difference between the DVS+ and DVS- membranes, in accordance with the role played by DVS in covalent immobilization of the oligonucleotide target. The hybridization observed on the DVS- paper can be attributed to a low level of physisorbed target sequence (non-covalent) to the unmodified cellulose. However, DVS yielded an order of magnitude higher response for the hybridization assay. The limit of detection (LOD) was determined to be 0.5 nM. This is on the same order of magnitude as that reported for short oligonucleotide hybridization on zirconia-modified filter paper (using FITC-labeled probe),[189] and on gold using surface plasmon resonance imaging (SPRi) (unlabeled probe).[190]

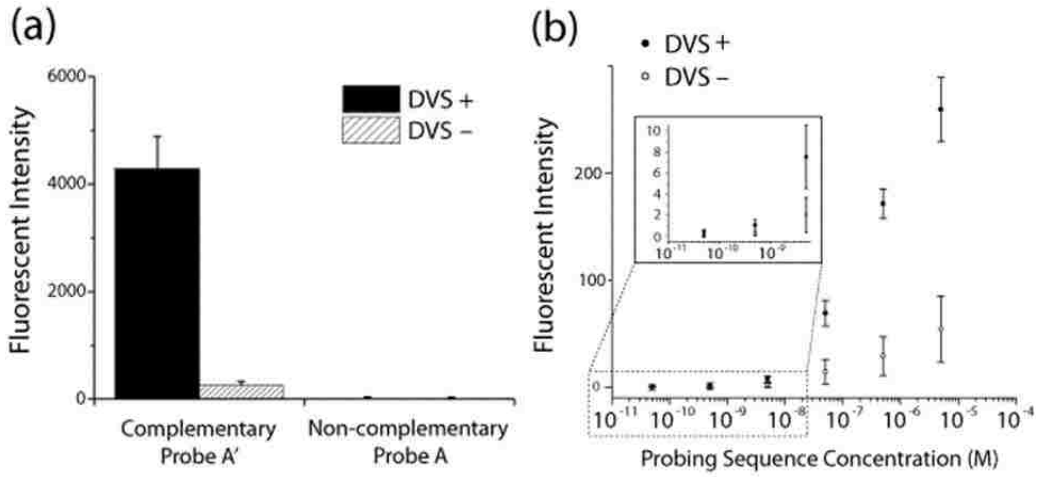

Figure B5. (a) The immobilized sequence (A) was probed by 5 μM of the complementary probe sequence (A'); bioactivity was observed on the DVS+ membrane but not the DVS- membrane. Labeled sequence (A) was also incubated as a negative control, and was not detected on either membrane. (b) Dose-dependent detection of immobilized sequence (A) was observed for concentrations of probe (A') from 0.5 nM to 5 μM.

Stability of DVS-activated Cellulose

To develop a reliable paper-based platform suitable for future point-of-care applications, the stability of DVS-activated and biofunctionalized cellulose is critical. A cellulose-based LF platform for low-resource settings needs to maintain its stability for extended periods of time. To gain a better understanding of the stability of our DVS-cellulose platform, we tested the stability of DVS-activated membranes after 60 days of storage in a dry, nitrogen-filled environment. Carbohydrates and the glycoprotein RNase B were spotted on the DVS-active cellulose membrane after the storage period and tested for specific binding to labeled Con A. The results in Figure B6a indicate that the activity of carbohydrates and glycoprotein spotted on the aged DVS-cellulose was very similar to that of freshly activated DVS-paper. Only minor variability was observed for the immobilized mannose solutions. We ascribe these minor differences to

physical irregularities within the manufactured chromatography paper used for this study. These inconsistencies within the membrane are visually apparent, and may affect the degree of DVS activation, biomolecule immobilization and therefore probe response. However, this heterogeneity results in only modest standard deviations for the bioactivity of the immobilized carbohydrates, glycoprotein and oligonucleotide. A similar experiment involving a membrane stored for 30 days on the bench top yielded similar results. These results demonstrate that DVS-activated cellulose is stable to prolonged storage while retaining reactivity for subsequent biomolecule immobilization.

Having established that DVS+ membranes retain their reactivity after prolonged storage, we investigated the ability of biofunctionalized DVS+ membranes to retain their bioactivity under the same storage conditions employed by us previously. We tested the stability of a DVS-activated membrane functionalized with carbohydrates and glycoprotein and stored in a dry, nitrogen-filled environment for 30 days. Con A binding following storage showed preservation of the bioactivity with differing amounts of loss, varying by specific glycans (Figure B6b). These results demonstrate that biofunctionalized cellulose using DVS chemistry has great potential to be used in a low-cost, portable and robust bioassay with long shelf-life for point-of-care diagnosis and other applications.

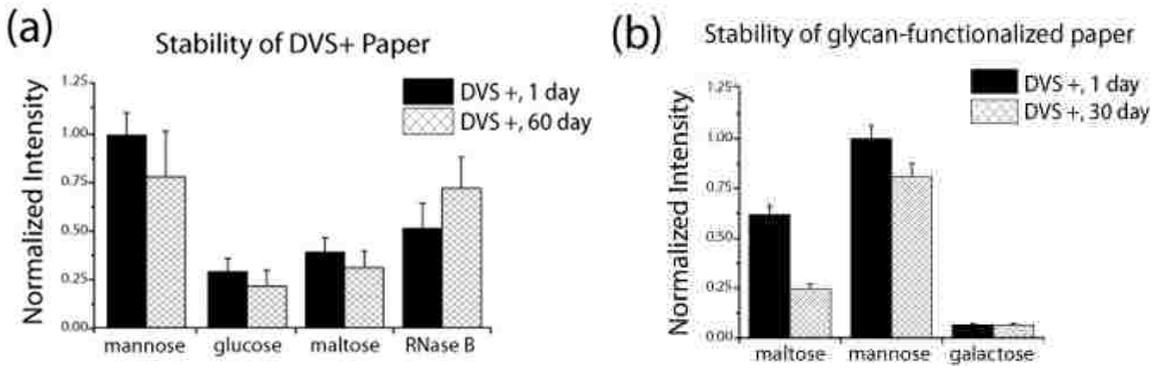

Figure B6. (a) DVS-activated membranes were stored for 60 days and subsequently functionalized with mannose (555 mM), glucose (555 mM), maltose (290 mM), and RNase B (7 mM). The bioactivity, as observed by fluorescent ConA detection, was minimally affected by storage of the DVS activated paper. (b) The DVS-activated membrane that was biofunctionalized and stored for 30 days experienced slight bioactivity loss for mannose (555 mM) and more significant loss for maltose (290 mM), when compared to a membrane freshly functionalized and assayed. Maltose bioactivity loss may be ascribed to its susceptibility as a disaccharide to enzyme digestion, as this loss was not pronounced with the monosaccharide mannose.

Printed Biomolecular Patterning

Fabrication of biomolecular patterns on LF-based cellulosic diagnostic devices may benefit from the development of facile bioprinting techniques. To demonstrate the adaptability of the DVS functionalization technique to bioprinting we have visualized patterns of immobilized galactose on DVS-activated cellulose membranes using fluorescently labeled RCA_{120}. An Epson R280 inkjet printer was modified for printing biological solutions. The printing solution we formulated (10% w/v galactose, 40% w/v sucrose and 5% w/v TWEEN® 20 in 0.1 M pH 10 sodium carbonate buffer) was previously immobilized and assayed on a DVS-activated membrane without the galactose component to ensure that the non-reducing sugar sucrose did not interfere with binding by RCA_{120} (not shown). Examples of the printed patterns are depicted in Scheme

B1. These visualizations indicate that DVS-activated cellulose is amenable to accurate, sub-millimeter patterning of biomolecules through bioprinting, and that the printed biomolecules retain their bioactivity during the printing process. The simplicity of this technique may facilitate the fabrication of LF-based cellulosic diagnostic devices because printing can be scaled up to produce many units simultaneously. Separation of the physical printing process from the digitized design process also allows design changes to be implemented immediately and conveniently. These advantages may be especially important for microfluidic-based techniques for muiltiplexed detection, in which complex channel designs on the substrate make manual fabrication labor-intensive and time-consuming.

Conclusions

We have presented a simple covalent immobilization method for cellulose using DVS chemistry. The DVS-activated cellulose membranes exhibit versatile conjugation capability for biomolecules presenting nucleophilic functional groups. The immobilized carbohydrates and oligonucleotides on DVS-activated cellulose membranes demonstrate specific response to lectins and complementary nucleotides, respectively. Probing of the functionalized surface with either lectins or oligonucleotides is dose-dependent, and the LOD of nucleic acid hybridization is comparable to results observed previously using SPR and zirconia-modified paper. In addition, DVS-activated and biofunctionalized cellulose membranes maintain their activity for prolonged storage under ambient conditions, which demonstrates the suitability of this technique for the fabrication of paper-based bioassays for low-cost and portable point-of-care diagnostics. Finally, the DVS strategy can be combined with an existing simple bioprinting technique to accurately produce biomolecular patterns, demonstrating the potential of cellulose for sophisticated

bioassay design and multiplexed detection. Together, these findings demonstrate that cellulose can be chemically activated with DVS for the generation of biofunctionalized surfaces with potential applications in cellulosic LF-based diagnostic devices, water pathogen-testing strips, and molecular detection papers for basic research.

References

1. Griffith, K., J. Wenzel, J. Shang, et al., *Impact of a walking intervention on cardiorespiratory fitness, self-reported physical function, and pain in patients undergoing treatment for solid tumors.* Cancer, 2009. **115**(20): p. 4874-84.
2. *Global HIV/AIDS response, progress report summary 2011.* World Health Organization, 2011.
3. Oyelaran, O. and J.C. Gildersleeve, *Glycan arrays: recent advances and future challenges.* Curr. Opin. Chem. Biol., 2009. **13**(4): p. 406-13.
4. Dhayal, M. and D.M. Ratner, *XPS and SPR analysis of glycoarray surface density.* Langmuir, 2009. **25**(4): p. 2181-7.
5. Zhi, Z.L., A.K. Powell, and J.E. Turnbull, *Fabrication of carbohydrate microarrays on gold surfaces: Direct attachment of nonderivatized oligosaccharides to hydrazide-modified self-assembled monolayers.* Anal. Chem., 2006. **78**(14): p. 4786-4793.
6. Tan, M. and X. Jiang, *Norovirus-host interaction: implications for disease control and prevention.* Expert Rev Mol Med, 2007. **9**(19): p. 1-22.
7. Tan, M., P. Fang, T. Chachiyo, et al., *Noroviral P particle: structure, function and applications in virus-host interaction.* Virology, 2008. **382**(1): p. 115-23.
8. Rydell, G.E., A.B. Dahlin, F. Hook, et al., *QCM-D studies of human norovirus VLPs binding to glycosphingolipids in supported lipid bilayers reveal strain-specific characteristics.* Glycobiology, 2009. **19**(11): p. 1176-1184.
9. Newburg, D.S., *Innate immunity and human milk.* J Nutr, 2005. **135**(5): p. 1308-12.
10. Jiang, X., P. Huang, W. Zhong, et al., *Human milk contains elements that block binding of noroviruses to human histo-blood group antigens in saliva.* J. Infect. Dis., 2004. **190**(10): p. 1850-9.
11. Morrow, A.L., G.M. Ruiz-Palacios, X. Jiang, et al., *Human-milk glycans that inhibit pathogen binding protect breast-feeding infants against infectious diarrhea.* J Nutr, 2005. **135**(5): p. 1304-1307.
12. Ernst, B. and J.L. Magnani, *From carbohydrate leads to glycomimetic drugs.* Nat Rev Drug Discov, 2009. **8**(8): p. 661-77.
13. David L. Nelson, M.M.C., *Lehninger Principles of Biochemistry, Fifth Edition*. 2005: W. H. Freeman.
14. Liang, P.H., C.Y. Wu, W.A. Greenberg, et al., *Glycan arrays: biological and medical applications.* Curr. Opin. Chem. Biol., 2008. **12**(1): p. 86-92.
15. Shirato, H., *Norovirus and histo-blood group antigens.* Jpn J Infect Dis, 2011. **64**(2): p. 95-103.
16. Huang, P., T. Farkas, W. Zhong, et al., *Norovirus and histo-blood group antigens: demonstration of a wide spectrum of strain specificities and classification of two major binding groups among multiple binding patterns.* J. Virol., 2005. **79**(11): p. 6714-22.
17. Seyrek, E. and P. Dubin, *Glycosaminoglycans as polyelectrolytes.* Adv. Colloid Interface Sci., 2010. **158**(1-2): p. 119-29.
18. Patel, M., M. Yanagishita, G. Roderiquez, et al., *Cell-surface heparan sulfate proteoglycan mediates HIV-1 infection of T-cell lines.* AIDS Research and Human Retroviruses, 1993. **9**(2): p. 167-74.
19. Crublet, E., J.P. Andrieu, R.R. Vives, et al., *The HIV-1 envelope glycoprotein gp120 features four heparan sulfate binding domains, including the co-receptor binding site.* J Biol Chem, 2008. **283**(22): p. 15193-200.
20. Moulard, M., H. Lortat-Jacob, I. Mondor, et al., *Selective Interactions of Polyanions with Basic Surfaces on Human Immunodeficiency Virus Type 1 gp120.* J. Virol., 2000. **74**(4): p. 1948-1960.
21. Newburg, D.S., G.M. Ruiz-Palacios, and A.L. Morrow, *Human milk glycans protect infants against enteric pathogens.* Annu Rev Nutr, 2005. **25**: p. 37-58.

22. Pereira, M.E. and E.A. Kabat, *Specificity of purified hemagglutinin (lectin) from Lotus tetragonolobus.* Biochemistry (Mosc). 1974. **13**(15): p. 3184-92.
23. Huang, P., A.L. Morrow, and X. Jiang, *The carbohydrate moiety and high molecular weight carrier of histo-blood group antigens are both required for norovirus-receptor recognition.* Glycoconjugate J., 2009. **26**(8): p. 1085-96.
24. Coutsoudis, A., K. Pillay, L. Kuhn, et al., *Method of feeding and transmission of HIV-1 from mothers to children by 15 months of age: prospective cohort study from Durban, South Africa.* AIDS, 2001. **15**(3): p. 379-87.
25. Lee, M.R. and I. Shin, *Facile preparation of carbohydrate microarrays by site-specific, covalent immobilization of unmodified carbohydrates on hydrazide-coated glass slides.* Org Lett, 2005. **7**(19): p. 4269-72.
26. Shankaran, D.R. and N. Miura, *Trends in interfacial design for surface plasmon resonance based immunoassays.* Journal of Physics D-Applied Physics, 2007. **40**(23): p. 7187-7200.
27. Shankaran, D.R., K.V.A. Gobi, and N. Miura, *Recent advancements in surface plasmon resonance immunosensors for detection of small molecules of biomedical, food and environmental interest.* Sensor Actuat B-Chem, 2007. **121**(1): p. 158-177.
28. Aldred, N., T. Ekblad, O. Andersson, et al., *Real-time quantification of microscale bioadhesion events in situ using imaging surface plasmon resonance (iSPR).* ACS Appl Mater Interfaces, 2011. **3**(6): p. 2085-91.
29. Lausted, C., Z. Hu, and L. Hood, *Label-free detection with surface plasmon resonance imaging.* Methods Mol. Biol., 2011. **723**: p. 321-33.
30. Bu, W., A. Mamedova, M. Tan, et al., *Structural basis for the receptor binding specificity of Norwalk virus.* J. Virol., 2008. **82**(11): p. 5340-7.
31. Song, E.-H. and N.L.B. Pohl, *Carbohydrate arrays: recent developments in fabrication and detection methods with applications.* Curr. Opin. Chem. Biol., 2009. **13**(5-6): p. 626-632.
32. Grant, C.F., V. Kanda, H. Yu, et al., *Optimization of immobilized bacterial disaccharides for surface plasmon resonance imaging measurements of antibody binding.* Langmuir, 2008. **24**(24): p. 14125-32.
33. Smith, E.A., W.D. Thomas, L.L. Kiessling, et al., *Surface plasmon resonance imaging studies of protein-carbohydrate interactions.* J. Am. Chem. Soc., 2003. **125**(20): p. 6140-6148.
34. Luyai, A., Y. Lasanajak, D.F. Smith, et al., *Facile preparation of fluorescent neoglycoproteins using p-nitrophenyl anthranilate as a heterobifunctional linker.* Bioconjugate Chem., 2009. **20**(8): p. 1618-24.
35. Park, S., M.R. Lee, and I. Shin, *Carbohydrate microarrays as powerful tools in studies of carbohydrate-mediated biological processes.* Chem Commun (Camb), 2008(37): p. 4389-99.
36. Shin, I., S. Park, and M.R. Lee, *Carbohydrate microarrays: An advanced technology for functional studies of glycans.* Chem-Eur J, 2005. **11**(10): p. 2894-2901.
37. Lee, M. and I. Shin, *Facile preparation of carbohydrate microarrays by site-specific, covalent immobilization of unmodified carbohydrates on hydrazide-coated glass slides.* Org. Lett., 2005. **7**(19): p. 4269-4272.
38. Liu, L.H., H. Dietsch, P. Schurtenberger, et al., *Photoinitiated coupling of unmodified monosaccharides to iron oxide nanoparticles for sensing proteins and bacteria.* Bioconjugate Chem., 2009. **20**(7): p. 1349-55.
39. Oyelaran, O. and J.C. Gildersleeve, *Glycan arrays: recent advances and future challenges.* Curr. Opin. Chem. Biol., 2009. **13**(4): p. 406-413.
40. Ratner, D.M., E.W. Adams, M.D. Disney, et al., *Tools for glycomics: mapping interactions of carbohydrates in biological systems.* Chembiochem, 2004. **5**(10): p. 1375-83.
41. Karamanska, R., J. Clarke, O. Blixt, et al., *Surface plasmon resonance imaging for real-time, label-free analysis of protein interactions with carbohydrate microarrays.* Glycoconjugate J., 2008. **25**(1): p. 69-74.

42. Lazcka, O., F.J. Del Campo, and F.X. Munoz, *Pathogen detection: a perspective of traditional methods and biosensors.* Biosens. Bioelectron., 2007. **22**(7): p. 1205-17.
43. Lee, H., E. Sun, D. Ham, et al., *Chip-NMR biosensor for detection and molecular analysis of cells.* Nat. Med., 2008. **14**(8): p. 869-74.
44. Kirk, J.T., G.E. Fridley, J.W. Chamberlain, et al., *Multiplexed inkjet functionalization of silicon photonic biosensors.* Lab Chip, 2011. **11**(7): p. 1372-7.
45. Ramachandran, A., S. Wang, J. Clarke, et al., *A universal biosensing platform based on optical micro-ring resonators.* Biosens. Bioelectron., 2008. **23**(7): p. 939-44.
46. Washburn, A.L., M.S. Luchansky, A.L. Bowman, et al., *Quantitative, label-free detection of five protein biomarkers using multiplexed arrays of silicon photonic microring resonators.* Anal. Chem., 2010. **82**(1): p. 69-72.
47. Byeon, J.Y. and R.C. Bailey, *Multiplexed evaluation of capture agent binding kinetics using arrays of silicon photonic microring resonators.* Analyst, 2010.
48. Washburn, A.L., L.C. Gunn, and R.C. Bailey, *Label-free quantitation of a cancer biomarker in complex media using silicon photonic microring resonators.* Anal. Chem., 2009. **81**(22): p. 9499-506.
49. Lee, H., S.M. Dellatore, W.M. Miller, et al., *Mussel-inspired surface chemistry for multifunctional coatings.* Science, 2007. **318**(5849): p. 426-30.
50. Wang, D., S. Liu, B.J. Trummer, et al., *Carbohydrate microarrays for the recognition of cross-reactive molecular markers of microbes and host cells.* Nat Biotech, 2002. **20**(3): p. 275-81.
51. Reed, R.A., J. Mattai, and G.G. Shipley, *Interaction of cholera toxin with ganglioside GM1 receptors in supported lipid monolayers.* Biochemistry (Mosc). 1987. **26**(3): p. 824-32.
52. Shi, J., T. Yang, S. Kataoka, et al., *GM1 clustering inhibits cholera toxin binding in supported phospholipid membranes.* Journal of the American Chemical Society, 2007. **129**(18): p. 5954-61.
53. Blixt, O., S. Head, T. Mondala, et al., *Printed covalent glycan array for ligand profiling of diverse glycan binding proteins.* P Natl Acad Sci Usa, 2004. **101**(49): p. 17033-17038.
54. Rusmini, F., Z. Zhong, and J. Feijen, *Protein immobilization strategies for protein biochips.* Biomacromolecules, 2007. **8**(6): p. 1775-1789.
55. Willats, W.G.T., S.E. Rasmussen, T. Kristensen, et al., *Sugar-coated microarrays: A novel slide surface for the high-throughput analysis of glycans.* Proteomics, 2002. **2**(12): p. 1666-1671.
56. Pelton, R., *Bioactive paper provides a low-cost platform for diagnostics.* Trac-Trend Anal Chem, 2009. **28**(8): p. 925-942.
57. Park, S., M.R. Lee, and I. Shin, *Carbohydrate microarrays as powerful tools in studies of carbohydrate-mediated biological processes.* Chem. Commun., 2008(37): p. 4389-4399.
58. Hermanson, G.T., *Bioconjugate techniques*. 2008, Rockford, Il: Elsevier.
59. Dubey, M., K. Emoto, F. Cheng, et al., *Surface analysis of photolithographic patterns using ToF-SIMS and PCA.* Surf Interface Anal, 2009. **41**(8): p. 645-652.
60. Xia, N., Y.H. Hu, D.W. Grainger, et al., *Functionalized Poly(ethylene glycol)-Grafted Polysiloxane*

Monolayers for Control of Protein Binding. Langmuir, 2002. **18**(8): p. 3255-3262.
61. Martin, S.M., R. Ganapathy, T.K. Kim, et al., *Characterization and analysis of osteopontin-immobilized poly(2-hydroxyethyl methacrylate) surfaces.* Journal of biomedical materials research Part A, 2003. **67**(1): p. 334-43.
62. Takahashi, H., K. Emoto, M. Dubey, et al., *Imaging Surface Immobilization Chemistry: Correlation with Cell Patterning on Non-Adhesive Hydrogel Thin Films* Advanced Functional Materials, 2008. **18**(14).
63. Bradner, J.E., O.M. McPherson, R. Mazitschek, et al., *A robust small-molecule microarray platform for screening cell lysates.* Chemistry & Biology, 2006. **13**(5): p. 493-504.

64. Lockett, M.R., J.C. Carlisle, D.V. Le, et al., *Acyl Chloride-Modified Amorphous Carbon Substrates for the Attachment of Alcohol-, Thiol-, and Amine-Containing Molecules.* Langmuir, 2009. **25**(9): p. 5120-5126.
65. Song, X., B. Xia, S.R. Stowell, et al., *Novel Fluorescent Glycan Microarray Strategy Reveals Ligands for Galectins.* Chemistry & Biology, 2009. **16**(1): p. 36-47.
66. Cheng, F., L.J. Gamble, D.W. Grainger, et al., *X-ray photoelectron spectroscopy, time-of-flight secondary ion mass spectrometry, and principal component analysis of the hydrolysis, regeneration, and reactivity of N-hydroxysuccinimide-containing organic thin films.* Anal. Chem., 2007. **79**(22): p. 8781-8.
67. Gong, P. and D. Grainger, *Comparison of DNA immobilization efficiency on new and regenerated commercial amine-reactive polymer microarray surfaces.* Surf Sci, 2004.
68. Carroll, G.T., D. Wang, N.J. Turro, et al., *Photochemical micropatterning of carbohydrates on a surface.* Langmuir, 2006. **22**(6): p. 2899-905.
69. Liu, L.-H., H. Dietsch, P. Schurtenberger, et al., *Photoinitiated coupling of unmodified monosaccharides to iron oxide nanoparticles for sensing proteins and bacteria.* Bioconjug. Chem., 2009. **20**(7): p. 1349-55.
70. Porath, J., T. Låås, and J.C. Janson, *Agar derivatives for chromatography, electrophoresis and gel-bound enzymes. III. Rigid agarose gels cross-linked with divinyl sulphone (dvs).* J. Chromatogr., 1975. **103**(1): p. 49-62.
71. Fornstedt, N. and J. Porath, *Characterization studies on a new lectin found in seeds of Vicia ervilia.* FEBS Letters, 1975. **57**(2): p. 187.
72. Stayton, P.S., T. Shimoboji, C. Long, et al., *CONTROL OF PROTEIN-LIGAND RECOGNITION USING A STIMULI-RESPONSIVE POLYMER.* Nature, 1995. **378**(6556): p. 472-474.
73. Ding, Z., C.J. Long, Y. Hayashi, et al., *Temperature control of biotin binding and release with A streptavidin-poly(N-isopropylacrylamide) site-specific conjugate.* Bioconjug. Chem., 1999. **10**(3): p. 395-400.
74. Bulmus, V., Z. Ding, C. Long, et al., *Site-Specific Polymer− Streptavidin Bioconjugate for pH-Controlled Binding and Triggered Release of Biotin.* Bioconjugate Chem, 2000. **11**(1): p. 78-83.
75. Grover, G.N., S.N.S. Alconcel, N.M. Matsumoto, et al., *Trapping of Thiol-Terminated Acrylate Polymers with Divinyl Sulfone To Generate Well-Defined Semitelechelic Michael Acceptor Polymers.* Macromolecules, 2009. **42**(20): p. 7657-7663.
76. Morales-Sanfrutos, J., F.J. Lopez-Jaramillo, F. Hernandez-Mateo, et al., *Vinyl Sulfone Bifunctional Tag Reagents for Single-Point Modification of Proteins.* J Org Chem, 2010. **75**(12): p. 4039-4047.
77. Morales-Sanfrutos, J., J. Lopez-Jaramillo, M. Ortega-Munoz, et al., *Vinyl sulfone: a versatile function for simple bioconjugation and immobilization.* Org Biomol Chem, 2010. **8**(3): p. 667-675.
78. Hatakeyama, T., K. Murakami, Y. Miyamoto, et al., *An assay for lectin activity using microtiter plate with chemically immobilized carbohydrates.* Anal. Biochem., 1996. **237**(2): p. 188-192.
79. Hatakeyama, T., Y. Miyamoto, H. Nagatomo, et al., *Carbohydrate-binding properties of the hemolytic lectin CEL-III from the holothuroidea Cucumaria echinata as analyzed using carbohydrate-coated microplate.* J. Biochem., 1997. **121**(1): p. 63-67.
80. Qiao, T., J. Leon, T. Penner, et al., *Substrate for protein microarray containing functionalized polymer*. 2002, Google Patents.
81. Iwaki, Y., H. Shinoki, and O. Seshimoto, *Method for the detection of gene with DNA micro-array.* US Patent, 2007: p. 7,169,583.
82. Vigé, A., C. Gallou-Kabani, M. Gross, et al., *An oligonucleotide microarray for mouse imprinted genes profiling.* Cytogenet. Genome Res., 2006. **113**(1-4): p. 253-261.
83. Zhen, G.L., D. Falconnet, E. Kuennemann, et al., *Nitrilotriacetic acid functionalized graft copolymers: A polymeric interface for selective and reversible binding of histidine-tagged proteins.* Adv. Funct. Mater., 2006. **16**(2): p. 243-251.

84. Pathak, T. and R. Bhattacharya, *A vinyl sulfone-modified carbohydrate mediated new route to aminosugars and branched-chain sugars.* Carbohydr. Res., 2008. **343**(12): p. 1980-1998.
85. Pathak, T., *Vinyl sulfone-modified carbohydrates: an inconspicuous group of chiral building blocks.* Tetrahedron, 2008. **64**: p. 3605-3628.
86. Hayes, W., H. Osborn, S. Osborne, et al., *One-pot synthesis of multivalent arrays of mannose mono-and disaccharides.* Tetrahedron, 2003. **59**(40): p. 7983-7996.
87. Dhayal, M. and D.A. Ratner, *XPS and SPR Analysis of Glycoarray Surface Density.* Langmuir, 2009. **25**(4): p. 2181-2187.
88. Wei, Y. and R.A. Latour, *Determination of the Adsorption Free Energy for Peptide−Surface Interactions by SPR Spectroscopy.* Langmuir, 2008. **24**(13): p. 6721-6729.
89. Baio, J.E., T. Weidner, J. Brison, et al., *Amine terminated SAMs: Investigating why oxygen is present in these films.* J Electron Spectrosc, 2009. **172**(1-3): p. 2-8.
90. Castner, D., K. Hinds, and D. Grainger, *X-ray photoelectron spectroscopy sulfur 2p study of organic thiol and disulfide binding interactions with gold surfaces.* Langmuir, 1996. **12**: p. 5083-5086.
91. Cheng, F., L.J. Gamble, D.W. Grainger, et al., *X-ray photoelectron spectroscopy, time-of-flight secondary ion mass spectrometry, and principal component analysis of the hydrolysis, regeneration, and reactivity of N-hydroxysuccinimide-containing organic thin films.* Anal. Chem., 2007. **79**(22): p. 8781-8.
92. Berman, E.S.F., K.S. Kulp, M.G. Knize, et al., *Distinguishing monosaccharide stereo- and structural isomers with TOF-SIMS and multivariate statistical analysis.* Anal. Chem., 2006. **78**(18): p. 6497-503.
93. Biemann, K., D.C. DeJongh, and H.K. Schnoes, *Application of Mass Spectrometry to Structure Problems. XIII. Acetates of Pentoses and Hexaoses.* Journal of the American Chemical Society, 1962. **85**: p. 1763-1771.
94. Silva, A., C. Richard, M. Bessodes, et al., *Growth factor delivery approaches in hydrogels.* Biomacromolecules, 2009. **10**(1): p. 9-18.
95. Kim, J., B. Wacker, and D. Elbert, *Thin polymer layers formed using multiarm poly (ethylene glycol) vinylsulfone by a covalent layer-by-layer method.* Biomacromolecules, 2007. **8**(11): p. 3682-3686.
96. Hiemstra, C., L. van der Aa, Z. Zhong, et al., *Rapidly in situ-forming degradable hydrogels from dextran thiols through Michael addition.* Biomacromolecules, 2007. **8**(5): p. 1548-1556.
97. Masel, R., *Principles of adsorption and reaction on solid surfaces*. 1996: Wiley-Interscience.
98. Zhang, Y., S. Luo, Y. Tang, et al., *Carbohydrate-Protein Interactions by "Clicked" Carbohydrate Self-Assembled Monolayers.* Anal. Chem., 2006. **78**: p. 2001-2008.
99. Smith, E.A., W.D. Thomas, L.L. Kiessling, et al., *Surface plasmon resonance imaging studies of protein-carbohydrate interactions.* J. Am. Chem. Soc., 2003. **125**(20): p. 6140-8.
100. Mori, T., M. Toyoda, T. Ohtsuka, et al., *Kinetic analyses for bindings of concanavalin A to dispersed and condensed mannose surfaces on a quartz crystal microbalance.* Anal. Biochem., 2009. **395**(2): p. 211-216.
101. Lee, J., Y. Kim, Y. Chi, et al., *Grafting nitrilotriacetic groups onto carboxylic acid-terminated self-assembled monolayers on gold surfaces for immobilization of histidine-tagged proteins.* J Phys Chem B, 2004. **108**(23): p. 7665-7673.
102. Agrawal, P.K., *NMR Spectroscopy in the structural elucidation of oligosaccharides and glycosides.* Phytochemistry, 1992. **31**(10): p. 3307-3330.
103. Luchansky, M.S. and R.C. Bailey, *Silicon photonic microring resonators for quantitative cytokine detection and T-cell secretion analysis.* Anal. Chem., 2010. **82**(5): p. 1975-81.
104. Cattani-Scholz, A., D. Pedone, M. Dubey, et al., *Organophosphonate-based PNA-functionalization of silicon nanowires for label-free DNA detection.* ACS Nano, 2008. **2**(8): p. 1653-60.

105. Lapin, N.A. and Y.J. Chabal, *Infrared characterization of biotinylated silicon oxide surfaces, surface stability, and specific attachment of streptavidin.* J Phys Chem B, 2009. **113**(25): p. 8776-83.
106. Asenath-Smith, E. and W. Chen, *How To Prevent the Loss of Surface Functionality Derived from Aminosilanes.* Langmuir, 2008. **24**(21): p. 12405-12409.
107. Dubey, M., T. Weidner, L.J. Gamble, et al., *Structure and order of phosphonic acid-based self-assembled monolayers on Si(100).* Langmuir, 2010. **26**(18): p. 14747-54.
108. Hauffman, T., O. Blajiev, J. Snauwaert, et al., *Study of the self-assembling of n-octylphosphonic acid layers on aluminum oxide.* Langmuir, 2008. **24**(23): p. 13450-6.
109. Silverman, B.M., K.A. Wieghaus, and J. Schwartz, *Comparative properties of siloxane vs phosphonate monolayers on a key titanium alloy.* Langmuir, 2005. **21**(1): p. 225-8.
110. Midwood, K.S., M.D. Carolus, M.P. Danahy, et al., *Easy and efficient bonding of biomolecules to an oxide surface of silicon.* Langmuir, 2004. **20**(13): p. 5501-5.
111. Hanson, E.L., J. Schwartz, B. Nickel, et al., *Bonding self-assembled, compact organophosphonate monolayers to the native oxide surface of silicon.* J. Am. Chem. Soc., 2003. **125**(51): p. 16074-80.
112. Cattani-Scholz, A., D. Pedone, F. Blobner, et al., *PNA-PEG modified silicon platforms as functional bio-interfaces for applications in DNA microarrays and biosensors.* Biomacromolecules, 2009. **10**(3): p. 489-96.
113. Hoque, E., J.A. DeRose, G. Kulik, et al., *Alkylphosphonate modified aluminum oxide surfaces.* J Phys Chem B, 2006. **110**(22): p. 10855-61.
114. Klauk, H., U. Zschieschang, J. Pflaum, et al., *Ultralow-power organic complementary circuits.* Nature, 2007. **445**(7129): p. 745-8.
115. Zschieschang, U., M. Halik, and H. Klauk, *Microcontact-printed self-assembled monolayers as ultrathin gate dielectrics in organic thin-film transistors and complementary circuits.* Langmuir, 2008. **24**(5): p. 1665-9.
116. Luo, W., N.P. Westcott, A. Pulsipher, et al., *Renewable and optically transparent electroactive indium tin oxide surfaces for chemoselective ligand immobilization and biospecific cell adhesion.* Langmuir, 2008. **24**(22): p. 13096-101.
117. Adden, N., L.J. Gamble, D.G. Castner, et al., *Phosphonic acid monolayers for binding of bioactive molecules to titanium surfaces.* Langmuir, 2006. **22**(19): p. 8197-204.
118. Shirato, H., S. Ogawa, H. Ito, et al., *Noroviruses distinguish between type 1 and type 2 histo-blood group antigens for binding.* J. Virol., 2008. **82**(21): p. 10756-67.
119. Cheng, F., J. Shang, and D.M. Ratner, *A versatile method for functionalizing surfaces with bioactive glycans.* Bioconjugate Chem., 2011. **22**(1): p. 50-7.
120. Putvinski, T.M., M.L. Schilling, H.E. Katz, et al., *SELF-ASSEMBLY OF ORGANIC MULTILAYERS WITH POLAR ORDER USING ZIRCONIUM-PHOSPHATE BONDING BETWEEN LAYERS.* Langmuir, 1990. **6**(10): p. 1567-1571.
121. Tagawa, K., N. Sendai, K. Ohno, et al., *Recognition of novel amphiphiles with many pendent mannose residues by Con A.* Bioconjugate Chem., 1999. **10**(3): p. 354-360.
122. Newton, D.L., R. Wales, P.T. Richardson, et al., *Cell surface and intracellular functions for ricin galactose binding.* J. Biol. Chem., 1992. **267**(17): p. 11917-22.
123. Farr, A.G. and S.K. Anderson, *Epithelial heterogeneity in the murine thymus: fucose-specific lectins bind medullary epithelial cells.* J. Immunol., 1985. **134**(5): p. 2971-7.
124. Shang, J., F. Cheng, M. Dubey, et al., *An organophosphonate strategy for functionalizing silicon photonic biosensors.* Langmuir, 2012. **28**(6): p. 3338-44.
125. Itakura, Y., S. Nakamura-Tsuruta, J. Kominami, et al., *Systematic comparison of oligosaccharide specificity of Ricinus communis agglutinin I and Erythrina lectins: a search by frontal affinity chromatography.* J Biochem, 2007. **142**(4): p. 459-69.
126. Seitz, O., P.G. Fernandes, R.H. Tian, et al., *Control and stability of self-assembled monolayers under biosensing conditions.* J. Mater. Chem., 2011. **21**(12): p. 4384-4392.

127. Marcinko, S. and A.Y. Fadeev, *Hydrolytic stability of organic monolayers supported on TiO2 and ZrO2.* Langmuir, 2004. **20**(6): p. 2270-3.
128. Cao, S., Z.Y. Lou, M. Tan, et al., *Structural basis for the recognition of blood group trisaccharides by norovirus.* J. Virol., 2007. **81**(11): p. 5949-5957.
129. Baleux, F., L. Loureiro-Morais, Y. Hersant, et al., *A synthetic CD4-heparan sulfate glycoconjugate inhibits CCR5 and CXCR4 HIV-1 attachment and entry.* Nat Chem Biol, 2009. **5**(10): p. 743-8.
130. Luchansky, M.S., A.L. Washburn, T.A. Martin, et al., *Characterization of the evanescent field profile and bound mass sensitivity of a label-free silicon photonic microring resonator biosensing platform.* Biosens. Bioelectron., 2010. **26**(4): p. 1283-91.
131. Tan, M., P. Huang, J. Meller, et al., *Mutations within the P2 domain of norovirus capsid affect binding to human histo-blood group antigens: evidence for a binding pocket.* J. Virol., 2003. **77**(23): p. 12562-71.
132. Tan, M. and X. Jiang, *Association of histo-blood group antigens with susceptibility to norovirus infection may be strain-specific rather than genogroup dependent.* Journal of Infectious Diseases, 2008. **198**(6): p. 940-941.
133. Kawai, H., S. Deguchi, K. Deguchi, et al., *Synergistic benefit of combined amlodipine plus atorvastatin on neuronal damage after stroke in Zucker metabolic rat.* Brain Res, 2010.
134. Rydell, G.E., A.B. Dahlin, F. Hook, et al., *QCM-D studies of human norovirus VLPs binding to glycosphingolipids in supported lipid bilayers reveal strain-specific characteristics.* Glycobiology, 2009. **19**(11): p. 1176-84.
135. Zhang, Y., Q. Yao, C. Xia, et al., *Trapping norovirus by glycosylated hydrogels: a potential oral antiviral drug.* ChemMedChem, 2006. **1**(12): p. 1361-6.
136. Feng, X. and X. Jiang, *Library screen for inhibitors targeting norovirus binding to histo-blood group antigen receptors.* Antimicrob. Agents Chemother., 2007. **51**(1): p. 324-31.
137. Rademacher, C., J. Guiard, P.I. Kitov, et al., *Targeting norovirus infection-multivalent entry inhibitor design based on NMR experiments.* Chemistry, 2011. **17**(27): p. 7442-53.
138. Guiard, J., B. Fiege, P.I. Kitov, et al., *"Double-Click" Protocol for Synthesis of Heterobifunctional Multivalent Ligands: Toward a Focused Library of Specific Norovirus Inhibitors.* Chem-Eur J, 2011. **17**(27): p. 7438-7441.
139. Ruvoen-Clouet, N., E. Mas, S. Marionneau, et al., *Bile-salt-stimulated lipase and mucins from milk of 'secretor' mothers inhibit the binding of Norwalk virus capsids to their carbohydrate ligands.* Biochem. J, 2006. **393**: p. 627-634.
140. Kanda, V., J.K. Kariuki, D.J. Harrison, et al., *Label-free reading of microarray-based immunoassays with surface plasmon resonance imaging.* Anal. Chem., 2004. **76**(24): p. 7257-7262.
141. Mullett, W.M., E.P.C. Lai, and J.M. Yeung, *Surface plasmon resonance-based immunoassays.* Methods-a Companion to Methods in Enzymology, 2000. **22**(1): p. 77-91.
142. Yu, A., J. Shang, F. Cheng, et al., *Biofunctional Paper via the Covalent Modification of Cellulose.* Langmuir, 2012.
143. Gray, G.R., *The direct coupling of oligosaccharides to proteins and derivatized gels.* Arch Biochem Biophys, 1974. **163**(1): p. 426-8.
144. Likhosherstov, L.M., Novikova, O.S., Yamskov, I.A., Piskarev, V.E. , *Synthesis of N-glycyl-beta-glycosylamines of human milk fucooligosaccharides.* Rus. Chem. Bull. , 2012: p. In press.
145. Wu, A.M., J.H. Wu, T. Singh, et al., *Lectinochemical studies on the binding properties of a toxic lectin (ricin) isolated from the seeds of Ricinus communis.* Chang Gung Med J, 2005. **28**(8): p. 530-42.
146. Huang, P., T. Farkas, S. Marionneau, et al., *Noroviruses bind to human ABO, Lewis, and secretor histo-blood group antigens: identification of 4 distinct strain-specific patterns.* J. Infect. Dis., 2003. **188**(1): p. 19-31.

147. Marionneau, S., F. Airaud, N.V. Bovin, et al., *Influence of the combined ABO, FUT2, and FUT3 polymorphism on susceptibility to Norwalk virus attachment.* J. Infect. Dis., 2005. **192**(6): p. 1071-7.
148. Marionneau, S., N. Ruvoen, B. Le Moullac-Vaidye, et al., *Norwalk virus binds to histo-blood group antigens present on gastroduodenal epithelial cells of secretor individuals.* Gastroenterology, 2002. **122**(7): p. 1967-1977.
149. Bejugam, M. and S.L. Flitsch, *An efficient synthetic route to glycoamino acid building blocks for glycopeptide synthesis.* Org Lett, 2004. **6**(22): p. 4001-4.
150. Habte, H.H., C. de Beer, Z.E. Lotz, et al., *Inhibition of human immunodeficiency virus type 1 activity by purified human breast milk mucin (MUC1) in an inhibition assay.* Neonatology, 2008. **93**(3): p. 162-70.
151. Buranasin, P., M. Kunakorn, B. Petchclai, et al., *Detection of human immunodeficiency virus type 1 (HIV-1) proviral DNA in breast milk and colostrum of seropositive mothers.* J. Med. Assoc. Thai., 1993. **76**(1): p. 41-5.
152. Thior, I., S. Lockman, L.M. Smeaton, et al., *Breastfeeding plus infant zidovudine prophylaxis for 6 months vs formula feeding plus infant zidovudine for 1 month to reduce mother-to-child HIV transmission in Botswana: a randomized trial: the Mashi Study.* JAMA, 2006. **296**(7): p. 794-805.
153. Coovadia, H.M., N.C. Rollins, R.M. Bland, et al., *Mother-to-child transmission of HIV-1 infection during exclusive breastfeeding in the first 6 months of life: an intervention cohort study.* Lancet, 2007. **369**(9567): p. 1107-16.
154. Vives, R.R., A. Imberty, Q.J. Sattentau, et al., *Heparan sulfate targets the HIV-1 envelope glycoprotein gp120 coreceptor binding site.* J. Biol. Chem., 2005. **280**(22): p. 21353-7.
155. Platt, E.J., K. Wehrly, S.E. Kuhmann, et al., *Effects of CCR5 and CD4 cell surface concentrations on infections by macrophagetropic isolates of human immunodeficiency virus type 1.* J. Virol., 1998. **72**(4): p. 2855-2864.
156. Crublet, E., J.P. Andrieu, R.R. Vives, et al., *The HIV-1 envelope glycoprotein gp120 features four heparan sulfate binding domains, including the co-receptor binding site.* J. Biol. Chem., 2008. **283**(22): p. 15193-200.
157. de Parseval, A., M.D. Bobardt, A. Chatterji, et al., *A highly conserved arginine in gp120 governs HIV-1 binding to both syndecans and CCR5 via sulfated motifs.* J. Biol. Chem., 2005. **280**(47): p. 39493-39504.
158. Mourier, P.A. and C. Viskov, *Chromatographic analysis and sequencing approach of heparin oligosaccharides using cetyltrimethylammonium dynamically coated stationary phases.* Anal. Biochem., 2004. **332**(2): p. 299-313.
159. Cameron, N.R., S.G. Spain, J.A. Kingham, et al., *Synthesis of well-defined glycopolymers and some studies of their aqueous solution behaviour.* Faraday Discuss., 2008. **139**: p. 359-68; discussion 399-417, 419-20.
160. Wu, A.M., *Polyvalent GalNAcalpha1-->Ser/Thr (Tn) and Galbeta1-->3GalNAcalpha1-->Ser/Thr (T alpha) as the most potent recognition factors involved in Maclura pomifera agglutinin-glycan interactions.* J. Biomed. Sci., 2005. **12**(1): p. 135-52.
161. Mammen, M., G. Dahmann, and G.M. Whitesides, *Effective inhibitors of hemagglutination by influenza virus synthesized from polymers having active ester groups. Insight into mechanism of inhibition.* J. Med. Chem., 1995. **38**(21): p. 4179-90.
162. Engelhardt, W., H. Gorczytza, A. Butterweck, et al., *Structural requirements of the cytoplasmic domains of the human macrophage Fc gamma receptor IIa and B cell Fc gamma receptor IIb2 for the endocytosis of immune complexes.* Eur. J. Immunol., 1991. **21**(9): p. 2227-38.
163. Gibson, M.I., C.A. Barker, S.G. Spain, et al., *Inhibition of ice crystal growth by synthetic glycopolymers: implications for the rational design of antifreeze glycoprotein mimics.* Biomacromolecules, 2009. **10**(2): p. 328-33.
164. Mahkam, M., *New pH-sensitive glycopolymers for colon-specific drug delivery.* Drug Deliv, 2007. **14**(3): p. 147-53.

165. Kanda, V., P. Kitov, D.R. Bundle, et al., *Surface plasmon resonance imaging measurements of the inhibition of Shiga-like toxin by synthetic multivalent inhibitors.* Anal. Chem., 2005. **77**(23): p. 7497-504.
166. von Lode, P., *Point-of-care immunotesting: Approaching the analytical performance of central laboratory methods.* Clin. Biochem., 2005. **38**(7): p. 591-606.
167. Yager, P., T. Edwards, E. Fu, et al., *Microfluidic diagnostic technologies for global public health.* Nature, 2006. **442**(7101): p. 412-418.
168. Yager, P., G.J. Domingo, and J. Gerdes, *Point-of-care diagnostics for global health.* Annu Rev Biomed Eng, 2008. **10**: p. 107-144.
169. Tonkinson, J.L. and B.A. Stillman, *Nitrocellulose: A tried and true polymer finds utility as a post-genomic substrate.* Front. Biosci., 2002. **7**: p. C1-C12.
170. Martinez, A.W., S.T. Phillips, M.J. Butte, et al., *Patterned paper as a platform for inexpensive, low-volume, portable bioassays.* Angew Chem Int Edit, 2007. **46**(8): p. 1318-1320.
171. Martinez, A.W., S.T. Phillips, and G.M. Whitesides, *Three-dimensional microfluidic devices fabricated in layered paper and tape.* Proc. Natl. Acad. Sci. U. S. A., 2008. **105**(50): p. 19606-19611.
172. Martinez, A.W., S.T. Phillips, G.M. Whitesides, et al., *Diagnostics for the Developing World: Microfluidic Paper-Based Analytical Devices.* Anal. Chem., 2010. **82**(1): p. 3-10.
173. Fenton, E.M., M.R. Mascarenas, G.P. Lopez, et al., *Multiplex Lateral-Flow Test Strips Fabricated by Two-Dimensional Shaping.* Acs Appl Mater Inter, 2009. **1**(1): p. 124-129.
174. Xu, D.X., M. Vachon, A. Densmore, et al., *Label-free biosensor array based on silicon-on-insulator ring resonators addressed using a WDM approach.* Opt Lett, 2010. **35**(16): p. 2771-3.
175. Reches, M., K.A. Mirica, R. Dasgupta, et al., *Thread as a Matrix for Biomedical Assays.* Acs Appl Mater Inter, 2010. **2**(6): p. 1722-1728.
176. Towbin, H., T. Staehelin, and J. Gordon, *Electrophoretic Transfer of Proteins from Polyacrylamide Gels to Nitrocellulose Sheets - Procedure and Some Applications.* Proc. Natl. Acad. Sci. U. S. A., 1979. **76**(9): p. 4350-4354.
177. Bode, L., L. Beutin, and H. Kohler, *Nitrocellulose-Enzyme-Linked Immunosorbent-Assay (Nc-Elisa) - a Sensitive Technique for the Rapid Visual Detection of Both Viral-Antigens and Antibodies.* J. Virol. Methods, 1984. **8**(1-2): p. 111-121.
178. Tovey, E.R. and B.A. Baldo, *Protein-Binding to Nitrocellulose, Nylon and Pvdf Membranes in Immunoassays and Electroblotting.* J. Biochem. Bioph. Methods, 1989. **19**(2-3): p. 169-183.
179. Jones, K.L. and C.R. O'Melia, *Protein and humic acid adsorption onto hydrophilic membrane surfaces: effects of pH and ionic strength.* J Membrane Sci, 2000. **165**(1): p. 31-46.
180. Stollner, D., F.W. Scheller, and A. Warsinke, *Activation of cellulose membranes with 1,1 '-carbonyldiimidazole or 1-cyano-4-dimethylaminopyridinium tetrafluoroborate as a basis for the development of immunosensors.* Anal. Biochem., 2002. **304**(2): p. 157-165.
181. Bora, U., P. Sharma, K. Kannan, et al., *Photoreactive cellulose membrane - A novel matrix for covalent immobilization of biomolecules.* J. Biotechnol., 2006. **126**(2): p. 220-229.
182. Sharma, P., S.F. Basir, and P. Nahar, *Photoimmobilization of unmodified carbohydrates on activated surface.* J. Colloid Interface Sci., 2010. **342**(1): p. 202-204.
183. Bryjak, J., J. Liesiene, and V. Stefuca, *Man-tailored cellulose-based carriers for invertase immobilization.* Cellulose, 2008. **15**(4): p. 631-640.
184. Kong, D.L., W. Schuett, J. Dai, et al., *Development of cellulose-DNA immunoadsorbent.* Artif. Organs, 2002. **26**(2): p. 200-208.
185. Su, S.X., R. Nutiu, C.D.M. Filipe, et al., *Adsorption and covalent coupling of ATP-binding DNA aptamers onto cellulose.* Langmuir, 2007. **23**(3): p. 1300-1302.
186. Sereikaite, J., D. Bassus, R. Bobnis, et al., *Divinyl sulfone as a crosslinking reagent for oligomeric proteins.* uss. J. Bioorg. Chem., 2003. **29**(3): p. 227-230.

187. Porath, J., T. Laas, and J.C. Janson, *Agar derivatives for chromatography, electrophoresis and gel-bound enzymes. III. Rigid agarose gels cross-linked with divinyl sulphone (dvs).* J Chromatogr, 1975. **103**(1): p. 49-62.
188. Fornstedt, N. and J. Porath, *Characterization Studies on a New Lectin Found in Seeds of Vicia-Ervilia.* FEBS Lett., 1975. **57**(2): p. 187-191.
189. Xiao, W. and J.G. Huang, *Immobilization of Oligonucleotides onto Zirconia-Modified Filter Paper and Specific Molecular Recognition.* Langmuir, 2011. **27**(20): p. 12284-12288.
190. Nelson, B.P., T.E. Grimsrud, M.R. Liles, et al., *Surface plasmon resonance imaging measurements of DNA and RNA hybridization adsorption onto DNA microarrays.* Anal. Chem., 2001. **73**(1): p. 1-7.